

PROTEIN DIVERSITY IN AFRICAN TRYPANOSOMES: THE ROLE OF NOVEL AND  
MULTIFUNCTIONING MITOCHONDRIAL PROTEINS IN *TRYPANOSOMA BRUCEI*

by

STEVEN EDRIC SYKES

(Under the Direction of Stephen L. Hajduk)

ABSTRACT

*Trypanosoma brucei* differentiates into morphologically distinct forms as it inhabits two drastically different environments during its life cycle. In both stages, a single mitochondrion is required which differs greatly in the levels of activity during cell progression. The insect (procyclic) parasite has a very robust organelle that is active in energy processes such as the Krebs pathway and cytochrome mediated respiration while the mammalian (bloodstream) form has a repressed mitochondrion that is not active in these metabolic pathways. Despite these drastic differences, a diverse set of mitochondrial and nuclear encoded proteins is necessary for maintenance of this organelle in both developmental stages.

This work provides evidence of two contrasting mechanisms of protein diversity in *T. brucei*. The first part of this study further describes alternatively edited protein-1 (AEP-1), a polypeptide created from the post-transcriptional process of trypanosome mitochondrial RNA editing. Initially, I confirmed the presence of AEP-1 in procyclic and bloodstream form cells with a dual localization in their respective mitochondria. In both, AEP-1 resides in a nonionic detergent soluble complex associated with the inner mitochondrial membrane and a detergent resistant structure (tripartite attachment complex) that physically links the mitochondrial DNA

(kinetoplast) to the basal bodies of the single flagellum of the cell. A previous study has revealed the importance of AEP-1 in genome integrity and characterizes this structural protein as a kinetoplast maintenance factor.

Sequencing of the soluble AEP-1 integral mitochondrial membrane complex (A-IMM) unsuspectingly uncovered moonlighting metabolic enzymes, another means of diversification, and revealed single proteins that have multiple functions within a cell. Here, I show that one of these proteins, the dihydrolipoamide succinyltransferase (E2) subunit of the  $\alpha$ -ketoglutarate dehydrogenase, associates with the flagellum kinetoplast (kDNA) complex (FKC), which houses the tripartite attachment complex (TAC) and is important for kDNA distribution and mitochondrial biogenesis. Lastly, I demonstrate that depletion of a second enzyme from this Krebs pathway, the  $\alpha$ -ketoglutarate dehydrogenase (E1) subunit, causes rapid swelling of an organelle involved in endo- and exocytosis of the cell, the flagellar pocket.

INDEX WORDS: RNA editing, Moonlighting proteins, Mitochondria, Krebs cycle,  
Kinetoplast, *Trypanosoma brucei*

PROTEIN DIVERSITY IN AFRICAN TRYPANOSOMES: THE EFFECT OF NOVEL AND  
MULTIFUNCTIONING MITOCHONDRIAL PROTEINS IN *TRYPANOSOMA BRUCEI*

by

STEVEN EDRIC SYKES

B.S., Morehouse College, 2001

A Dissertation Submitted to the Graduate Faculty of The University of Georgia in Partial  
Fulfillment of the Requirements for the Degree

DOCTOR OF PHILOSOPHY

ATHENS, GEORGIA

2012

© 2012

STEVEN EDRIC SYKES

All Rights Reserved

PROTEIN DIVERSITY IN AFRICAN TRYPANOSOMES: THE EFFECT OF NOVEL AND  
MULTIFUNCTIONING MITOCHONDRIAL PROTEINS IN *TRYPANOSOMA BRUCEI*

by

STEVEN EDRIC SYKES

Major Professor: Stephen L. Hajduk  
Committee: Marcus Fechheimer  
Kojo Mensa-Wilmot  
Robert Sabatini  
Roberto Docampo

Electronic Version Approved:

Maureen Grasso  
Dean of the Graduate School  
The University of Georgia  
December 2012

DEDICATION

To the Sykes family.

My parents—Ellis and Shirley Sykes, Jr.

My brother—Ellis Sykes, III

My grandparents—Ellis and Sarah Sykes, Sr.

## ACKNOWLEDGEMENTS

My deepest expression of appreciation goes to Sykes family. I thank my father and mother, Ellis and Shirley Sykes, for grooming me into a person who could use the tools they made available to prepare me for this specific purpose. My parents showed me that life's most important rewards come with hard work. My brother, Ellis Sykes III, has taught me that your personal journey is full of obstacles and you must use these experiences as the stepping-stones of success. I'm indebted to my grandparents, the late Ellis and Sarah Sykes, for their support and words of encouragement throughout my academic process. I also want to thank my "other half", Renelsa Lewis, for always being there when I needed her and making Athens a great place to live.

I am extremely grateful to my advisor, Steve Hajduk. He was in my corner from the beginning and overly supportive of any situation I presented to him. I am also grateful for the lessons in independent thinking and brainstorming. He showed an unyielding devotion to science that was dedicated to resolving some of the most perplexing problems in the field. That kind of science foundation is ingrained in my being and will aid me in anything I strive for in the future.

I want to give a special thanks to past and present lab members who helped to create the perfect work environment! I first want like to thank the mitochondrial crew, which includes David Seidman and Tony Szempruch, for all of the fun times in and out of lab and also the deep discussions about research. I also want to thank the "TLFers" and this long list of great individuals includes Natalie Stephens, John Harrington, Justin Widener, April Shiflett and Rudo

Kieft. Also, I would like to thank Amanda Johns, one of my best undergrads who undoubtedly had “golden hands” and made significant contributions to my research.

I am thankful for my committee members for all of the good advice and strategies over the years. I am grateful for Bob Sabatini, Roberto Docampo, Marcus Fechheimer and Kojo Mensa-Wilmot for aiding in the progression of my research. I want to especially thank Kojo Mensa-Wilmot and Marcus Fechheimer for believing in me and helping in my grad school trials. Lastly, I would like to thank Kris Miller for helping me become the best teaching assistant I could be.

## TABLE OF CONTENTS

|   | Page |
|---|------|
| ACKNOWLEDGEMENTS .....  | v    |
| LIST OF TABLES .....  | x    |
| LIST OF FIGURES .....   | xi   |
| CHAPTER   |      |
| 1 GENERAL INTRODUCTION AND LITERATURE REVIEW .....            | 1    |
| African Trypanosomiasis .....                                 | 3    |
| The Cellular Structure of <i>Trypanosoma brucei</i> .....     | 4    |
| The Extraordinary Life Cycle of <i>T. brucei</i> .....        | 5    |
| The <i>T. brucei</i> Cell Cycle .....                         | 8    |
| The Flagellar Pocket .....                                    | 10   |
| The Nucleus of <i>T. brucei</i> .....                         | 11   |
| Glycolysis and Glycosomes .....                               | 13   |
| The <i>T. brucei</i> Mitochondrion .....                      | 14   |
| The kDNA .....  | 15   |
| The Tripartite Attachment Complex .....                       | 18   |
| Energy Metabolism in the <i>T. brucei</i> Mitochondrion ..... | 20   |
| Mitochondrial RNA Editing .....                               | 24   |
| Alternative RNA Editing .....                                 | 24   |
| Alternatively Edited Protein-1 .....                          | 27   |

|   |     |
|---|-----|
| Moonlighting Proteins .....   | 31  |
| Moonlighting Metabolic Enzymes in Parasitic Protozoa .....  | 35  |
| References.....   | 37  |
|   |     |
| 2 IDENTIFICATION OF A NOVEL MITOCHONDRIAL MEMBRANE COMPLEX:<br>AEP-1 INTERACTS WITH COMPONENTS OF THE $\alpha$ -KETOGLUTARATE<br>DEHYDROGENASE MULTIENZYME..... | 50  |
| Abstract.....   | 51  |
| Introduction.....   | 52  |
| Results.....  | 55  |
| Discussion.....   | 65  |
| Materials and Methods.....  | 71  |
| Acknowledgements.....   | 75  |
| References.....   | 75  |
| Supplemental Figures and Tables.....  | 79  |
|   |     |
| 3 DUAL FUNCTIONS OF $\alpha$ -KETOGLUTARATE DEHYDROGENASE E2 IN THE<br>KREBS CYCLE AND MITOCHONDRIAL DNA INHERITANCE IN<br><i>TRYPANOSOMA BRUCEI</i> .....      | 88  |
| Abstract.....   | 89  |
| Introduction.....   | 90  |
| Results.....  | 95  |
| Discussion.....   | 117 |
| Materials and Methods.....  | 122 |

|  |     |
|--|-----|
| Acknowledgements.....  | 129 |
| References.....  | 130 |
| 4 RNAi MEDIATED KNOCKDOWN OF $\alpha$ -KETOGLUTARATE<br>DEHYDROGENASE E1 CAUSES RAPID SWELLING OF THE<br>TRYPANOSOME FLAGELLAR POCKET..... | 136 |
| Introduction.....  | 136 |
| Reduction in the Levels of $\alpha$ -KDE1 mRNA Causes Rapid Morphological<br>Changes in BF <i>T. brucei</i> .....                          | 138 |
| $\alpha$ -KDE1 Depletion Causes FP Swelling.....   | 140 |
| Discussion.....  | 142 |
| Materials and Methods.....   | 145 |
| References.....  | 147 |
| 5 CONCLUSIONS AND DISCUSSION .....   | 151 |
| References.....  | 158 |

## LIST OF TABLES

|  | Page |
|--|------|
| Table 2.1: LC-MS/MS analysis of anion exchange purified mitochondrial complexes.....                         | 69   |
| Table S2.1: Subunits of the PF A-IMM identified by LC-MS/MS .....  | 81   |
| Table S2.2: Subunits of the PF ATPase-F <sub>1</sub> F <sub>0</sub> identified by LC-MS/MS .....             | 82   |
| Table S2.3: Subunits of the PF alternative ATPase-F <sub>1</sub> F <sub>0</sub> identified by LC-MS/MS ..... | 83   |
| Table S2.4: Subunits of the PF cytochrome c reductase identified by LC-MS/MS .....                           | 84   |
| Table S2.5: Subunits of the PF cytochrome c oxidase identified by LC-MS/MS .....                             | 85   |
| Table S2.6: Subunits of the BF A-IMM identified by LC-MS/MS.....   | 86   |
| Table S2.7: Subunits of the BF ATPase-F <sub>1</sub> F <sub>0</sub> identified by LC-MS/MS.....              | 87   |

## LIST OF FIGURES

|  | Page |
|--|------|
| Figure 1.1: The ultrastructure of <i>T. brucei</i> .....   | 5    |
| Figure 1.2: The digenetic life cycle of <i>T. brucei</i> alternates between mammalian and insect host ..                                 | 7    |
| Figure 1.3: Diagram of the <i>T. brucei</i> duplication cycle.....   | 9    |
| Figure 1.4: Schematic of kDNA replication .....  | 17   |
| Figure 1.5: Schematic diagram of TAC structure and duplication in trypanosomes.....  | 19   |
| Figure 1.6: Schematic diagram of pathways in procyclic form <i>T. brucei</i> involved in amino acid<br>and carbohydrate metabolism ..... | 21   |
| Figure 1.7: Simplified mechanism for uridine insertion and deletion editing in trypanosomes....  | 23   |
| Figure 1.8: AEP-1 mRNA and amino acid sequences.....   | 26   |
| Figure 1.9: AEP-1 orientation in the mitochondrial inner membrane .....  | 29   |
| Figure 1.10: A schematic of Krebs cycle enzymes with observed moonlighting functions.....  | 32   |
| Figure 2.1: Localization and distribution of AEP-1 in PF <i>T. brucei</i> .....  | 56   |
| Figure 2.2: Detection of mitochondrial membrane proteins in PF <i>T. brucei</i> .....  | 58   |
| Figure 2.3: Native and 2D electrophoresis of mitochondrial membrane complexes from PF <i>T.</i><br><i>brucei</i> .....                   | 60   |
| Figure 2.4: Differential migration of the PF and BF A-IMM.....   | 63   |
| Figure 2.5: Identification of AEP-1 .....  | 65   |
| Figure 2.6: Purification of the A-IMM by anion exchange chromatography .....   | 67   |
| Figure S2.1: Native and 2D electrophoresis of mitochondrial membrane complexes from BF <i>T.</i>   |      |

|   |     |
|---|-----|
| <i>brucei</i> .....   | 79  |
| Figure S2.2: LC-MS/MS identification of AEP-1 .....   | 80  |
| Figure 3.1: Stage specific mRNA expression of $\alpha$ -KD subunits and complex activity in<br>developmental stages ..... | 96  |
| Figure 3.2: Localization and subcellular fractionation of $\alpha$ -KDE2-PTP.....   | 98  |
| Figure 3.3: $\alpha$ -KDE2-PTP associates with the FKC.....   | 101 |
| Figure 3.4: Antipodal localization and stable association of $\alpha$ -KDE2-PTP with the FKC .....                        | 104 |
| Figure 3.5: Effect of $\alpha$ -KDE2 RNAi knockdown in BF <i>T. brucei</i> .....  | 107 |
| Figure 3.6: Effect of $\alpha$ -KDE2 RNAi on minicircle and maxicircle abundance .....                                    | 110 |
| Figure 3.7: Mitochondrial function and morphology are altered in dyskinetoplastic cells .....                             | 113 |
| Figure 4.1: Effect of $\alpha$ -KDE1 mRNA knockdown in BF <i>T. brucei</i> .....  | 139 |
| Figure 4.2: Cellular localization of the FP in $\alpha$ -KDE1 RNAi cells.....   | 141 |

## CHAPTER 1

### GENERAL INTRODUCTION AND LITERATURE REVIEW

In the late 1800s, a group of single-celled protozoa called trypanosomes were first identified. These organisms represent some of the most unique parasitic flagellates in nature (1). Their genus name describes their unique fluid movement and is derived from the Greek words “trypano” which means “screw-like”, and “soma” meaning body. Different species infect a wide variety of hosts and usually have a life cycle that alternates between mammalian hosts and blood feeding invertebrates (2, 3). Their pleomorphic nature allows for appropriate adaptation to these varying environments and permits successful cell replication and transmission between the hosts (4). One species of trypanosomes, *Trypanosoma cruzi*, is native to regions in South America and causes severe pathology in human heart and digestive tissues (Chagas disease) (5). Like *T. cruzi*, the *Leishmania* subspecies spend a portion of their life cycle in the intracellular environment of the host and specifically causes either the severe visceral or cutaneous leishmaniasis (6). African trypanosomes cause debilitating diseases in both domesticated cattle (Nagana) and humans (Human African trypanosomiasis) and is mediated by the bite of the tsetse fly vector (7). The veterinary pathogen *T. b. brucei* is unable to infect humans due to its susceptibility to a subclass of high density lipoproteins in human serum called the trypanosome lytic factor (TLF) that must be trafficked via the endosomal pathway to the trypanosome lysosome in order for parasite killing to occur (8).

Trypanosomes possess a very large and complex DNA nucleoid in their single mitochondrion called the kinetoplast (kDNA) (9). This feature places this genus within Kinetoplastida, one of the most highly divergent eukaryotic Orders. Ribosomal RNA studies revealed that these parasites branched soon after the formation of the initial eukaryote resulting in a plethora of unique biological features (10). This fact along with their relatively simple biology and ease of genetic manipulation make trypanosomes model organisms for the study of essential processes such as vesicular trafficking and mitochondrial protein diversity.

Interestingly, the *T. brucei* kDNA contains incomplete genetic information for proteins involved in cytochrome mediated respiration and ATP synthesis (11-14). Mitochondrial RNA editing is the post-transcriptional correction of these cryptic sequences by the insertion and deletion of uridine residues in these mRNA transcripts and is directed by guide RNAs (gRNAs) (15, 16). The gene for cytochrome oxidase III (COXIII), which is one of the final electron acceptors in the procyclic form respiration pathway, encodes an mRNA that is differentially edited to produce multiple transcripts with open reading frames (17). A novel protein product was identified from a single alternatively edited mRNA and the majority of this polypeptide resembled COXIII outside of a novel N-terminal region (18). Initial studies revealed that this DNA-binding alternatively edited protein-1 (AEP-1) maintained the structural integrity of the kDNA (19). Additionally, AEP-1 assembled into a large mitochondrial inner membrane complex, but the specific biological function of this structure is unknown.

The focus of this research is to further understand the relationship between mitochondrial protein diversity, biogenesis and function by discovering the components of the novel AEP-1 containing complex. In Chapter 1 of this work, I review the basic pathology, cellular makeup, energy metabolism and two approaches to creating protein diversity in *T.*

*brucei*. Additionally, mitochondrial proteins encoded by the kDNA historically evade positive sequencing by conventional mass spectrometry methods. I used a proteomics approach in Chapter 2 to sequence AEP-1 and identified a single N-terminal peptide, along with members of the high molecular weight membrane complex. Discovery of these subunits revealed the presence of two moonlighting (multifunctioning) proteins of the energy generating tricarboxylic acid (TCA) cycle and Chapters 3 and 4 further characterize their functions in the trypanosome. The final conclusions of this research are discussed in Chapter 5.

## AFRICAN TRYPANOSOMIASIS

As reviewed in Brun *et al.* (2010), African trypanosomiasis is a parasitic disease of humans and animals that is caused by the transmission of *T. brucei* through the bite of an infected tsetse fly (20). These diseases are endemic to the rural regions of sub-Saharan Africa where the insect vector largely inhabits and is considered a major problem. Human African Trypanosomiasis or African sleeping sickness is caused by the *T. b. rhodesiense* and *T. b. gambiense* subspecies and is divided into two major phases. Symptoms of the hemolymphatic phase include fever, headaches, joint pain and the swelling of lymph nodes to tremendous sizes. The second phase targets and irreversibly damages the central nervous system where parasites cross the blood brain barrier and cause confusion, reduced coordination, fatigue and interrupted sleep cycles. Historically it was thought that this disease is deadly if left untreated and the administration of medicine is very complex and highly toxic at advanced stages. However, a recent report identified two alternative courses of the *T. b. gambiense* associated disease that are not fatal in the absence of medication (21). Additionally due to increased surveillance and

management, the number of reported sleeping sickness cases in the year 2010 has dropped below 8,000 and represents a major achievement in disease control (22).

Animal trypanosomiasis or Nagana affects both wild (to a lesser extent) and domesticated animals and is caused by *T. b. congolense*, *T. b. vivax* and *T. b. brucei* subspecies (2). The pathology for most domestic vertebrates is severe and the symptoms include intermittent fever, anemia, lethargy, emaciation and even paralysis. Nagana decimates millions of cattle per year and estimated agricultural economic losses are in the billions.

#### THE CELLULAR STRUCTURE OF *TRYPANOSOMA BRUCEI*

*T. brucei* is described as a single, elongated cell that measures over 20  $\mu\text{m}$  long and about 5  $\mu\text{m}$  wide and is stabilized by a complex system of microtubules that serves as a frame for cell shape and positioning of cellular organelles (Figure 1.1). The cytoskeleton is partly formed by a parallel arrangement of subpellicular microtubules that reside beneath the plasma membrane and outline the body of the cell (23). The encased cytoplasm is home for organelles that are important for eukaryotic vitality with some features that are unique to trypanosomes such as a single mitochondrion that runs the length of the cell, a single Golgi apparatus and glycosomes (24). Positioning of the organelles within the cytoplasm is polarized with the majority situated at the posterior portion of the cell. The skeletal structure also coordinates the two genomes of the organism, the nucleus and the kDNA. The nucleus is localized to the center of the cell. The kDNA has a unique physical attachment that transverses the mitochondrial membranes and connects to the basal bodies of the single 9+2 microtubule flagellum that emerges from the endo- and exocytotic organelle that encompasses only a small portion of the cellular plasma membrane,

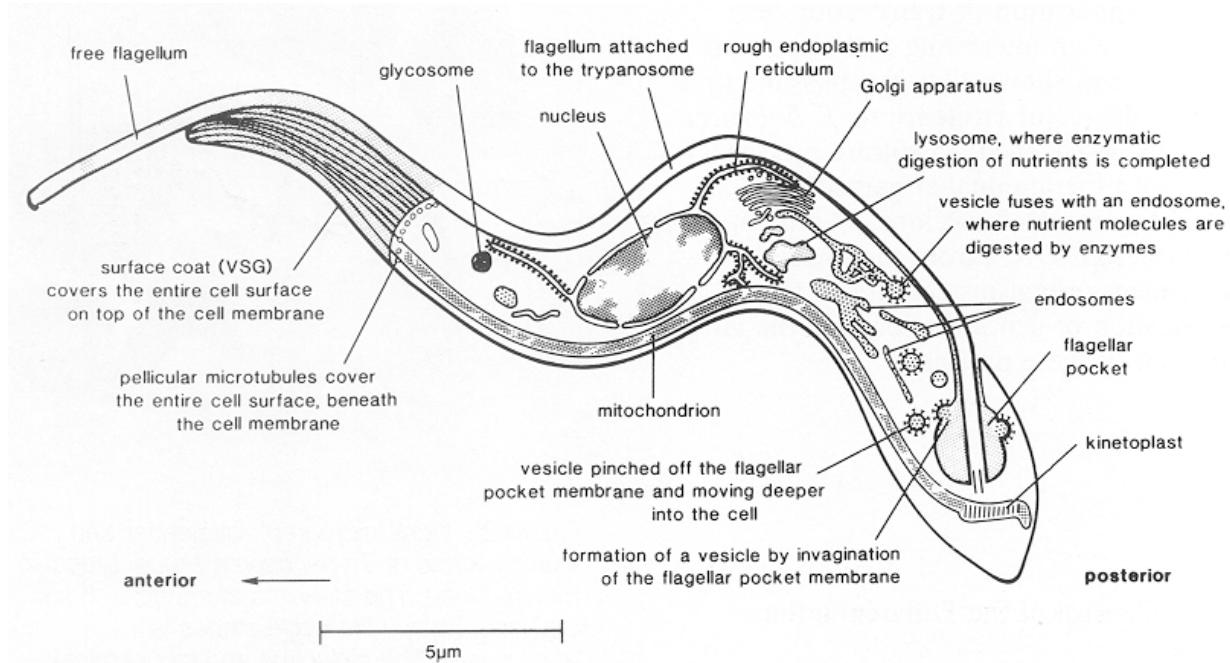


**Figure 1.1.** The ultrastructure of *T. brucei*. Schematic diagram of long slender bloodstream form illustrating major cellular organelles. Image adapted from the International Livestock Research Institute website (25).

the flagellar pocket (26, 27). The flagellum, which is responsible for the bihelical motion that provides the propulsive force for motility, extends alongside the cell body via the flagellum attachment zone (FAZ) and extends past the anterior tip of the trypanosome (28, 29).

### THE EXTRAORDINARY LIFE CYCLE OF *T. BRUCEI*

*T. brucei* is infamous for the various ultrastructural changes it undergoes during its life cycle (Figure 1.2). These adaptations allow for successful parasite proliferation in the insect and mammal environments and also transmission from one host to another. As reviewed in

Vickerman (1985), an infected tsetse fly bite injects mammalian infective metacyclic cells into dermal tissues where an inflammatory sore called a chancre develops (30). This sore allows for entry into the lymphatics and bloodstream, where subsequent morphological changes occur that lead to the proliferative long slender form. Long slender bloodstream forms are highly motile, undergo a high rate of endocytosis and divide by binary fission approximately every six hours. They retain a surface coat composed of the major surface antigen, variant surface glycoprotein (VSG), initially expressed in metacyclics that protects the cells against the host immune defenses. Due to the high glucose content in the blood, bloodstream trypanosomes undergo glycolysis in specialized organelles called the glycosomes, which contain most of the enzymes that catalyze this energy-producing pathway (24). The metabolic requirements of this form result in the secretion of certain glycolytic products and repression of the single mitochondrion that appears tubular and lacks cristae. No change is observed in the morphology or content of the kDNA and it is positioned furthest away from the nucleus at this stage. High parasitemia during the later stages of infection results in differentiation of long slender forms into the non-dividing short stumpy forms (31). To prepare for the amino acid rich environment of the tsetse fly, the mitochondria in this form become more active with an increase in size and the appearance of cristae.

Development in the insect begins when the fly takes an infected blood meal and short stumpy trypanosomes are deposited into the midgut, which morphologically transform into the proliferative procyclic form. Slender procyclics acquire a new protective extracellular coat (procyclin) and the rate of endocytosis begins to decline. The purine-rich and glucose-starved environment causes a suppression of glycosomes and a total activation of the mitochondria. The volume of this organelle and number of discoid cristae increases dramatically and denotes the

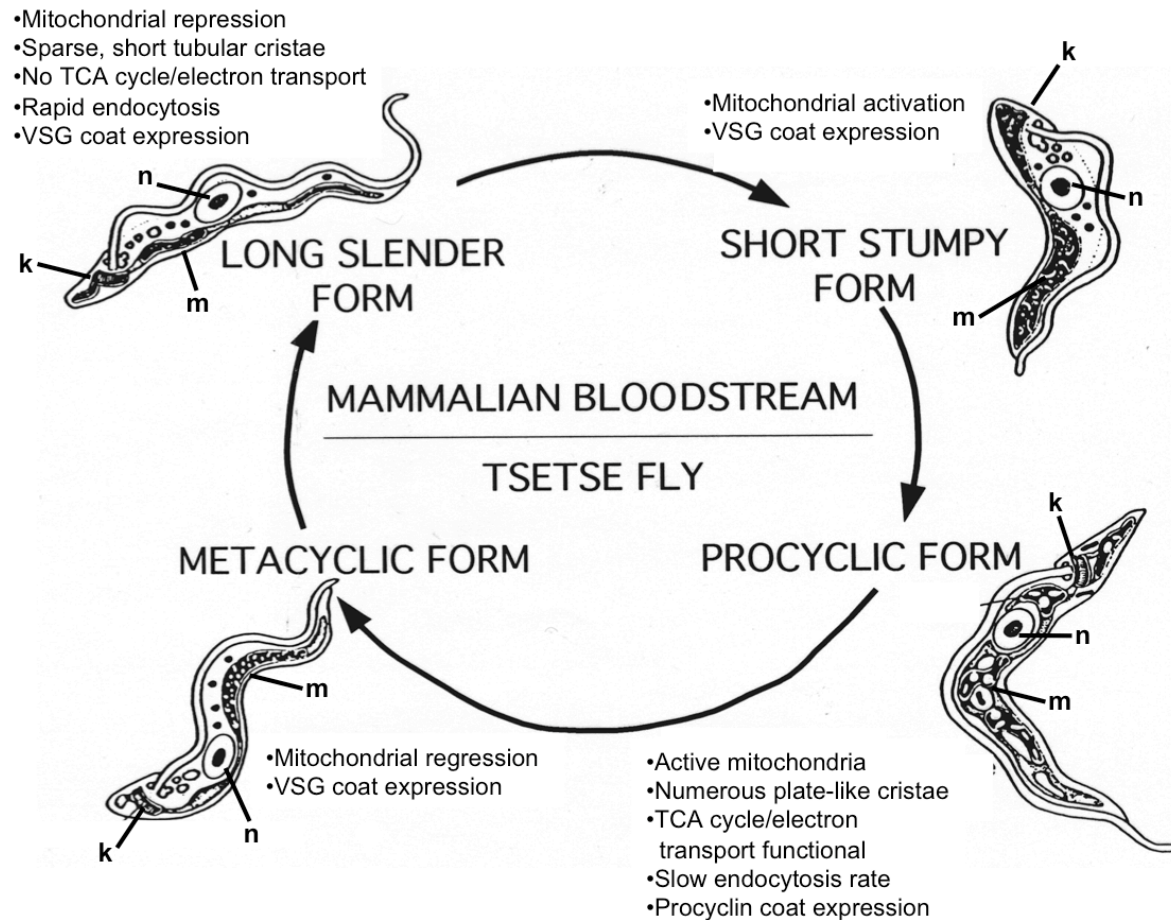


**Figure 1.2.** The digenetic life cycle of *T. brucei* alternates between mammalian and insect host. This schematic shows specific adaptations of the major proliferative and infective forms during the cycle. Abbreviations: k – kDNA; n – nucleus; m – mitochondrion (Adapted from Vickerman, British Medical Bulletin, 1985)

activation of important mitochondrial pathways such as the TCA cycle and cytochrome-mediated respiration.

Additionally, this stage denotes a reduced distance between the nucleus and kDNA. Almost one week into the infection, procyclics begin to migrate out of the midgut toward the salivary glands. Mitochondrial repression begins as the cells differentiate into epimastigotes that are physically attached to the glands' microvilli by the flagellum (32). Epimastigotes can further transform into the non-dividing metacyclics and the cycle begins again once the fly bites a vertebrate host.

### THE *T. BRUCEI* CELL CYCLE

The proliferative stages in bloodstream and procyclic form *T. brucei* are managed by an intricate set of events that includes faithful duplication of cellular structures and mitotic division to form two complete cells (Figure 1.3). This spatial order of events is defined by four distinct periods that fall under the categories of either interphase (growth and synthesis) or mitosis (cytokinesis). Non-synchronous timing for nuclear and kDNA duplication during this cycle gives both genomes a discrete synthesis (S) phase and is a phenomenon unique to *T. brucei* (33). As described in Hammarton *et al.* (2006), G<sub>1</sub> (the initial gap phase) describes a cell that has single copy organelles and undergoes increased growth and production of factors needed for DNA replication (34). These cells contain one kDNA, nucleus and flagellum and are designated 1K1N1F. Next, S phase occurs and involves replication of the nuclear and mitochondrial genomes. The kDNA enters S phase prior to the nucleus and DNA synthesis for both structures require multiple factors working in concert. Also, the immature pro-basal body begins to elongate along with the nucleation of a new flagellum (1K1N2F) at an early interval during this period. This daughter flagellum continues to extend throughout the remainder of the cycle.

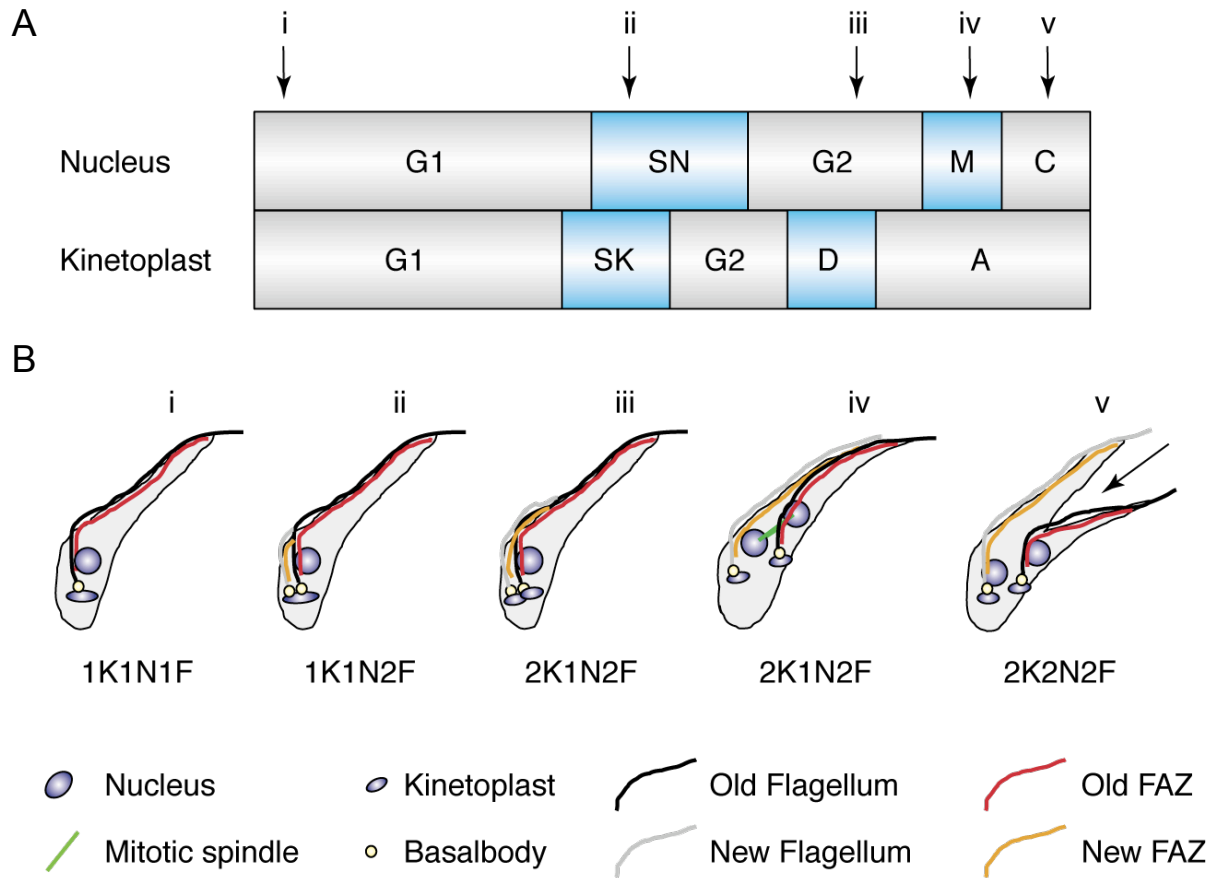


**Figure 1.3.** Diagram of the *T. brucei* duplication cycle. A) Nuclear and kDNA replication cycles. B) Schematic of the major morphological events during the cell cycle. Abbreviations: G1 – first growth phase; SN – nuclear synthesis phase; SK – kDNA synthesis phase; G2 – second growth phase; D – kDNA segregation; A – apportioning phase; M – nuclear mitosis; C – cytokinesis; 1K1N1F – a single kinetoplast, nucleus and flagellum; 1K1N2F – a single kDNA, nucleus and two flagella; 2K1N2F – two kinetoplast, one nucleus and two flagella; 2K2N2F – two kinetoplasts, nuclei and flagella; FAZ – flagellum attachment zone (Adapted from McKean, *Current Opinion in Microbiology*, 2003).

Duplicated basal body pairs and double sized kDNA are separated simultaneously during the second growth phase ( $G_2$ ) and this coordinated segregation is tethered by sets of protein filaments, leading to 2K1N2F cells. Nuclear division occurs during the mitotic (M) phase (2K2N2F) followed by the final step of the cell cycle, cytokinesis, which happens along a cleavage furrow that runs longitudinally along the organism.

Limited data is available concerning duplication of other organelles during the cell cycle. For instance, it is known that Golgi replication and division closely follows that of the basal bodies, but many mechanisms of this process are poorly defined (35). Contrastingly, the single large mitochondrion is mainly duplicated during M phase and is mediated by dynamin-like proteins (36)

## THE FLAGELLAR POCKET

The subpellicular array of microtubules forms an impenetrable cage surrounding the body of the trypanosome and these interlinked skeletal structures must allow for the required cellular adaptations and vesicular trafficking. The latter is mediated by a specialized invagination of the plasma membrane where the single flagellum of the basal bodies exits the cell through a discontinuity in the array (Figure 1.1). This region is termed the flagellar pocket and is defined by two cytoskeletal-associated boundaries, one being proximal to the basal bodies and the other being the collar, which delineates the neck of this structure (27). The beginning of the pocket can also be denoted by the start of the paraflagellar rod, a proposed biomechanical spring of the flagellum and also exits this region parallel to the flagellum (37, 38). Additionally the lumen of

this pocket is carbohydrate-rich and contains GPI-anchored glycoproteins that can be bound with high affinity by lectins such as concavalin A, which is a marker for endocytotic structures (39).

The trypanosome endomembrane system is polarized and well placed to make vesicle trafficking a highly efficient process. This is evident due to the abnormally high rate of endocytosis seen in bloodstream form cells and the small surface area of the flagellar pocket (40, 41). Procyclic cells share some similarities, but they endocytose at a much slower rate and differences in this process have been observed. For instance, both life forms are dependent on the role of clathrin in vesicle formation during endocytosis. Depletion of this protein by RNA interference (RNAi) halted endocytosis, growth and caused a rapid swelling of the procyclic and bloodstream flagellar pockets, referred to as the “Big Eye” phenotype (39). On the other hand, the eukaryotic vesicle scission protein dynamin is not required in bloodstream cells, but reduction of this protein in procyclic cells also causes flagellar pocket enlargement (36).

#### THE NUCLEUS OF *T. BRUCEI*

Located at the midpoint of the cell is the *T. brucei* nucleus, which is similar to the nuclear genome of other protists. The chromatin of trypanosomes is less condensed and is sensitive to nuclease digestion despite the nucleosome organization of the DNA (42). Additionally, during mitosis, the nuclear membrane does not break down nor does the DNA condense to a point where individual chromosomes are observed. Spindle formation, chromosome segregation and cytokinesis are mediated by a highly divergent chromosomal passenger complex and kinesins, which have varying localizations throughout the cell cycle (43).

The diploid nucleus is composed of 11 megabase chromosome pairs (1-6 megabase pairs), 1-5 intermediate chromosomes (200-900 kilobase pairs) and 100 minichromosomes (50-100 kilobase pairs) (44-47). Genes on the larger chromosomes are arranged in large polycistronic transcription units and are transcribed by RNA polymerase II (48). Non-housekeeping genes such as the stage-specific surface coat sequences are transcribed by RNA polymerase I. The majority of these sequences do not contain introns and the resulting mature mRNAs must be made stable by the post-transcriptional process of 5' trans-splicing, which is mediated by the spliceosome (49). Varying mRNAs that are stage-specific are also detected due to the presence of alternative splice sites and subsequently encode for proteins that could have novel functions and localizations in the cell (50). Once the 3' end is modified by the addition of a poly (A) tail, the information contained in the mRNAs is ready to be translated by cytosolic ribosomes.

The nuclear genome of *T. brucei* has been sequenced ([www.genedb.org](http://www.genedb.org)) and is predicted to encode over 9,000 proteins, including a large portion of polypeptides that are required by the membranous organelles. For example, in 2009 the Stuart group performed a shotgun proteomic analysis on the total cell and purified mitochondrial fractions of the procyclic form cells (51). This analysis identified 2,897 proteins including 1,333 with validated or putative functions. Additionally, the contribution of the nucleus to the mitochondrial proteome is further substantiated by the identification of 1,008 mitochondrial proteins. kDNA encoded proteins were not identified in this analysis and these sequences have historically been elusive using conventional mass spectrometry methods. The Maslov group (2000) positively identified the mitochondrial encoded cytochrome b and cytochrome c oxidase subunit I, proteins of the cytochrome c reductase and cytochrome c oxidase complexes of the electron transport chain

respectively, by an alternative sequencing method termed Edman degradation (52, 53). More recently, tandem mass spectrometry identified a unique peptide for both cytochrome c oxidase subunits II and III (54).

## GLYCOLYSIS AND GLYCOSOMES

Long slender bloodstream *T. brucei* use the abundant glucose in the surrounding environment to meet their energy needs by a process called glycolysis, which systematically degrades glucose into pyruvate. This is the only process that provides a carbon source for ATP production since the mitochondrion is limited at this stage of the life cycle (30). The initial seven enzymatic steps of this pathway (catalyzed by hexokinase, phosphoglucose isomerase, phosphofructokinase, fructose bisphosphate aldolase, triosephosphate isomerase, glyceraldehyde phosphate dehydrogenase and phosphoglycerate kinase) are held in specialized single membrane peroxisome-like organelles called glycosomes, which convert glucose to 3-phosphoglycerate under aerobic conditions (24). The remaining steps (catalyzed by phosphoglycerate mutase, enolase and pyruvate kinase) further metabolize 3-phosphoglycerate to pyruvate and occur in the cytosol. The final reaction catalyzed by pyruvate kinase results in the synthesis of ATP that is used by the cell and pyruvate is subsequently secreted.

The compartmentalization of glycolysis by glycosomes is a very important regulator of energy metabolism. Encapsulation of certain enzymes that aren't regulated prevents the wasteful consumption of ATP and makes glycolysis around 50 times more efficient than in mammalian cells (55, 56). Also, 2-fold ATP is produced because of a secondary glycerol-3-phosphate shuttle pathway that also leads to the production of the waste product pyruvate. Maintaining glycosome

number, homeostatic levels, formation, enzyme import from the cytosol and remodeling during the life cycle is critical for cell survival.

### THE *T. BRUCEI* MITOCHONDRION

In the 1890s, mitochondria were first discovered and described as a simple organism that executed essential functions within a cell (57). Later, the endosymbiotic theory further characterized this body and postulated that the eukaryotic mitochondrion was a free-living  $\alpha$ -Proteobacteria endosymbiont that implanted itself in a cell that contained its own genome (58). Even though they differ in shape and structure, mitochondria are all encapsulated by a double-membrane, contain a genome and have redox activity.

The adaptive trypanosome mitochondrion has many unique morphological, structural and metabolic features that are essential for cell vitality. *T. brucei* is defined by one of the extraordinary features occurring in the mitochondrion, the kDNA. This electron dense body, which is proximal to the basal bodies, is composed of a concatenated network of circular DNA molecules (maxi- and minicircles) that contain the coding information for RNAs and proteins involved in the multiple processes in the organelle (59). Additionally, the kDNA is maintained by a diverse set of proteins that sequester this structure to the posterior portion of the mitochondrion, replicate the constituent DNA molecules and segregate the duplicated genomes post replication (26, 60).

Varying levels of mitochondrial activity are reached during the biphasic life cycle of *T. brucei* and this is apparent by observing organelle morphology during the major proliferative stages (30). The large branching mitochondria of the procyclic form contains many nuclear and

mitochondrial encoded proteins in the matrix and membranes of the organelle that are involved in fatty acid synthesis, energy metabolism, iron sulfur cluster assembly and  $\text{Ca}^{2+}$  signaling.

Alternatively, the tubular mitochondria of the bloodstream form lack the complexity of the procyclic organelle and many of these proteins are under developmental regulation. Even with these drastic differences, processes such as protein/tRNA import, kDNA maintenance, gene expression and generation of a membrane potential are required in both (18, 61, 62).

## THE KDNA

The circular configuration of bacterial and mitochondrial DNA were two important discoveries made in the 1960s and 70s (63-65). Both prokaryotic and eukaryotic types contain the information for protein-coding genes, rRNAs and tRNAs (in most cases). In contrast to the nucleus, both of these genomes lack histones and are packaged into structures called nucleoids by DNA interacting proteins (66, 67). Mitochondrial nucleoid proteins, which are similar to the proteins contained in the nucleoids of their bacterial ancestors, are diverse, often basic and involved in genome compaction, replication and gene expression. In certain cases, mitochondrial DNA has been shown to associate with cell cytoskeletal elements, but many of these interactions have yet to be defined (26, 68).

Trypanosomes have one of the largest and most complex mitochondrial DNA bodies in nature, having a diameter of 650 nm and a 100 nm breadth. Maxi- and minicircles are the constituent supercoiled DNA molecules and they differ in size and copy number. As reviewed in Feagin (2000) and Lukes *et al.* (2005), the homogeneous population of maxicircles in *T. brucei* is approximately 20 kb in length and there are 50 sequences per network (69, 70). The smaller

heterogeneous minicircles are only 1 kb in length and represent about 90% (5000 circles) of the total mass of the genome. The completely sequenced maxicircles contain information for 18 to 20 mRNAs including three subunits of the cytochrome c oxidase complex (COX I-III), cytochrome b of the cytochrome c reductase complex, the A6 subunit of the adenosine triphosphatase/triphosphate synthase, six subunits of the NADH dehydrogenase (ND 1, 4, 5, 7, 8 and 9) and also the 9S and 12S ribosomal RNAs. Interestingly, no transfer RNAs (tRNAs) are encoded by the kDNA and must be imported from the cytosol for mitochondrial translation.

An abnormality of maxicircles is that some of the sequences are cryptogenic, meaning the genes contain incomplete coding information for proteins involved in cytochrome-mediated respiration (11-14). The incomplete mRNAs from 12 maxicircle genes were cloned and sequenced and this analysis revealed additional or missing uridines in the transcripts (71, 72). An extreme example is the COX III subunit since the full-length mRNA transcript is detectable but no corresponding maxicircle or nuclear sequence has been identified. However, a contrasting sequence that is highly divergent from other species of trypanosome, because of the number and placement of thymidines, was identified upstream of the cytochrome b gene (17). The transcript from this sequence is missing over 50% of the coding information and must undergo the unique process of mitochondrial RNA editing to become functional (73). This post-transcriptional process remodels these pre-mRNAs by the enzymatic insertion and deletion of uridine residues and is templated by guide RNA (gRNA) sequences that are transcribed from minicircles. It creates open reading frames by correcting stop codons, frame shifts and the formation of initiation codons.

kDNA replication is another complex process undertaken by the DNA and a diverse set of proteins. Proteins that are housed in specialized domains surrounding the genome catalyze

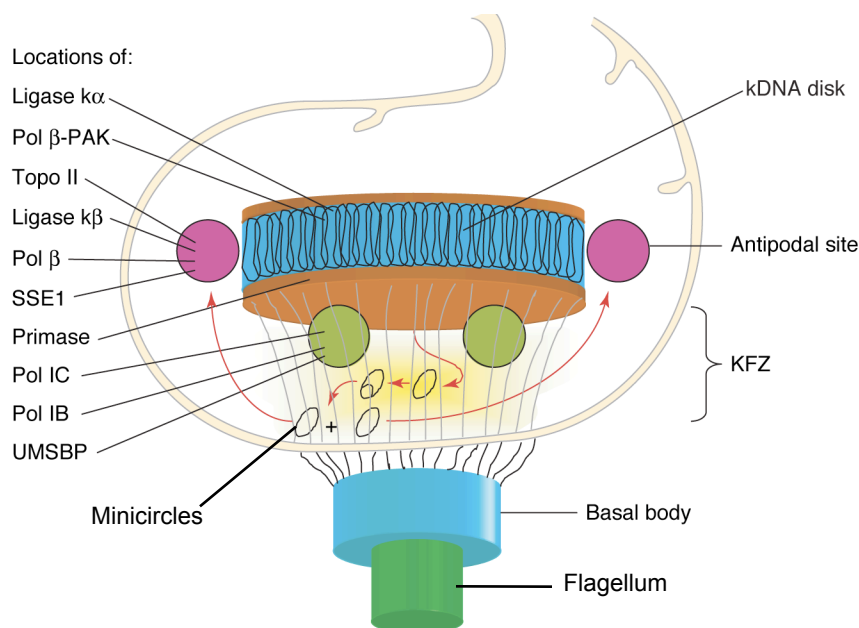


**Figure 1.4.** Schematic of kDNA replication. Proteins surrounding the disk catalyze the release of covalently closed minicircles from the network into the KFZ, in which they initiate replication as theta structures. The progeny free minicircles then migrate to the antipodal sites at which the next stages of replication occur (primer removal, gap filling and the sealing of most of the nicks). The minicircles are then linked to the network periphery and the remaining sequence gaps are repaired when replication is complete. Abbreviations: Pol  $\beta$ -PAK – polymerase  $\beta$ -PAK (N-terminal prolines, alanines and lysines domain); Topo II – topoisomerase II; Pol  $\beta$  - polymerase  $\beta$ ; SSE1 – structure-specific endonuclease-1; Pol1B – polymerase 1B; Pol1C – polymerase 1C; UMSBP – universal minicircle-sequence-binding protein; KFZ – kinetoflagellar zone (Adapted from Liu *et al.*, Trends in Parasitology, 2005).

maxi- and minicircle replication. Once replication is complete, the tripartite attachment complex mediates separation of the daughter kinetoplasts (26). As reviewed in Liu *et al.* (2005), *T. brucei*

kDNA minicircle replication initiates with release of the DNA from the network and depositing of these individual sequences into the kinetoflagellar zone (KFZ) by an undiscovered mechanism (Figure 1.4) (60). The KFZ is the space between a single face of the kDNA and the mitochondrial membranes and is the site where sequence duplication commences. The universal minicircle sequence binding protein (UMSBP) is located in the KFZ and binds to the replication origin of the free minicircles, which activates replication (74). Replication is semi conservative and is mediated by proteins recruited to the origin, which includes a primase and polymerases (IB and IC) (75, 76). RNA primers are generated and bound, a replication fork is created and DNA strand synthesis proceeds unidirectionally through theta-structure intermediates. Progeny minicircles are separated in the KFZ and migrate toward the antipodal sites, which are two structural assemblies that flank the kDNA. In these regions, primers are removed from minicircles, gaps are filled between Okazaki fragments and minicircles are reattached to the network by multiple proteins (77-82). Bromodeoxyuridine (BrdU) is a synthetic thymidine analogue used to observe cell proliferation and can also be employed as a marker for newly replicated minicircle incorporation at the antipodal sites (33). Maxicircle replication is much less defined. Unlike minicircles, maxicircles do not leave the network to duplicate (83). In a similar fashion, maxicircles replicate unidirectionally from a single origin and the progeny circles contain gaps.

### THE TRIPARTITE ATTACHMENT COMPLEX

The *T. brucei* kDNA is positioned and maintained by a structural trichotomy that is located in the posterior region of the cell. Ogbadoyi *et al.* (2003) describes the tripartite

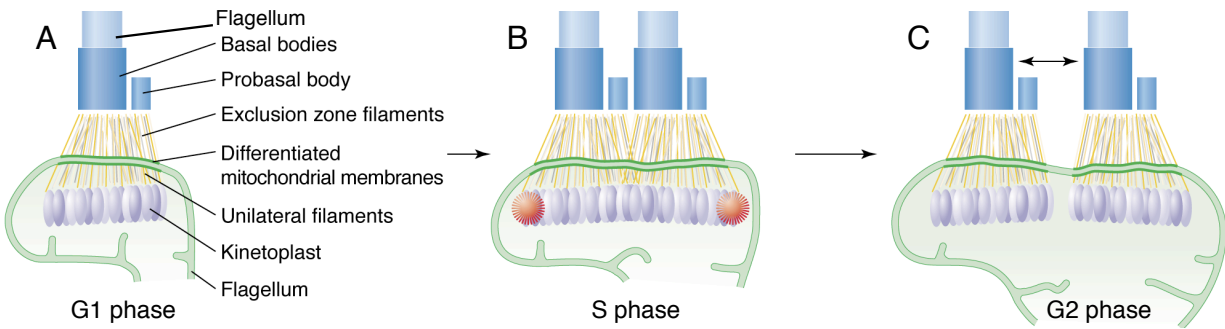


**Figure 1.5.** Schematic diagram of TAC structure and duplication in trypanosomes. A) G1 phase cell contains single copy organelles and structures. B) S phase cell contains two pairs of basal bodies, nascent TACs and a bilobed kDNA with the appearance of antipodal sites. C) G2 phase cell contains double copy TACs and organelles (Adapted from Gull, *Current Opinion in Microbiology*, 2003).

attachment complex (TAC) as a specialized portion of the cytoskeleton that transverses the mitochondrial membrane and maintains a physical association between the kDNA and the basal bodies of the single flagellum (26). This complex is evident through transmission electron microscopy and the tight association of the kDNA to the flagellum after flagellum kinetoplast complex (FKC) extraction using nonionic detergents and  $\text{Ca}^{2+}$ . Only three proteins of the TAC have been identified, all through indirect methods due to its structural makeup.

The TAC is composed of proteinaceous filaments that pass through a specialized membrane region at the posterior portion of the mitochondrion (Figure 1.5) (84). Exclusion zone filaments are external to the mitochondrion and this region was described by Vickerman as a zone that excluded cytosolic ribosomes. The filaments connect the pro- and mature basal bodies to the differentiated mitochondrial membranes. Differentiated refers to a few unique features of

these membranes that separate them from a basic lipid bilayer. One of the most striking features is that this cristae-free zone resists nonionic detergent extraction and is reminiscent of a lipid raft. Additionally, the unilateral filaments attach the kDNA to the differentiated membranes and maintain the position and integrity of the genome in the mitochondrial lumen. Since these unilateral filaments are composed of two zones distinguished by negative staining that transverse the KFZ, they are also thought to be involved in kDNA replication (85).

The first protein identified in the TAC, p166, confirms the role of this structure in kDNA segregation (86). This large nuclear encoded protein was identified through an RNA interference (RNAi) library screen and contains an N-terminal mitochondrial import signal and a small transmembrane domain at its carboxyl C-terminus. The transmembrane region is not necessary for stable incorporation and full-length p166 remains associated with the unilateral filaments after FKC extraction. Knockdown of p166 mRNA by RNAi altered kDNA structure due to the asymmetric segregation of the genome. This resulted in varying kDNA sizes, including cells with no mitochondrial genome (dyskinetoplasmic cells), but did not affect replication of the constituent DNA circles (86).

#### ENERGY METABOLISM IN THE *T. BRUCEI* MITOCHONDRION

In the procyclic mitochondrion, the degradation of carbohydrates and amino acids is mediated by the nuclear encoded proteins of the TCA cycle, which produce substrates that can be further processed by the respiratory chain. The TCA cycle is composed of eight enzymes (citrate synthase, aconitase, isocitrate dehydrogenase,  $\alpha$ -ketoglutarate dehydrogenase, succinate

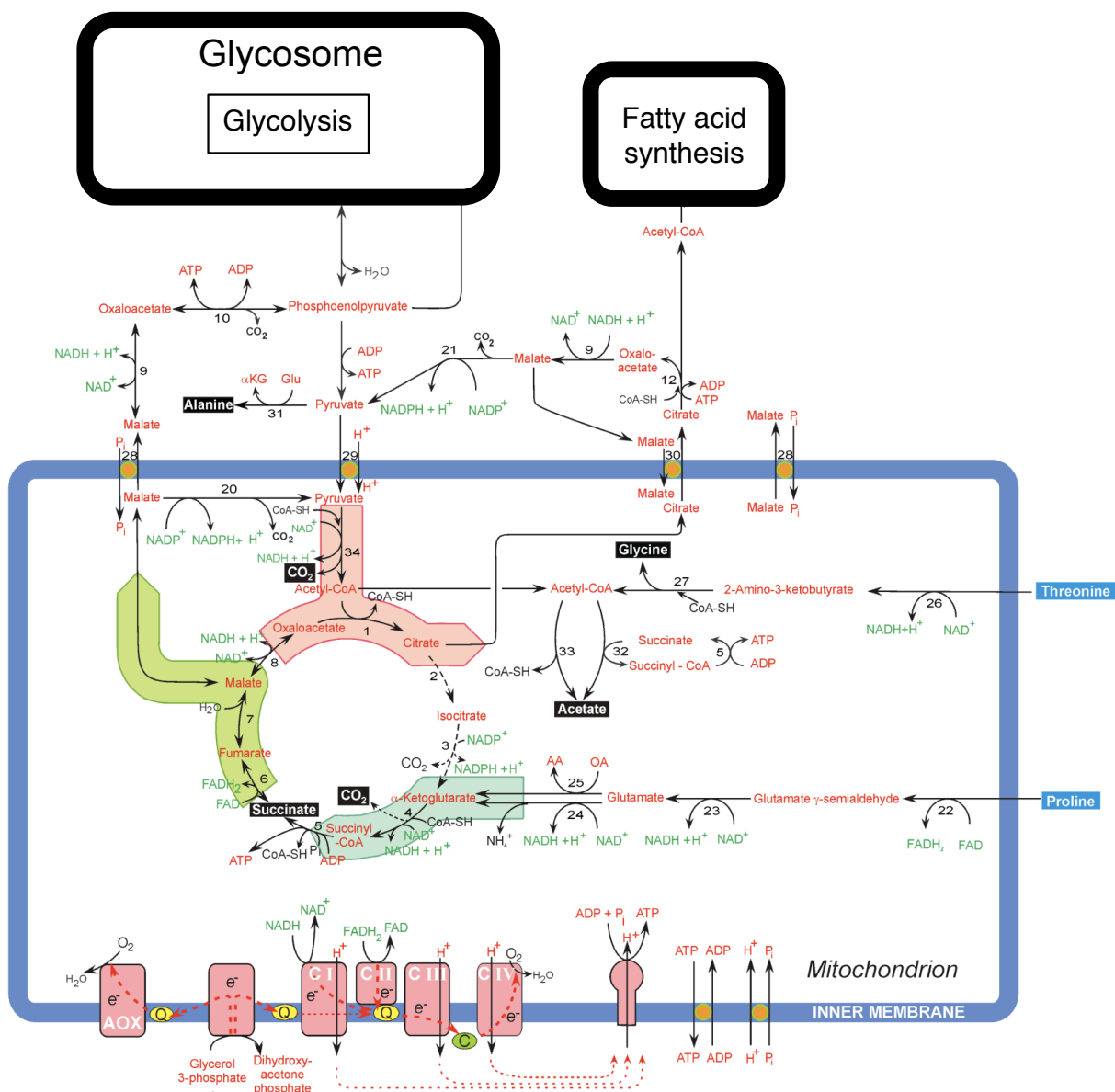


**Figure 1.6.** Schematic diagram of pathways in procyclic form *T. brucei* involved in amino acid and carbohydrate metabolism, followed by flux of reducing equivalents down the electron transport chain and the subsequent production of ATP. The pink, light green and pea green arrows represent the degradation of pyruvate and oxaloacetate to citrate, proline and glutamate to succinate and fumarate to malate, respectively. Abbreviations: AOX – alternative oxidase; C I – NADH dehydrogenase; C II – succinate dehydrogenase; C III – cytochrome bc1; C IV

cytochrome c oxidase (Adapted from van Weelden *et al.*, Journal of Biological Chemistry, 2005).

thiokinase, succinate dehydrogenase, fumarate hydratase, malate dehydrogenase) that are known to catalyze the stepwise conversion of acetyl-CoA to oxaloacetate. However, only six out of the eight enzymes are necessary for energy metabolism and the low activities of aconitase and isocitrate dehydrogenase have no discernable metabolic function in procyclics (87, 88). Aconitase deletions did not perturb the end products and suggest that the TCA cycle is not complete and may have other functions (89). Alternative functions of the cycle include proline metabolism, fatty acid synthesis, production of substrates used for gluconeogenesis and other sources of electrons for the electron transport chain (Figure 1.6) (87, 90).

The *T. brucei* branched electron transport chain is the major pathway for the reoxidation of the cofactor NADH that is produced in large amounts by pyruvate and amino acid metabolism (87). This chain is composed of complexes containing nuclear and mitochondrial encoded proteins and includes two NADH dehydrogenases (complex I and a rotenone insensitive complex), a FADH oxidizing succinate dehydrogenase (complex II), a ubiquinol oxidizing cytochrome bc1 (complex III) and the final electron acceptor cytochrome c oxidase (complex IV). The procyclic chain also contains an electron accepting glycerol-3-phosphate dehydrogenase and an alternative oxidase (TAO), but the latter does not aid in forming a proton gradient like complex IV (91). The intermembrane space protons move back into the matrix by an ATP synthase (complex V), which produces ATP via the proton motive force (Figure 1.6).

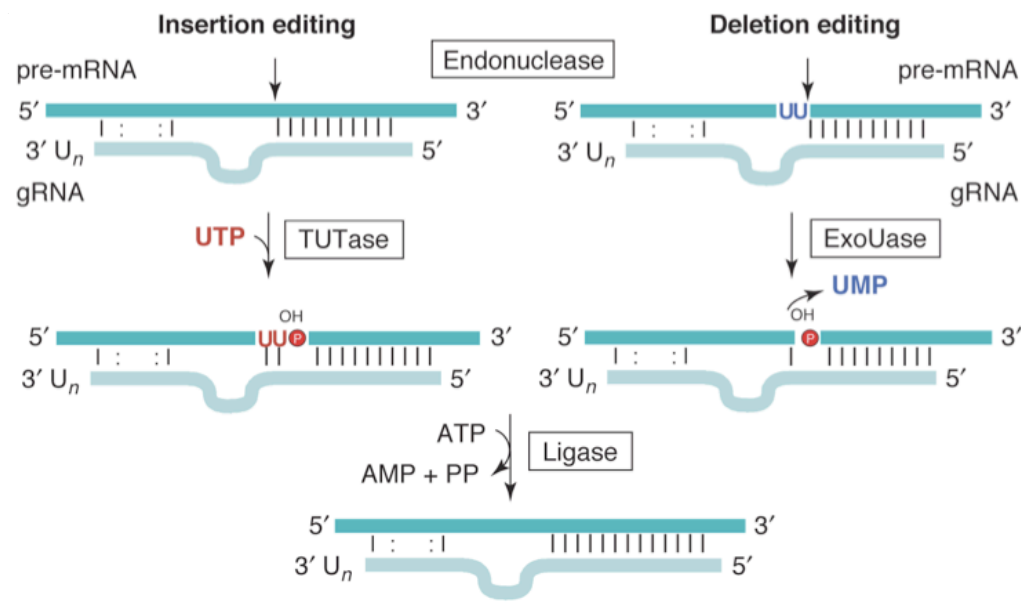


**Figure 1.7.** Simplified mechanism for uridine insertion and deletion editing in trypanosomes. Guide RNAs bind to their pre-mRNAs via the anchor region on the 5' end of the gRNA transcript and is facilitated mainly through Watson Crick (solid lines) and G:U (:) base pairing. The 3' poly U tail of the guide stabilizes the gRNA: mRNA duplex. The first mismatch between gRNA and pre-mRNA signals for the endonuclease to cleave the pre-mRNA, generating a 3' and 5' mRNA cleavage product. Insertional editing adds uridines to the 3' hydroxyl of the cleavage product by a terminal uridylyl transferase (TUTase). In deletion editing, an exonuclease removes uridines from the 3' end of the cleavage product. The 5' and 3' cleavage sequences are joined by a ligase using ATP hydrolysis. (Adapted from Stuart *et al.*, *Trends in Biochemical Sciences*, 2005).

## MITOCHONDRIAL RNA EDITING

Trypanosome mitochondrial mRNA editing is defined as an enzyme cascade consisting of transcript cleavage by an endonuclease, uridine insertion or deletion and RNA ligation and is catalyzed by large complexes called editosomes, which sediment at 20S on a glycerol gradient and are composed of more than 20 proteins (92). This process is initiated when a complementary gRNA binds an mRNA and forms a short anchor duplex between the 5' region of the guide and 3' end of the transcript editing site (Figure 1.7) (73, 93). The editosome recognizes the remaining mismatched sequence adjacent to the duplex and cleaves the RNA using a site-specific endoribonuclease, which subsequently generates a 5' phosphate and a 3' hydroxyl. This creates an opportunity for uridine insertion or deletion by a terminal U transferase or exonuclease, respectively. Editing is complete when RNA ligase rejoins the ends of the modified mRNA.

## ALTERNATIVE RNA EDITING

Trypanosome mitochondrial mRNA editing was first thought of as a transcript repair process that functioned by creating initiation codons, open reading frames or by the correction of frame shift mutations. A trend observed among mammals is the use of this process to create protein diversity, which can generate multiple RNAs and protein sequences from a single gene. For instance, adenosine to inosine editing of neuronal receptors and ion channels in the mammalian

brain results in different protein isoforms with dramatic changes in function (94). Strangely, some of these alterations have been linked to neurological disorders (95).

Trypanosome mitochondrial mRNA editing is critical for the production of multiple proteins including the conventional oxidative phosphorylation proteins. Surprisingly, sequencing of three extensively edited transcripts (COXIII, A6 and ND7) revealed a collection of differentially edited mRNAs stemming from single genes in bloodstream form *T. brucei* (96). Initially, these incompletely edited mRNAs were thought of as an anomaly of this process and were unable to be functional. Our lab (Ochsenreiter and Hajduk 2006) diverged from this assumption by identifying a stable partially edited transcript of the COXIII in bloodstream form *T. brucei* that contained a mix of the 3' pre- and 5' fully edited mRNA (18). This truncated transcript (636 nucleotides) contained an alternative start site and the pre- and edited portions were brought into frame by the insertion of two uridines by a single gRNA (Figure 1.8). Translation of this mRNA creates a protein with a hydrophobic C-terminus that is identical to COXIII and a highly charged N-terminus that is novel in sequence, called alternatively edited protein-1 (AEP-1). Another mRNA, COXIII-K12 (similar to AEP-1 mRNA) and three other variations of this transcript were identified using a bloodstream mitochondrial cDNA library (96). AEP-1, along with transcription and editing of mitochondrial respiratory genes in the



acceptor (87). Analysis of three extensively edited mRNAs from subunits ND7, 8, and 9 revealed eleven alternative sequences and three corresponding gRNAs (96). ND7-G10 mRNA is formed from a frame shift caused by a single uridine insertion at nucleotide 1183 and extends the sequence by twenty-one bases. Another alternative transcript, ND7-N12, is differentially edited at four different sites on the mRNA and results in four amino acid substitutions. Both mRNAs use the conventional AUG start codon. ND8-F04, an alternative mRNA from the ND8 gene, contained two open reading frames that initiated from alternative start codons. The shorter of the two mRNAs encodes a predicted sequence that has high homology to a hypothetical protein of *Plasmodium chabaudi*. Additionally, analysis of ND9 transcripts revealed a sequence (ND9-F12) that contained an alternate start and fusion of pre- and edited mRNAs.

Lastly, the *bona fide* A6, an important protein of the ATPase/ATP synthase in both proliferative stages, contains an alternative mRNA that is edited uniquely in three different regions (87, 96). The A6-D08 open reading frame is initiated at an alternative start codon and these three unique regions must be aligned in two areas, one between the pre-edited and edited sequences and in alternatively edited region II. Additional studies are needed to confirm the expression and function of these proteins in *T. brucei*.

#### ALTERNATIVELY EDITED PROTEIN-1

AEP-1 is a novel protein that is encoded by an alternative mRNA that is a fusion of pre-transcript and fully edited COXIII sequences (18). Since the C-terminus is identical to a portion of the *bona fide* COXIII, our lab created antibodies to the hydrophilic N-terminus to verify translation of a stable protein. Initial localization of the protein by immunofluorescence

microscopy revealed the association of AEP-1 with the mitochondria in bloodstream form *T. brucei*. The predicted molecular weight of AEP-1 is 27 kDa, but it migrates much slower (49 kDa) by Western blot analysis, probably due to the hydrophobic nature of the protein. Fractions from total cell, cytosol, total purified mitochondria, mitochondrial matrix and mitochondrial membrane were also analyzed to further localize AEP-1. The transmembrane domains of the protein suggest a membrane association in the mitochondrion and this is confirmed by this fractionation analysis. Many of the mitochondrial-encoded proteins reside in large membrane complexes that can be isolated by treating mitochondria with detergents. Blue native-PAGE (BN-PAGE) analysis of the mitochondrial membrane fraction by nonionic detergents and Western blot analysis revealed the association of AEP-1 with a large complex that migrates at approximately 550 kDa.

By immunofluorescence microscopy, AEP-1 has a polarized distribution in bloodstream mitochondrion where 65% localized to the kDNA region and the remainder was distributed throughout the organelle (19). Since the area surrounding the kDNA is highly specialized, our lab isolated FKCs and performed additional immunofluorescence localization studies to confirm the association of AEP-1 with this structure. AEP-1 stably associated with this structure where it apposed the kDNA and both signals comprised an average distance of  $320 \pm 20$  nm, which is more proximal to the DNA than the basal bodies ( $810 \pm 20$  nm). A homology model of AEP-1 was created against the crystal structure of the *bona fide* bovine COXIII and this data along with other prediction software confirmed the five transmembrane helices of this sequence and gave AEP-1 directionality (Figure 1.9). The novel N-terminus of AEP-1 points toward the

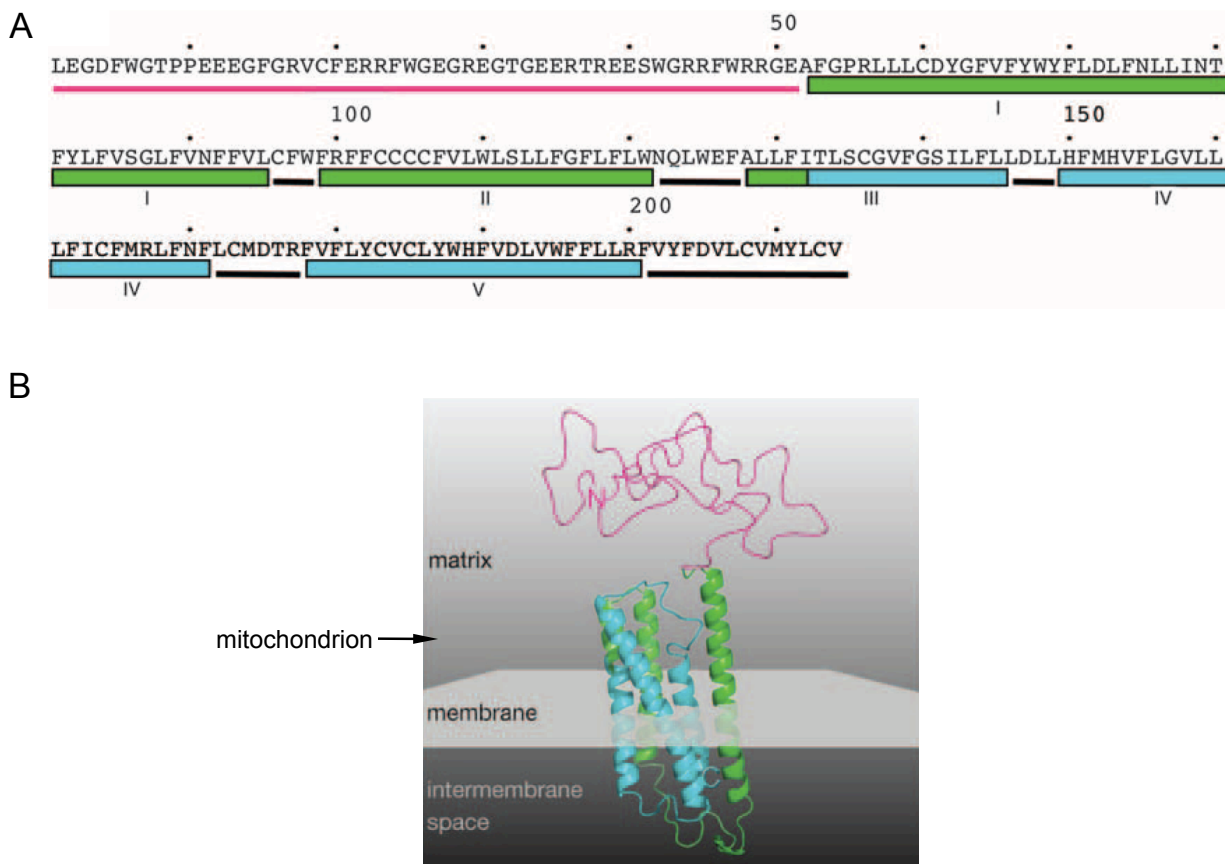


**Figure 1.9.** AEP-1 orientation in the mitochondrial inner membrane. A) AEP-1 amino acid sequence and color-coded secondary structures. Magenta amino acids denote the hydrophilic N-terminus, followed by five transmembrane domains that could be mapped against the bovine COXIII (cyan) and two that were predicted using an additional topology program (green). B) Homology model of AEP-1 revealing that the N-terminus is pointed toward the mitochondrial matrix (Adapted from Ochsenreiter *et al.*, Molecular and Cellular Biology, 2008).

mitochondrial matrix and its distance from the kDNA suggest the protein resides in the unilateral filaments of the TAC (19, 26). Recombinant expression of the hydrophilic N-terminal

portion of AEP-1 (amino acids 1-59) and electrophoretic mobility shift assays revealed its ability to nonspecifically bind DNA. These data suggest that AEP-1 is a mitochondrial membrane protein that assembles into the TAC, contains an N-terminus that extends through the unilateral filaments and possibly interacts with the kDNA in some way. To test for this interaction, our lab created a fusion protein of truncated AEP-1 (amino acids 1-59) that was linked C-terminally to green fluorescent protein (GFP), along with an N-terminal mitochondrial localization signal (mt-AEP-1<sup>(1-59)</sup>-GFP) that was expressed from the nucleus and imported into the mitochondria (19). More commonly known as a dominant negative mutation, this ectopic expression of truncated AEP-1 competed for the endogenous protein and this was advantageous because of the inability to manipulate mitochondrial genes by more conventional methods. The mt-AEP-1<sup>(1-59)</sup>-GFP expressing *T. brucei* showed a growth defect with an increase in G<sub>1</sub> phase cells. 13% of the population lacked kDNA along with an increase in cells with two kinetoplasts. A visible association of mt-AEP-1<sup>(1-59)</sup>-GFP with the kDNA is observed and this truncated protein remains stably attached after FKC purification. In 2k cells, mt-AEP-1<sup>(1-59)</sup>GFP only associated with a single genome that had a more diffuse fluorescent staining. This suggests that mt-AEP-1<sup>(1-59)</sup>-GFP disrupted the structure of the kDNA maintained by the endogenous AEP-1 and only accessed the junction between the unilateral filaments and the DNA at a certain phase during the cell cycle. Despite ample research characterizing AEP-1, it has yet to be identified by protein sequencing methods.

## MOONLIGHTING PROTEINS

Moonlighting proteins, a term coined by Jeffery (1999), are defined by having at least two unrelated biological functions in an organism (97). Despite differing activities, these proteins are encoded by a single gene that is neither genetically modified, nor altered in amino acid composition of the polypeptide chain. To date, many moonlighting proteins have been identified and their alternate functions include DNA maintenance, cytoskeletal structure binding, lipid metabolism, apoptosis and transcriptional activation. One of the initially discovered family of proteins, the crystallins, serves as a refractive medium in the lens of the eye in many vertebrates and invertebrates (98). Beginning in the mid-1990s, studies revealed homology between these proteins and some of the well-characterized metabolic enzymes. It is not clear if these water soluble and translucent enzymes perform their metabolic functions in the environment of the eye. Piatigorsky (1998) suggested that proteins such as aldehyde dehydrogenase are recruited to the lens as structural proteins where they can perform additional functions (99, 100).

Multi-functioning proteins possibly emerged during organismal evolution as an adaptation to a change in biological demands and there are advantages to this type of phenomenon. First, Jeffery (1999) proposed that multiple functions for a single gene leads to a reduced genome size and maintenance, but this was later refuted since many genomes contain large regions that are not transcribed (97). Alternatively, Gancedo (2008) suggested that adaptations in existing activities create novel functions and these are preferentially adopted if they create advantages for an organism (101). These functions are revealed under specific circumstances such as sublocalization changes or expression in dissimilar cell forms.

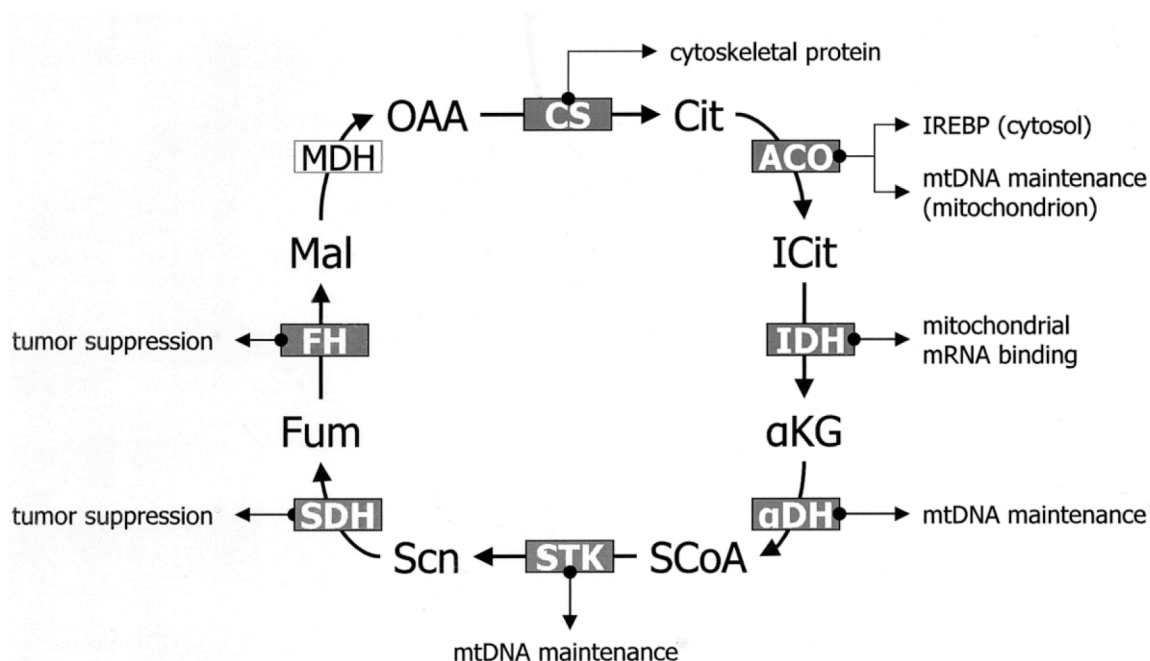


**Figure 1.10.** A schematic of Krebs cycle enzymes with observed moonlighting functions. Abbreviations: CS – citrate synthase; ACO – aconitase; IDH – isocitrate dehydrogenase;  $\alpha$ DH -  $\alpha$ -ketoglutarate dehydrogenase; STK – succinate thiokinase; SDH – succinate dehydrogenase; FH – fumarate hydratase; MDH – malate dehydrogenase; Cit – citrate; ICit – isocitrate;  $\alpha$ KG -  $\alpha$ -ketoglutarate; SCoA – succinyl coenzyme A; Scn – succinate; Fum – fumarate; Mal – malate; OAA – oxaloacetate; IREBP – iron-responsive element-binding protein. (Adapted from Sriram *et al.*, Am J Hum Genet, 2005).

Oligomeric states, availability of specific domains, substrate concentration and phosphorylation also influences these novel activities.

Metabolic enzymes represent a large portion of the identified moonlighting proteins. Though these proteins have specific enzymatic functions, there is a high prevalence for these enzymes to have some type of structural secondary function. Additionally, many historic

metabolic pathways contain multiple well-characterized enzymes with additional functions that are very diverse. For instance, seven of the ten glycolytic enzymes and some that are linked to this pathway have diverse alternative functions (102). A prime example is the metalloenzyme enolase, which is responsible for catalyzing the conversion of 2-phosphoglycerate to phosphoenolpyruvate. Enolase moonlights as a lens crystallin, heat shock protein, plasminogen receptor and a structural factor for chromatin and the cytoskeleton (103-105).

The classic TCA cycle has a similar trend where seven of its eight metabolic enzymes have been identified as moonlighting proteins (Figure 1.10) (102). Tumor suppression has been observed with fumarate hydratase and succinate dehydrogenase, while mitochondrial mRNA, cytoskeletal and iron-responsive element binding is mediated by isocitrate dehydrogenase, citrate synthase and aconitase, respectively (106-109). Aconitase,  $\alpha$ -ketoglutarate dehydrogenase and succinate thiokinase have DNA maintenance roles in the mitochondrion and all exemplify the extent of genome upkeep by metabolic proteins in this organelle (110). A secondary function for malate dehydrogenase has yet to be discovered.

Interestingly,  $\alpha$ -ketoglutarate dehydrogenase involvement in mitochondrial DNA maintenance is a unique case. This complex is a part of a larger group called  $\alpha$ -keto acid dehydrogenases (pyruvate dehydrogenase,  $\alpha$ -ketoglutarate dehydrogenase and branched chain  $\alpha$ -ketoacid dehydrogenase) and they play a critical role in redox regulation in the mitochondrion. As reviewed in Perham (1991), each is composed of a  $\alpha$ -keto acid dehydrogenase (E1), dihydrolipoamide acyltransferase (E2) and dihydrolipoamide dehydrogenase (E3), which catalyzes the breakdown of a specific 2-oxo acid and transfers its energy to acyl-CoA and NADH (111). The stoichiometry and structure of these complexes can vary greatly in different organisms and their size surpasses the ribosome. E2 comprises the structural oligomeric core

and has been shown to be present as three, twenty-four or sixty copies per complex (111, 112). E1 and E3 dimers are noncovalently attached to this core, completely surrounding and burying most of E2 from the surrounding environment. A special feature of E2 is a covalently attached lipoic acid group that is linked to domains that protrude from the inner core and interweave between the E1 and E3. This lipoyl group freely rotates in the complex and transfers the substrate between the active sites (111). Of the three subunits, E2 is the only component in these complexes that has been linked to mitochondrial nucleoids. The association of E2 with DNA has been observed in highly divergent organisms and has mainly been demonstrated through crosslinking, sedimentation, immunoprecipitation and sequencing studies (113, 114). The E2 of the pyruvate and branched chain dehydrogenase is linked to the nucleoids of mammals and bacteria while the transferase of  $\alpha$ -ketoglutarate dehydrogenase attaches to mitochondrial genomes in yeast (68, 114, 115). Additionally, deletion of this E2 in yeast, which are also deficient in a mitochondrial transcription factor, results in augmentation of genome stability (114).

Details surrounding the interaction of E2 with DNA are presently obscure. There are variations in the sequence and lipoic acid content between the  $\alpha$ -keto acid complexes and species, but each shares a similar quaternary structure and enzymatic function. The fact that the different E2s assemble with nucleoids suggests an additional capacity for these proteins to interact with DNA (116). This DNA interaction is likely mediated by a novel domain on the exposed surface of the protein that would only be accessible if the enzyme was free from the obstructing E1 and E3 subunits (113). Alternatively, a well-characterized stretch of amino acids, known as the peripheral subunit-binding domain, contains positively charged residues that bind to the two external enzymes (E1 and E3) and could potentially bind the negatively charged DNA

(117). Also, Bogenhagen (2003) proposed that the soluble E2 might aid in the positioning and anchoring of the nucleoid to the inner mitochondrial membrane by the covalently linked lipoic acid (113).

Many metabolic moonlighting enzymes have clinical importance due to their role in a vast number of human disorders. E2 subunits from each  $\alpha$ -keto acid dehydrogenase complex are the etiological agents of a chronic autoimmune disease called primary biliary cirrhosis (118, 119). This disease is described by inflammation and progressive destruction of the intrahepatic bile ducts in the liver. High levels of anti-mitochondrial antibodies are produced against the autoantigen (E2), which induces an immune response against the target tissues. There is also evidence of nucleotide-binding proteins that render the associated DNA immunogenic thereby inducing conditions such as lupus erythematosus (120).

#### MOONLIGHTING METABOLIC ENZYMES IN PARASITIC PROTOZOA

Dual-functionality of enzymes is not a new concept in parasitic eukaryotes. This adds complexity to the overall makeup of these organisms and fits with the overall reductionism in traits that are linked to parasitism. Collingridge *et al.* (2010) reviews the contribution of the unique biology of these protists to the evolution of moonlighting proteins and discusses the findings in multiple parasites (121). The Apicomplexa *Plasmodium falciparum* and *Toxoplasma gondii*, that are for the causative agents of malaria and toxoplasmosis, respectively, have unique localizations of the glycolytic enzyme enolase (122, 123). Another glycolytic protein, aldolase, is involved in the gliding motility of both parasites by its interaction with actin and this binding has also been observed in other organisms (124-126). It is suggested that the moonlighting

function of aldolase was acquired during the evolution of Apicomplexa since this secondary activity is conserved.

A similar trend for glycolytic enzymes is also seen in trypanosomes. Enolase also moonlights as a plasminogen-binding protein on the extracellular face of the plasma membrane of *Leishmania mexicana* (127). *T. brucei* expresses two hexokinase enzymes, but only one is found outside of glycosomes. This second hexokinase is essential for glycolysis, but also localizes to the flagellum (unpublished research by the Jim Morris lab, Clemson University). These studies led to the realization that compartmentalization of these proteins in glycosomes offers a level of control over these secondary functions, since these novel activities are observed in other regions of the cell.

*T. brucei* also gives an example of this dual localization for a mitochondrial TCA cycle enzyme. Aconitase catalyzes the conversion of citrate to isocitrate via stereo-specific isomerization. Saas *et al.* (2000) found 30% of this total protein in the single mitochondrion and the remainder in the cytosol, which differs from mammalian cells that encode a separate mitochondrial and cytoplasmic enzyme from discrete genes (128). The cytosolic mammalian aconitase resembles an iron-regulatory protein that post-transcriptionally regulates mRNAs in the absence of iron-sulfur clusters and in the presence of iron it retains its normal enzymatic activity. Despite trypanosomes' early eukaryotic divergence, aconitase resembles this iron-regulatory protein, though a similar function in the cytosol has not been resolved (128, 129).

The developmental regulation of energy metabolism pathways and mitochondrion structure remains one of the most unique and puzzling features of trypanosome biology. Additionally, the complex nature of the kDNA demands faithful replication, segregation and maintenance throughout the cell cycle by a diverse set of nuclear and mitochondrial encoded

proteins. The discovery of AEP-1 suggests that differential editing of mitochondrial mRNAs is one approach to creating protein diversity in this organelle. The focus of this dissertation is to further understand the contribution of RNA editing to mitochondrion function by evaluating the alternate locale of AEP-1 in the mitochondrial membrane. Examining the AEP-1 complex by protein sequencing resulted in the identification of a single peptide in the novel N-terminal region of the protein. These studies also led to the identification of  $\alpha$ -ketoglutarate dehydrogenase E1 and E2 subunits, which are moonlighting metabolic enzymes that have effects on flagellar pocket morphology and kDNA inheritance, respectively. The specific functions of these three proteins remain unresolved.

#### REFERENCES

1. **Bruce, D.** 1985. Preliminary report on the tsetse fly disease or nagana in Zululand Durban: Bennett and Davis.
2. **Losos, G. J. a. I., B.O.** 1972. Review of Pathology of Diseases in Domestic and Laboratory Animals Caused by *Trypanosoma congolense*, *T. vivax*, *T. brucei*, *T. rhodesiense* and *T.gambiense*. *Vet Pathol* **9**.
3. **Enanga, B., R. J. Burchmore, M. L. Stewart, and M. P. Barrett.** 2002. Sleeping sickness and the brain. *Cell Mol Life Sci* **59**:845-858.
4. **Matthews, K. R.** 1999. Developments in the differentiation of *Trypanosoma brucei*. *Parasitol Today* **15**:76-80.
5. **Tarleton, R. L.** 2001. Parasite persistence in the aetiology of Chagas disease. *Int J Parasitol* **31**:550-554.
6. **Desjeux, P.** 2004. Leishmaniasis: current situation and new perspectives. *Comp Immunol Microbiol Infect Dis* **27**:305-318.

7. **Murray, M., W. I. Morrison, and D. D. Whitelaw.** 1982. Host susceptibility to African trypanosomiasis: trypanotolerance. *Adv Parasitol* **21**:1-68.
8. **Bishop, J. R., M. Shimamura, and S. L. Hajduk.** 2001. Insight into the mechanism of trypanosome lytic factor-1 killing of *Trypanosoma brucei brucei*. *Mol Biochem Parasitol* **118**:33-40.
9. **Stuart, K.** 1983. Kinetoplast DNA, mitochondrial DNA with a difference. *Mol Biochem Parasitol* **9**:93-104.
10. **Haag, J., C. O'HUigin, and P. Overath.** 1998. The molecular phylogeny of trypanosomes: evidence for an early divergence of the Salivaria. *Mol Biochem Parasitol* **91**:37-49.
11. **Benne, R., B. F. De Vries, J. Van den Burg, and B. Klaver.** 1983. The nucleotide sequence of a segment of *Trypanosoma brucei* mitochondrial maxi-circle DNA that contains the gene for apocytochrome b and some unusual unassigned reading frames. *Nucleic Acids Res* **11**:6925-6941.
12. **Eperon, I. C., J. W. Janssen, J. H. Hoeijmakers, and P. Borst.** 1983. The major transcripts of the kinetoplast DNA of *Trypanosoma brucei* are very small ribosomal RNAs. *Nucleic Acids Res* **11**:105-125.
13. **Hensgens, L. A., J. Brakenhoff, B. F. De Vries, P. Sloof, M. C. Tromp, J. H. Van Boom, and R. Benne.** 1984. The sequence of the gene for cytochrome c oxidase subunit I, a frameshift containing gene for cytochrome c oxidase subunit II and seven unassigned reading frames in *Trypanosoma brucei* mitochondrial maxi-circle DNA. *Nucleic Acids Res* **12**:7327-7344.
14. **Payne, M., V. Rothwell, D. P. Jasmer, J. E. Feagin, and K. Stuart.** 1985. Identification of mitochondrial genes in *Trypanosoma brucei* and homology to cytochrome c oxidase II in two different reading frames. *Mol Biochem Parasitol* **15**:159-170.
15. **Benne, R., J. Van den Burg, J. P. Brakenhoff, P. Sloof, J. H. Van Boom, and M. C. Tromp.** 1986. Major transcript of the frameshifted coxII gene from trypanosome mitochondria contains four nucleotides that are not encoded in the DNA. *Cell* **46**:819-826.
16. **Benne, R.** 1994. RNA editing in trypanosomes. *Eur J Biochem* **221**:9-23.

17. **Feagin, J. E., J. M. Abraham, and K. Stuart.** 1988. Extensive editing of the cytochrome c oxidase III transcript in *Trypanosoma brucei*. *Cell* **53**:413-422.
18. **Ochsenreiter, T., and S. L. Hajduk.** 2006. Alternative editing of cytochrome c oxidase III mRNA in trypanosome mitochondria generates protein diversity. *EMBO Rep* **7**:1128-1133.
19. **Ochsenreiter, T., S. Anderson, Z. A. Wood, and S. L. Hajduk.** 2008. Alternative RNA editing produces a novel protein involved in mitochondrial DNA maintenance in trypanosomes. *Mol Cell Biol* **28**:5595-5604.
20. **Brun, R., J. Blum, F. Chappuis, and C. Burri.** 2010. Human African trypanosomiasis. *Lancet* **375**:148-159.
21. **Jamonneau, V., H. Ilboudo, J. Kabore, D. Kaba, M. Koffi, P. Solano, A. Garcia, D. Courtin, C. Laveissiere, K. Lingue, P. Buscher, and B. Bucheton.** 2012. Untreated human infections by *Trypanosoma brucei gambiense* are not 100% fatal. *PLoS Negl Trop Dis* **6**:e1691.
22. **(WHO), W. H. O.** 23 May 2011. New cases of human African trypanosomiasis continue to drop  
[http://www.who.int/neglected\\_diseases/disease\\_management/HAT\\_cases\\_drop/en/index.html](http://www.who.int/neglected_diseases/disease_management/HAT_cases_drop/en/index.html)2012.
23. **Hemphill, A., D. Lawson, and T. Seebeck.** 1991. The cytoskeletal architecture of *Trypanosoma brucei*. *J Parasitol* **77**:603-612.
24. **Coley, A. F., H. C. Dodson, M. T. Morris, and J. C. Morris.** 2011. Glycolysis in the african trypanosome: targeting enzymes and their subcellular compartments for therapeutic development. *Mol Biol Int* **2011**:123702.
25. **(ILRI), I. L. R. I.** *Schematic diagram of a trypanosome of the Trypanosoma brucei group in its intermediate bloodstream form, illustrating the major organelles.*  
<http://ilri.org/InfoServ/Webpub/fulldocs/Ilrad88/Trypanosomiasis.htm>  
<http://www.ilri.org/InfoServ/Webpub/fulldocs/Ilrad90/Figures/fig%2025%20p45.gif>.
26. **Ogbadoyi, E. O., D. R. Robinson, and K. Gull.** 2003. A high-order trans-membrane structural linkage is responsible for mitochondrial genome positioning and segregation by flagellar basal bodies in trypanosomes. *Mol Biol Cell* **14**:1769-1779.

27. **Field, M. C., and M. Carrington.** 2009. The trypanosome flagellar pocket. *Nat Rev Microbiol* **7**:775-786.
28. **Bastin, P., T. J. Pullen, F. F. Moreira-Leite, and K. Gull.** 2000. Inside and outside of the trypanosome flagellum: a multifunctional organelle. *Microbes Infect* **2**:1865-1874.
29. **Hill, K. L.** 2010. Parasites in motion: flagellum-driven cell motility in African trypanosomes. *Curr Opin Microbiol* **13**:459-465.
30. **Vickerman, K.** 1985. Developmental cycles and biology of pathogenic trypanosomes. *Br Med Bull* **41**:105-114.
31. **Seed, J. R., and J. B. Sechelski.** 1989. Mechanism of long slender (LS) to short stumpy (SS) transformation in the African trypanosomes. *J Protozool* **36**:572-577.
32. **Jenni, L., S. Marti, J. Schweizer, B. Betschart, R. W. Le Page, J. M. Wells, A. Tait, P. Paindavoine, E. Pays, and M. Steinert.** 1986. Hybrid formation between African trypanosomes during cyclical transmission. *Nature* **322**:173-175.
33. **Woodward, R., and K. Gull.** 1990. Timing of nuclear and kinetoplast DNA replication and early morphological events in the cell cycle of *Trypanosoma brucei*. *J Cell Sci* **95 ( Pt 1)**:49-57.
34. **Hammarton, T. C., Wickstead, B., McKean, P.G.** 2006. Cell structure, cell division and cell cycle. In J. D. Barry, Mottram, J.C., McCulloch, R., Acosta-Serrano, A. (ed.), *Trypanosomes-after the genome*. Horizon Scientific Press.
35. **Hall, B. S., C. Gabernet-Castello, A. Voak, D. Goulding, S. K. Natesan, and M. C. Field.** 2006. TbVps34, the trypanosome orthologue of Vps34, is required for Golgi complex segregation. *J Biol Chem* **281**:27600-27612.
36. **Chanez, A. L., A. B. Hehl, M. Engstler, and A. Schneider.** 2006. Ablation of the single dynamin of *T. brucei* blocks mitochondrial fission and endocytosis and leads to a precise cytokinesis arrest. *J Cell Sci* **119**:2968-2974.
37. **Hughes, L. C., K. S. Ralston, K. L. Hill, and Z. H. Zhou.** 2012. Three-dimensional structure of the Trypanosome flagellum suggests that the paraflagellar rod functions as a biomechanical spring. *PLoS One* **7**:e25700.

38. **Ralston, K. S., Z. P. Kabututu, J. H. Melehani, M. Oberholzer, and K. L. Hill.** 2009. The *Trypanosoma brucei* flagellum: moving parasites in new directions. *Annu Rev Microbiol* **63**:335-362.
  
39. **Allen, C. L., D. Goulding, and M. C. Field.** 2003. Clathrin-mediated endocytosis is essential in *Trypanosoma brucei*. *EMBO J* **22**:4991-5002.
  
40. **Thilo, L.** 1985. Quantification of endocytosis-derived membrane traffic. *Biochim Biophys Acta* **822**:243-266.
  
41. **Webster, P., and W. R. Fish.** 1989. Endocytosis by African trypanosomes. II. Occurrence in different life-cycle stages and intracellular sorting. *Eur J Cell Biol* **49**:303-310.
  
42. **Hecker, H., B. Betschart, K. Bender, M. Burri, and W. Schlimme.** 1994. The chromatin of trypanosomes. *Int J Parasitol* **24**:809-819.
  
43. **Li, Z., J. H. Lee, F. Chu, A. L. Burlingame, A. Gunzl, and C. C. Wang.** 2008. Identification of a novel chromosomal passenger complex and its unique localization during cytokinesis in *Trypanosoma brucei*. *PLoS One* **3**:e2354.
  
44. **Ersfeld, K., S. E. Melville, and K. Gull.** 1999. Nuclear and genome organization of *Trypanosoma brucei*. *Parasitol Today* **15**:58-63.
  
45. **Van der Ploeg, L. H., D. C. Schwartz, C. R. Cantor, and P. Borst.** 1984. Antigenic variation in *Trypanosoma brucei* analyzed by electrophoretic separation of chromosome-sized DNA molecules. *Cell* **37**:77-84.
  
46. **Sloof, P., J. L. Bos, A. F. Konings, H. H. Menke, P. Borst, W. E. Gutteridge, and W. Leon.** 1983. Characterization of satellite DNA in *Trypanosoma brucei* and *Trypanosoma cruzi*. *J Mol Biol* **167**:1-21.
  
47. **Weiden, M., Y. N. Osheim, A. L. Beyer, and L. H. Van der Ploeg.** 1991. Chromosome structure: DNA nucleotide sequence elements of a subset of the minichromosomes of the protozoan *Trypanosoma brucei*. *Mol Cell Biol* **11**:3823-3834.
  
48. **Barry, D., McCulloch, R., Mottram, J. and Acosta-Serrano, A.** 2007. *Trypanosomes: After The Genome*. Horizon Scientific Press.

49. **Gunzl, A.** 2010. The pre-mRNA splicing machinery of trypanosomes: complex or simplified? *Eukaryot Cell* **9**:1159-1170.
50. **Nilsson, D., K. Gunasekera, J. Mani, M. Osteras, L. Farinelli, L. Baerlocher, I. Roditi, and T. Ochsenreiter.** 2010. Spliced leader trapping reveals widespread alternative splicing patterns in the highly dynamic transcriptome of *Trypanosoma brucei*. *PLoS Pathog* **6**:e1001037.
51. **Panigrahi, A. K., Y. Ogata, A. Zikova, A. Anupama, R. A. Dalley, N. Acestor, P. J. Myler, and K. D. Stuart.** 2009. A comprehensive analysis of *Trypanosoma brucei* mitochondrial proteome. *Proteomics* **9**:434-450.
52. **Horvath, A., E. A. Berry, and D. A. Maslov.** 2000. Translation of the edited mRNA for cytochrome b in trypanosome mitochondria. *Science* **287**:1639-1640.
53. **Horvath, A., T. G. Kingan, and D. A. Maslov.** 2000. Detection of the mitochondrially encoded cytochrome c oxidase subunit I in the trypanosomatid protozoan *Leishmania tarentolae*. Evidence for translation of unedited mRNA in the kinetoplast. *J Biol Chem* **275**:17160-17165.
54. **Acestor, N., A. Zikova, R. A. Dalley, A. Anupama, A. K. Panigrahi, and K. D. Stuart.** 2011. *Trypanosoma brucei* mitochondrial respiratome: composition and organization in procyclic form. *Mol Cell Proteomics* **10**:M110 006908.
55. **Bakker, B. M., F. I. Mensonides, B. Teusink, P. van Hoek, P. A. Michels, and H. V. Westerhoff.** 2000. Compartmentation protects trypanosomes from the dangerous design of glycolysis. *Proc Natl Acad Sci U S A* **97**:2087-2092.
56. **Fairlamb, A. H. a. O., F.R.** 1986. Carbohydrate metabolism in African trypanosomes with special reference to the glycosome, p. 183-224. *In* M. J. Morgan (ed.), *Carbohydrate metabolism in cultured cells*, Plenum, New York.
57. **Altman, R.** 1890. *Die Elementarorganismen und ihre Beziehungen zu den Zellen*, Veit, Leipzig.
58. **Gray, M. W., G. Burger, and B. F. Lang.** 1999. Mitochondrial evolution. *Science* **283**:1476-1481.
59. **Englund, P. T., S. L. Hajduk, and J. C. Marini.** 1982. The molecular biology of trypanosomes. *Annu Rev Biochem* **51**:695-726.

60. **Liu, B., Y. Liu, S. A. Motyka, E. E. Agbo, and P. T. Englund.** 2005. Fellowship of the rings: the replication of kinetoplast DNA. *Trends Parasitol* **21**:363-369.
  
61. **Seidman, D., D. Johnson, V. Gerbasi, D. Golden, R. Orlando, and S. Hajduk.** 2012. Mitochondrial membrane complex that contains proteins necessary for tRNA import in *Trypanosoma brucei*. *J Biol Chem* **287**:8892-8903.
  
62. **Brown, S. V., P. Hosking, J. Li, and N. Williams.** 2006. ATP synthase is responsible for maintaining mitochondrial membrane potential in bloodstream form *Trypanosoma brucei*. *Eukaryot Cell* **5**:45-53.
  
63. **Nass, M. M.** 1966. The circularity of mitochondrial DNA. *Proc Natl Acad Sci U S A* **56**:1215-1222.
  
64. **van Bruggen, E. F., P. Borst, G. J. Rutenberg, M. Gruber, and A. M. Kroon.** 1966. Circular mitochondrial DNA. *Biochim Biophys Acta* **119**:437-439.
  
65. **Delius, H., and A. Worcel.** 1974. Electron microscopic studies on the folded chromosome of *Escherichia coli*. *Cold Spring Harb Symp Quant Biol* **38**:53-58.
  
66. **Kornberg, R. D.** 1974. Chromatin structure: a repeating unit of histones and DNA. *Science* **184**:868-871.
  
67. **Bogenhagen, D. F.** 2011. Mitochondrial DNA nucleoid structure. *Biochim Biophys Acta*.
  
68. **Wang, Y., and D. F. Bogenhagen.** 2006. Human mitochondrial DNA nucleoids are linked to protein folding machinery and metabolic enzymes at the mitochondrial inner membrane. *J Biol Chem* **281**:25791-25802.
  
69. **Lukes, J., H. Hashimi, and A. Zikova.** 2005. Unexplained complexity of the mitochondrial genome and transcriptome in kinetoplastid flagellates. *Curr Genet* **48**:277-299.
  
70. **Feagin, J. E.** 2000. Mitochondrial genome diversity in parasites. *Int J Parasitol* **30**:371-390.
  
71. **Hajduk, S. L., M. E. Harris, and V. W. Pollard.** 1993. RNA editing in kinetoplastid mitochondria. *FASEB J* **7**:54-63.

72. **Estevez, A. M., and L. Simpson.** 1999. Uridine insertion/deletion RNA editing in trypanosome mitochondria--a review. *Gene* **240**:247-260.
73. **Ochsenreiter, T. a. H., S.L.** 2008. The Function of RNA Editing in Trypanosomes *In* H. U. Goringer (ed.), RNA Editing. Nucleic Acids and Molecular Biology vol. 20. Springer-Verlag, Berlin Heidelberg.
74. **Abu-Elneel, K., D. R. Robinson, M. E. Drew, P. T. Englund, and J. Shlomai.** 2001. Intramitochondrial localization of universal minicircle sequence-binding protein, a trypanosomatid protein that binds kinetoplast minicircle replication origins. *J Cell Biol* **153**:725-734.
75. **Li, C., and P. T. Englund.** 1997. A mitochondrial DNA primase from the trypanosomatid *Crithidia fasciculata*. *J Biol Chem* **272**:20787-20792.
76. **Klingbeil, M. M., S. A. Motyka, and P. T. Englund.** 2002. Multiple mitochondrial DNA polymerases in *Trypanosoma brucei*. *Mol Cell* **10**:175-186.
77. **Engel, M. L., and D. S. Ray.** 1999. The kinetoplast structure-specific endonuclease I is related to the 5' exo/endonuclease domain of bacterial DNA polymerase I and colocalizes with the kinetoplast topoisomerase II and DNA polymerase beta during replication. *Proc Natl Acad Sci U S A* **96**:8455-8460.
78. **Ferguson, M., A. F. Torri, D. C. Ward, and P. T. Englund.** 1992. In situ hybridization to the *Crithidia fasciculata* kinetoplast reveals two antipodal sites involved in kinetoplast DNA replication. *Cell* **70**:621-629.
79. **Torri, A. F., and P. T. Englund.** 1995. A DNA polymerase beta in the mitochondrion of the trypanosomatid *Crithidia fasciculata*. *J Biol Chem* **270**:3495-3497.
80. **Sinha, K. M., J. C. Hines, N. Downey, and D. S. Ray.** 2004. Mitochondrial DNA ligase in *Crithidia fasciculata*. *Proc Natl Acad Sci U S A* **101**:4361-4366.
81. **Downey, N., J. C. Hines, K. M. Sinha, and D. S. Ray.** 2005. Mitochondrial DNA ligases of *Trypanosoma brucei*. *Eukaryot Cell* **4**:765-774.
82. **Wang, Z., and P. T. Englund.** 2001. RNA interference of a trypanosome topoisomerase II causes progressive loss of mitochondrial DNA. *EMBO J* **20**:4674-4683.

83. **Carpenter, L. R., and P. T. Englund.** 1995. Kinetoplast maxicircle DNA replication in *Crithidia fasciculata* and *Trypanosoma brucei*. *Mol Cell Biol* **15**:6794-6803.
84. **Gull, K.** 2003. Host-parasite interactions and trypanosome morphogenesis: a flagellar pocketful of goodies. *Curr Opin Microbiol* **6**:365-370.
85. **Gluezn, E., M. K. Shaw, and K. Gull.** 2007. Structural asymmetry and discrete nucleic acid subdomains in the *Trypanosoma brucei* kinetoplast. *Mol Microbiol* **64**:1529-1539.
86. **Zhao, Z., M. E. Lindsay, A. Roy Chowdhury, D. R. Robinson, and P. T. Englund.** 2008. p166, a link between the trypanosome mitochondrial DNA and flagellum, mediates genome segregation. *EMBO J* **27**:143-154.
87. **van Hellemond, J. J., F. R. Opperdoes, and A. G. Tielens.** 2005. The extraordinary mitochondrion and unusual citric acid cycle in *Trypanosoma brucei*. *Biochem Soc Trans* **33**:967-971.
88. **Durieux, P. O., P. Schutz, R. Brun, and P. Kohler.** 1991. Alterations in Krebs cycle enzyme activities and carbohydrate catabolism in two strains of *Trypanosoma brucei* during *in vitro* differentiation of their bloodstream to procyclic stages. *Mol Biochem Parasitol* **45**:19-27.
89. **van Weelden, S. W., B. Fast, A. Vogt, P. van der Meer, J. Saas, J. J. van Hellemond, A. G. Tielens, and M. Boshart.** 2003. Procyclic *Trypanosoma brucei* do not use Krebs cycle activity for energy generation. *J Biol Chem* **278**:12854-12863.
90. **van Weelden, S. W., J. J. van Hellemond, F. R. Opperdoes, and A. G. Tielens.** 2005. New functions for parts of the Krebs cycle in procyclic *Trypanosoma brucei*, a cycle not operating as a cycle. *J Biol Chem* **280**:12451-12460.
91. **Walker, R., Jr., L. Saha, G. C. Hill, and M. Chaudhuri.** 2005. The effect of over-expression of the alternative oxidase in the procyclic forms of *Trypanosoma brucei*. *Mol Biochem Parasitol* **139**:153-162.
92. **Panigrahi, A. K., N. L. Ernst, G. J. Domingo, M. Fleck, R. Salavati, and K. D. Stuart.** 2006. Compositionally and functionally distinct editosomes in *Trypanosoma brucei*. *RNA* **12**:1038-1049.
93. **Stuart, K. D., A. Schnauffer, N. L. Ernst, and A. K. Panigrahi.** 2005. Complex management: RNA editing in trypanosomes. *Trends Biochem Sci* **30**:97-105.

94. **Sommer, B., M. Kohler, R. Sprengel, and P. H. Seeburg.** 1991. RNA editing in brain controls a determinant of ion flow in glutamate-gated channels. *Cell* **67**:11-19.
95. **Siegel, G. J.** 1999. Excessive Glutamate Receptor Activation and Neurological Disorders. In G. J. Siegel, Agranoff, B.W., Albers, R.W., et al. (ed.), *Basic Neurochemistry: Molecular, Cellular and Medical Aspects*. 6th edition. American Society for Neurochemistry., Philadelphia.
96. **Ochsenreiter, T., M. Cipriano, and S. L. Hajduk.** 2008. Alternative mRNA editing in trypanosomes is extensive and may contribute to mitochondrial protein diversity. *PLoS One* **3**:e1566.
97. **Jeffery, C. J.** 1999. Moonlighting proteins. *Trends Biochem Sci* **24**:8-11.
98. **Piatigorsky, J.** 1993. Puzzle of crystallin diversity in eye lenses. *Dev Dyn* **196**:267-272.
99. **Piatigorsky, J.** 1998. Gene sharing in lens and cornea: facts and implications. *Prog Retin Eye Res* **17**:145-174.
100. **Piatigorsky, J.** 1998. Multifunctional lens crystallins and corneal enzymes. More than meets the eye. *Ann N Y Acad Sci* **842**:7-15.
101. **Gancedo, C., and C. L. Flores.** 2008. Moonlighting proteins in yeasts. *Microbiol Mol Biol Rev* **72**:197-210, table of contents.
102. **Sriram, G., J. A. Martinez, E. R. McCabe, J. C. Liao, and K. M. Dipple.** 2005. Single-gene disorders: what role could moonlighting enzymes play? *Am J Hum Genet* **76**:911-924.
103. **Nakajima, K., M. Hamanoue, N. Takemoto, T. Hattori, K. Kato, and S. Kohsaka.** 1994. Plasminogen binds specifically to alpha-enolase on rat neuronal plasma membrane. *J Neurochem* **63**:2048-2057.
104. **Pancholi, V.** 2001. Multifunctional alpha-enolase: its role in diseases. *Cell Mol Life Sci* **58**:902-920.

105. **Wistow, G. J., T. Lietman, L. A. Williams, S. O. Stapel, W. W. de Jong, J. Horwitz, and J. Piatigorsky.** 1988. Tau-crystallin/alpha-enolase: one gene encodes both an enzyme and a lens structural protein. *J Cell Biol* **107**:2729-2736.
106. **Jeffery, C. J.** 2003. Moonlighting proteins: old proteins learning new tricks. *Trends Genet* **19**:415-417.
107. **Basilion, J. P., T. A. Rouault, C. M. Massinople, R. D. Klausner, and W. H. Burgess.** 1994. The iron-responsive element-binding protein: localization of the RNA-binding site to the aconitase active-site cleft. *Proc Natl Acad Sci U S A* **91**:574-578.
108. **Elzinga, S. D., A. L. Bednarz, K. van Oosterum, P. J. Dekker, and L. A. Grivell.** 1993. Yeast mitochondrial NAD(+)-dependent isocitrate dehydrogenase is an RNA-binding protein. *Nucleic Acids Res* **21**:5328-5331.
109. **Numata, O.** 1996. Multifunctional proteins in Tetrahymena: 14-nm filament protein/citrate synthase and translation elongation factor-1 alpha. *Int Rev Cytol* **164**:1-35.
110. **Chen, X. J., X. Wang, B. A. Kaufman, and R. A. Butow.** 2005. Aconitase couples metabolic regulation to mitochondrial DNA maintenance. *Science* **307**:714-717.
111. **Perham, R. N.** 1991. Domains, motifs, and linkers in 2-oxo acid dehydrogenase multienzyme complexes: a paradigm in the design of a multifunctional protein. *Biochemistry* **30**:8501-8512.
112. **Bunik, V. I.** 2003. 2-Oxo acid dehydrogenase complexes in redox regulation. *Eur J Biochem* **270**:1036-1042.
113. **Bogenhagen, D. F., Y. Wang, E. L. Shen, and R. Kobayashi.** 2003. Protein components of mitochondrial DNA nucleoids in higher eukaryotes. *Mol Cell Proteomics* **2**:1205-1216.
114. **Kaufman, B. A., S. M. Newman, R. L. Hallberg, C. A. Slaughter, P. S. Perlman, and R. A. Butow.** 2000. In organello formaldehyde crosslinking of proteins to mtDNA: identification of bifunctional proteins. *Proc Natl Acad Sci U S A* **97**:7772-7777.
115. **Stein, A., and W. Firshein.** 2000. Probable identification of a membrane-associated repressor of *Bacillus subtilis* DNA replication as the E2 subunit of the pyruvate dehydrogenase complex. *J Bacteriol* **182**:2119-2124.

116. **Spelbrink, J. N.** 2010. Functional organization of mammalian mitochondrial DNA in nucleoids: history, recent developments, and future challenges. *IUBMB Life* **62**:19-32.
117. **Perham, R. N.** 2000. Swinging arms and swinging domains in multifunctional enzymes: catalytic machines for multistep reactions. *Annu Rev Biochem* **69**:961-1004.
118. **Coppel, R. L., L. J. McNeilage, C. D. Surh, J. Van de Water, T. W. Spithill, S. Whittingham, and M. E. Gershwin.** 1988. Primary structure of the human M2 mitochondrial autoantigen of primary biliary cirrhosis: dihydrolipoamide acetyltransferase. *Proc Natl Acad Sci U S A* **85**:7317-7321.
119. **Fussey, S. P., J. R. Guest, O. F. James, M. F. Bassendine, and S. J. Yeaman.** 1988. Identification and analysis of the major M2 autoantigens in primary biliary cirrhosis. *Proc Natl Acad Sci U S A* **85**:8654-8658.
120. **Moens, U., O. M. Seternes, A. W. Hey, Y. Silsand, T. Traavik, B. Johansen, and O. P. Rekvig.** 1995. In vivo expression of a single viral DNA-binding protein generates systemic lupus erythematosus-related autoimmunity to double-stranded DNA and histones. *Proc Natl Acad Sci U S A* **92**:12393-12397.
121. **Collingridge, P. W., R. W. Brown, and M. L. Ginger.** 2010. Moonlighting enzymes in parasitic protozoa. *Parasitology* **137**:1467-1475.
122. **Bhowmick, I. P., N. Kumar, S. Sharma, I. Coppens, and G. K. Jarori.** 2009. Plasmodium falciparum enolase: stage-specific expression and sub-cellular localization. *Malar J* **8**:179.
123. **Ferguson, D. J., S. F. Parmley, and S. Tomavo.** 2002. Evidence for nuclear localisation of two stage-specific isoenzymes of enolase in Toxoplasma gondii correlates with active parasite replication. *Int J Parasitol* **32**:1399-1410.
124. **Bosch, J., C. A. Buscaglia, B. Krumm, B. P. Ingason, R. Lucas, C. Roach, T. Cardozo, V. Nussenzweig, and W. G. Hol.** 2007. Aldolase provides an unusual binding site for thrombospondin-related anonymous protein in the invasion machinery of the malaria parasite. *Proc Natl Acad Sci U S A* **104**:7015-7020.
125. **Starnes, G. L., M. Coincon, J. Sygusch, and L. D. Sibley.** 2009. Aldolase is essential for energy production and bridging adhesin-actin cytoskeletal interactions during parasite invasion of host cells. *Cell Host Microbe* **5**:353-364.

126. **Buscaglia, C. A., I. Coppens, W. G. Hol, and V. Nussenzweig.** 2003. Sites of interaction between aldolase and thrombospondin-related anonymous protein in plasmodium. *Mol Biol Cell* **14**:4947-4957.
127. **Quinones, W., P. Pena, M. Domingo-Sananes, A. Caceres, P. A. Michels, L. Avilan, and J. L. Concepcion.** 2007. *Leishmania mexicana*: molecular cloning and characterization of enolase. *Exp Parasitol* **116**:241-251.
128. **Saas, J., K. Ziegelbauer, A. von Haeseler, B. Fast, and M. Boshart.** 2000. A developmentally regulated aconitase related to iron-regulatory protein-1 is localized in the cytoplasm and in the mitochondrion of *Trypanosoma brucei*. *J Biol Chem* **275**:2745-2755.
129. **Theil, E. C.** 1994. Iron regulatory elements (IREs): a family of mRNA non-coding sequences. *Biochem J* **304 ( Pt 1)**:1-11.

## CHAPTER 2

IDENTIFICATION OF A NOVEL MITOCHONDRIAL MEMBRANE COMPLEX:

AEP-1 INTERACTS WITH COMPONENTS OF THE  $\alpha$ -KETOGLUTARATE

DEHYDROGENASE MULTIENZYME<sup>1</sup>

---

<sup>1</sup> Sykes, S.E., Zhu, X., Orlando, R.C., Hajduk, S.L. To be submitted to J. Biol. Chem.

## ABSTRACT

Mitochondrial alternative editing of the cytochrome c oxidase III pre-mRNA in *Trypanosoma brucei* produces a novel membrane protein in bloodstream cells called alternatively edited protein-1 (AEP-1). Previously, it has been shown that the role for AEP-1 in bloodstream form (BF) *T. brucei* is assembly into the tripartite attachment complex (TAC) and maintenance of the mitochondrial nucleoid, the kinetoplast DNA (kDNA). However, little is known about the AEP-1 assembled into an integral membrane complex (A-IMM) distributed throughout mitochondrion. Here we describe the expression and localization of AEP-1 in the mitochondrion of procyclic form (PF) *T. brucei*, which also has a TAC and mitochondrial membrane distribution as BF cells. Native fractionation of both the PF and BF mitochondrial inner membrane proteins revealed differential expression of oxidative phosphorylation complexes and a developmentally regulated A-IMM. Tandem mass spectrometry (LC-MS/MS) analysis of the PF A-IMM identified the alternatively edited protein and further purification of the A-IMM by anion exchange chromatography revealed subunits from the Krebs pathway enzyme, the  $\alpha$ -ketoglutarate dehydrogenase complex ( $\alpha$ -KD). These data suggest that AEP-1 provides a unique localization for historically soluble proteins in the dynamic mitochondrion of *T. brucei*.

## INTRODUCTION

The protozoan parasite *Trypanosoma brucei* possesses very distinctive biological and physiological characteristics including an adaptive mitochondrion that cycles through levels of activity during development (1-3). Bloodstream form (BF) trypanosomes have a repressed mitochondrion due to the rich glucose content of the mammalian blood and is metabolized by the glycolytic pathway in glycosomes for energy (4). Alternatively, the robust procyclic form (PF) mitochondrion in the insect host expresses a full complement of proteins involved in essential mitochondrial pathways such as the Krebs cycle and cytochrome mediated respiration (5). Carbohydrate and amino acid degradation by pathways such as the Krebs cycle produces reduced cofactors (NADH and FADH<sub>2</sub>) that are further utilized by oxidoreductase complexes I-IV (NADH dehydrogenase [I], succinate dehydrogenase [II], cytochrome c reductase [III] and cytochrome c oxidase [IV]). The pumping of protons by complexes I, III and IV aids in generating a proton motive force that powers ATP production by the ATPase-F<sub>1</sub>F<sub>0</sub> (complex V).

Protein expression in the mitochondrion requires a concerted effort between genes in the nucleus and kinetoplast (kDNA), the DNA body of the mitochondrion (5, 6). Genes for nuclear encoded mitochondrial proteins are RNA polymerase II transcribed, translated by cytosolic ribosomes and actively imported into the mitochondrion (7, 8). The kDNA, which is composed of catenated deoxyribonucleic circles (maxicircles and minicircles), houses information for the other mitochondrial components such as the oxidoreductase complexes, ATPase-F<sub>1</sub>F<sub>0</sub> and rRNAs (9). Interestingly, many of these

kDNA sequences are cryptic and require posttranscriptional modification to become functional (10-12).

Mitochondrial RNA editing is a guided process (by minicircle-encoded guide RNAs) catalyzed by a large protein complex where maxicircle transcribed pre-mRNAs are cleaved, uridines are inserted and deleted into the transcript and the altered fragments are ligated together (13). This mechanism partially edits some sequences while other transcripts, such as cytochrome c oxidase III (COXIII), are pan edited to create a functional mRNAs (10, 11). A diverse population of incompletely edited mRNAs, created by alternative RNA editing, has been observed for some subunits of the electron transport chain (NADH dehydrogenase subunits 7,8,9 and COXIII) and the A6 component of the ATPase-F<sub>1</sub>F<sub>0</sub> in BF *T. brucei* (14). Our lab has shown that alternative RNA editing produced a non-canonical mRNA that is a fusion product between pre- and fully edited COXIII sequences which are both brought into frame by the insertion of two uridines in a junction region (15). This mRNA is stable and is translated into a novel protein called alternatively edited protein-1 (AEP-1), which is composed of a unique N-terminal region and the C-terminal domain contains the identical amino acid sequence of COXIII. Ochsenreiter et al. (2008) revealed that 65% of this protein is focused at the kDNA and it assembles into the tripartite attachment complex (TAC), a highly ordered filamentous structure that connects the single mitochondrial nucleoid to the flagellum and is responsible for DNA locality, partitioning and upkeep in this organelle (16). To date, the functional characterization of AEP-1 deals with only the TAC-associated protein in BF *T. brucei* and little is known about the remaining detergent-soluble form distributed throughout the mitochondria or its expression in PF cells. The discovery of alternatively

edited protein-1 (AEP-1) suggests that RNA editing is not just a repair process, but also a way of creating protein diversity in the mitochondrion.

kDNA-encoded proteins remain to be a challenge for positive identification by conventional mass spectrometry methods (6, 17-19). The extreme hydrophobic nature of these polypeptides is thought to be the main cause of this phenomenon. Mitochondrial-encoded cytochrome b and cytochrome c oxidase subunit I, subunits of complexes III and IV respectively, were sequenced by the Edman degradation method in *Leishmania tarentolae* (12, 20). Recently, Acestor et al. (2011) identified peptides in *T. brucei* for two subunits of the cytochrome c oxidase through the affinity purification of mitochondrial membrane complexes (21). Due to the hydrophobic nature of AEP-1 and assembly into the stable TAC, early attempts to sequence this protein by mass spectrometry were unsuccessful and the only evidence of translation is by an N-terminal specific antibody (15, 22).

This present study gives the first translational evidence of an alternatively edited mRNA encoded from the cytochrome c oxidase subunit III gene in PF *T. brucei*. We show in this cell form that AEP-1 is localized throughout the mitochondria and to the TAC. Mitochondrial membrane protein purification, anion exchange chromatography and blue native PAGE (BNPAGE) fractionation affirms AEP-1's association with an integral mitochondrial membrane complex (A-IMM) in PF cells. Tandem mass spectrometry (LC-MS/MS) of the mitochondrial membrane complexes revealed 107 nuclear encoded proteins and the first reported identification of a single peptide for AEP-1. Additionally, three subunits of the Krebs pathway associated multimeric  $\alpha$ -ketoglutarate dehydrogenase ( $\alpha$ -KD) enzyme (two protein isoforms of  $\alpha$ -KDE1 and the

$\alpha$ -KDE2) were also discovered in a highly purified A-IMM fraction and provide an additional facet of matrix metabolic enzymes assembling into a membrane complex.

## RESULTS

### **AEP-1 identification in the PF mitochondrion.**

It was previously shown that AEP-1 is expressed and purifies with the mitochondrion in BF *T. brucei* (15). The AEP-1 mRNA is also expressed in PF cells (data not shown) and immunofluorescence microscopy was used to localize AEP-1 subcellularly (Figure 2.1A and B). AEP-1 antibodies reacted with the PF mitochondrion and showed a distribution similar to the mitotracker staining (Figure 2.1A). In contrast to the BF cells, there was no discernable increase in staining at the kDNA (22) and PF cells were treated further with Triton X-100 to ablate the majority of the signal in the mitochondrion (Figure 2.1B). The resulting cell ghost revealed a stable association with AEP-1 proximal to the kinetoplast and basal bodies and suggests this protein also assembles into the TAC in PF cells.

To assess whether the detergent soluble AEP-1 in PF cells associates with mitochondrial membrane, intact mitochondria were isolated hypotonically and subjected to a tandem nonionic detergent treatment to purify the membrane fraction from the matrix (15, 23). Membrane proteins were purified, fractionated by SDS-PAGE and analyzed further by Western Blot (Figure 2.2A). Subunits of the F<sub>1</sub> domain ( $\beta, \alpha, \gamma, \delta, \epsilon$ ) of the ATPase-F<sub>1</sub>F<sub>0</sub>

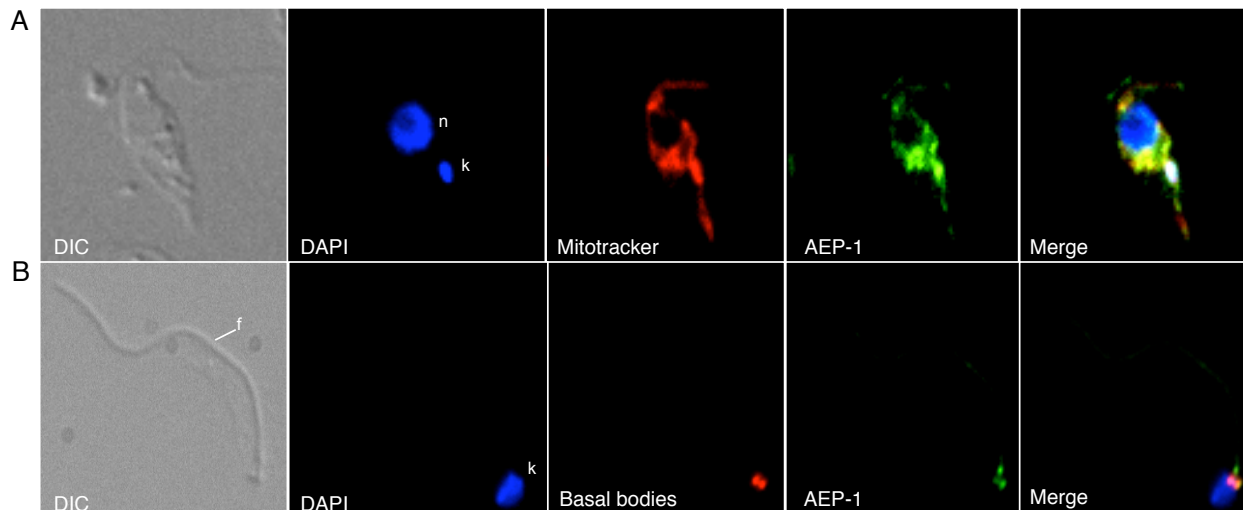


**Figure 2.1.** Localization and distribution of AEP-1 in PF *T. brucei*. A) Fluorescence microscopy of intact PF trypanosomes (DIC) stained with DAPI, MitoTracker and an antibody against AEP-1. B) (Fluorescence microscopy of PF cells treated with 0.5% Triton X-100 to reveal skeletal elements. The resulting cell ghosts shown (DIC) were stained with DAPI and antibodies against the basal bodies and AEP-1. The position of the nucleus (n), kDNA (k) and flagellum (f) are indicated.

(complex V), subunit IV of the cytochrome c oxidase (complex IV) and the Rieske iron sulfur protein (ISP) of the cytochrome reductase (complex III) are all mitochondrial inner membrane proteins that are expressed in PF trypanosomes (Figure 2.2B). AEP-1 also fractionates in this preparation as a 49 kDa protein. These results indicate that despite developmental regulation of the *T. brucei* mitochondrion, a small fraction of AEP-1 is expressed and localizes to the TAC and the mitochondrial membranes of PF *T. brucei*.

**AEP-1 assembles into an integral membrane complex.**

Many of the well-characterized mitochondrial proteins associate with complexes to perform specific functions (24-26). Extracted membrane proteins from BF and PF mitochondria were fractionated by BNPAGE (1D) to identify these complexes including a potential assembly containing AEP-1 in PF cells. The PF analysis revealed five complexes that were resolved further by SDSPAGE (2D) and analyzed by Western Blot to identify associated subunits (Figure 2.3). This 1D profile was similar to what was observed in *L. tarentolae* (20) with additional complexes observed (Figure 2.3A). The fastest migrating PF complex contained a subunit (32 kDa) that reacted with antibodies against ISP (complex III) and above that ran the COXIV (36 kDa) reactive complex (complex IV) (Figure 2.3B and C). Migrating two complexes above that is the complex V ( $\alpha$  [52 kDa],  $\beta$  [60 kDa]) and the largest structure resolved on the 1D gel contains AEP-1 (50 kDa) (Figure 3B and C). The A-IMM (>1.2 Mda, based on Figure 2.5A) fractionates as a smudge on the native gel and may reveal the heterogeneous nature of this high molecular weight assembly (Figure 2.3A and B). The complex with an intermediate position between IV and V had minor reactivity with the ATPase-F<sub>1</sub> domain antibodies ( $\alpha$  and  $\beta$ ) and was thought to be smaller oligomeric form of complex V (complex Va) (Figure 2.3B and C).

In contrast to the PF results, a drastically different profile was observed for the BF mitochondrial membrane complexes and also emphasizes developmental regulation of the organelle and proteins (Figure S2.1). Only complexes containing AEP-1 and ATPase-F<sub>1</sub> subunits ( $\alpha$  and  $\beta$ ) were identified and a similar distribution to the PF

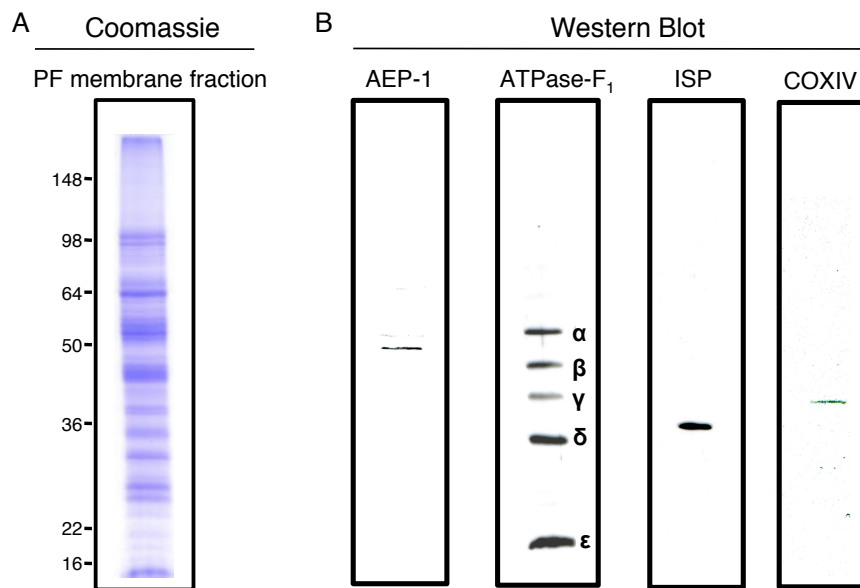


**Figure 2.2.** Detection of mitochondrial membrane proteins in PF *T. brucei*. Total mitochondrial membrane protein lysate from PF cells fractionated by SDS-PAGE. A) Coomassie-stained proteins from PF mitochondrial membrane lysates. B) Western blot analysis with AEP-1, ATPase-F<sub>1</sub>, ISP and COXIV antibodies. The five different subunits of ATPase-F<sub>1</sub> are represented by  $\alpha$ ,  $\beta$ ,  $\gamma$ ,  $\delta$  and  $\epsilon$ .

assemblies was observed (Figure 2.3 and Figure S2.1), but different from what was published in Ochsenreiter and Hajduk (2006) (15) and are possibly attributable to varying BN-PAGE conditions. Despite this distribution, the PF A-IMM migrated much slower than the BF complex and suggests developmental regulation of the structure (Figure 2.4A and B). This data confirms the expression of a differential A-IMM in PF and BF *T. brucei*.

### Sequence analysis of mitochondrial membrane complexes.

Sequencing by mass spectrometry was used to determine the composition of each complex that reacted with antibodies for both the developmental forms. The seven protein bands (five PF and two BF) were excised from blue native gels, digested with trypsin and resulting peptides were subjected to rounds of LC-MS/MS. Proteins were selected based on a  $\geq 0.9$  probability score and a total of 107 nuclear encoded sequences, but no mitochondrial-encoded, were identified by multiple peptide (minimum of 2) matches (Tables S2.1-7). Chaperones and many proteins involved in respiration, Krebs pathway, amino acid and carbon metabolism were detected. The remaining 35 non-annotated hypothetical proteins were confirmed for mitochondrial localization by the TargetP database (<http://www.cbs.dtu.dk/services/TargetP/>).

Multiple peptides for four subunits of the F1 portion of complex V ( $\beta$  [Tb927.3.1380],  $\alpha$  [LMJF\_05\_0500],  $\gamma$  [Tb10.100.0070] and  $\epsilon$  [Tb927.6.4990]) in PF *T. brucei* were detected, but only  $\beta$  and  $\gamma$  were identified in the smaller reacting structure (Tables S2.2 and 3). This smaller complex also contained a diverse group of proteins (a trend observed in all identified complexes) including chaperones (Tb11.02.0250 and Tb10.70.0430), cytochrome c oxidase subunits (Tb927.1.4100 and Tb09.160.1820) and a Krebs pathway enzyme (Tb10.6k15.3250). Also, guide RNA binding ribonucleoprotein p18 (Tb927.5.1710) was also identified with this complex (Table S2.3) and has been designated as a homologue of the  $\beta$  subunit in other trypanosomes (18). Sequencing of the BF reactive complex revealed the detection of the F1  $\beta$ ,  $\gamma$ ,  $\epsilon$  and p18 subunits (Table S2.7).

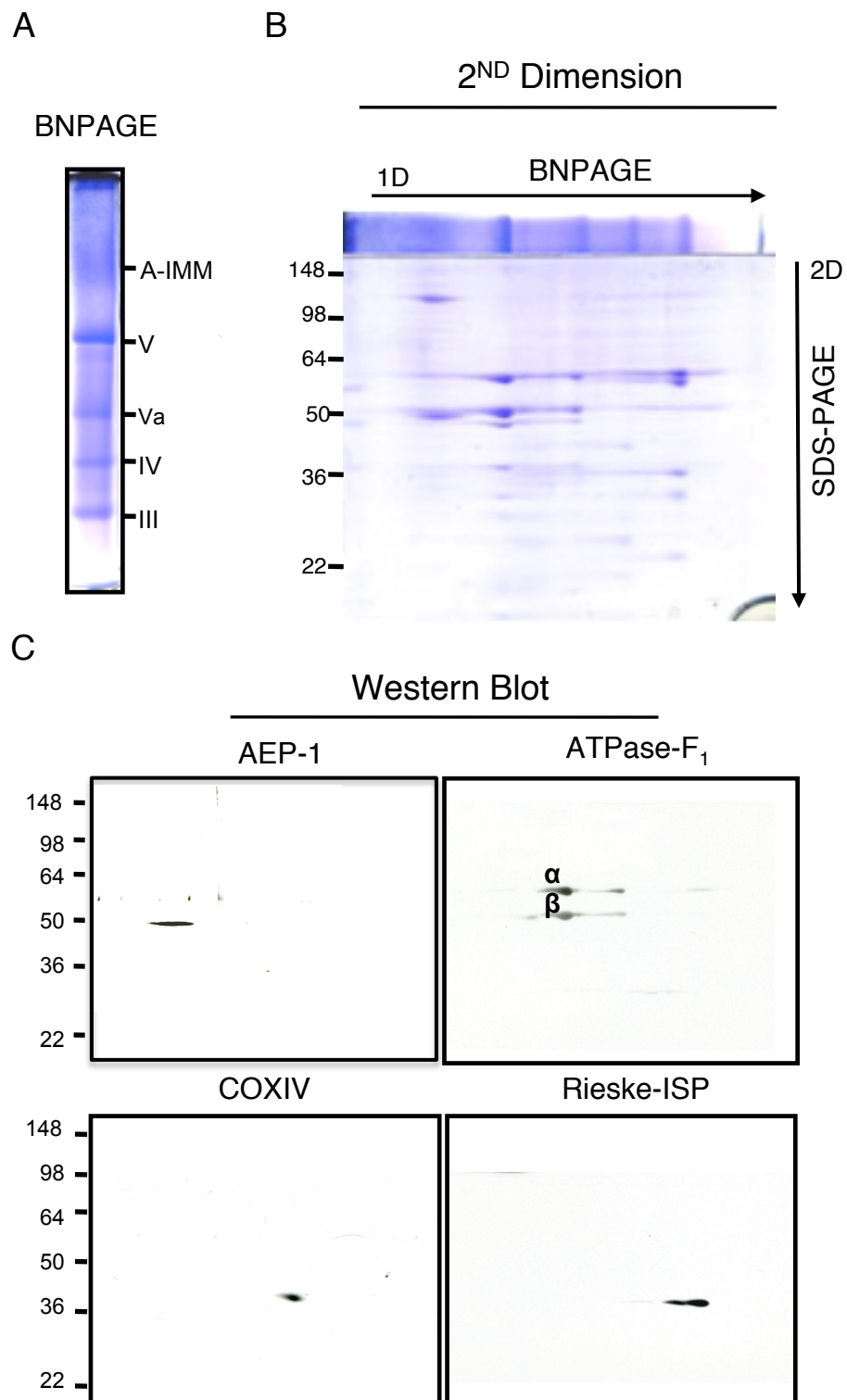


**Figure 2.3.** Native and 2D electrophoresis of mitochondrial membrane complexes from PF *T. brucei*. A) Mitochondria from PF *T. brucei* were solubilized in 0.5% Triton X-100 and 2% n-dodecyl- $\beta$ -D-maltoside, loaded on a BNPAGE gradient gel (4-13%) and coomassie-stained. B) Subunits of the native complexes were separated by SDS-PAGE (2D) and stained by coomassie. C) Western blot analysis of 2D gels. Western blots were analyzed using antibodies against AEP-1, ATPase-F<sub>1</sub>, COXIV and ISP. Positions of the A-IMM and complexes III, IV, V and Va are indicated. The  $\alpha$  and  $\beta$  subunits of the ATPase-F<sub>1</sub> are also shown.

COXIV (Tb927.1.4100), COXV (Tb09.160.1820), COXVI (Tb10.100.0160), COXVII (Tb927.3.1410) and COX10 (Tb11.01.4702), were identified for complex IV (Table S2.5), while ISP (Tb09.211.4700) and cytochrome c1 (Tb927.8.1890) were found in complex III (Table S2.4). Uniquely, analysis of the PF A-IMM gel bands from BNPAGE and SDS-PAGE (Figure 2.3A) revealed the presence of the soluble  $\alpha$ -KD enzymes (E1 [Tb11.01.1740, Tb11.47.0004], E2 [Tb11.01.3550] and E3 [Tb11.01.8470]). E2 was also identified in the BF A-IMM (Tables S2.1 and 6).

These data confirm that our cellular fractionation and purification of mitochondrial membrane proteins was achieved. However, many of the identified proteins were ubiquitous in these complexes and may support the phenomenon that these structures can assemble into supramolecular assemblies termed respirasomes (27). Alternatively, the high frequency of shared proteins could be due to comigration of membrane complexes (21) or artifacts caused by sample preparation and BNPAGE.

**Identification of a single N-terminal AEP-1 peptide.**

Accessibility of target proteins by conventional mass spectrometry techniques, such as enzyme digestion and peptide extraction, may be further complicated by BNPAGE and it would be advantageous to resolve individual subunits by SDS-PAGE prior to sequencing. Since we lacked antibodies to positively detect kinetoplast-encoded respiratory subunits by this method, these proteins were no longer pursued in this study. The antibody to the N-terminal region of AEP-1 identifies a Coomassie-stained band around 50 kDa on the 2D in PF cells (Figure 2.3). The PF gel band was excised and peptides were generated using trypsin. Four possible AEP-1 N-terminal peptides were found amenable to mass spectrometry by the MS-Digest tool developed by the UCSF Mass Spectrometry Facility (<http://prospector.ucsf.edu/prospector/mshome.htm>). These sequences were preferentially scanned for during this analysis and a nine amino acid peptide, EGTGEERTR (residues 30 – 38), was identified in a single LC-MS/MS run (Figure 2.5). Figure 5 displays a partial alignment of the AEP-1 and COXIII amino acid sequences with corresponding mRNAs and shows that the EGTGEERTR peptide was identified from the unique N-terminal pre-edited sequence of AEP-1. The generated spectrum for this sequence is shown in Supplemental Figure 2 and only 13 out of the 82 generated fragment ions were identified (shown in red), which resulted in an ion score of five. This is thought to be a result of the charged nature of these amino acids and preliminary results from an identical sequence generated from a synthetic N-terminal AEP-1 peptide (residues 1 – 59) agreed with these findings (data not shown).

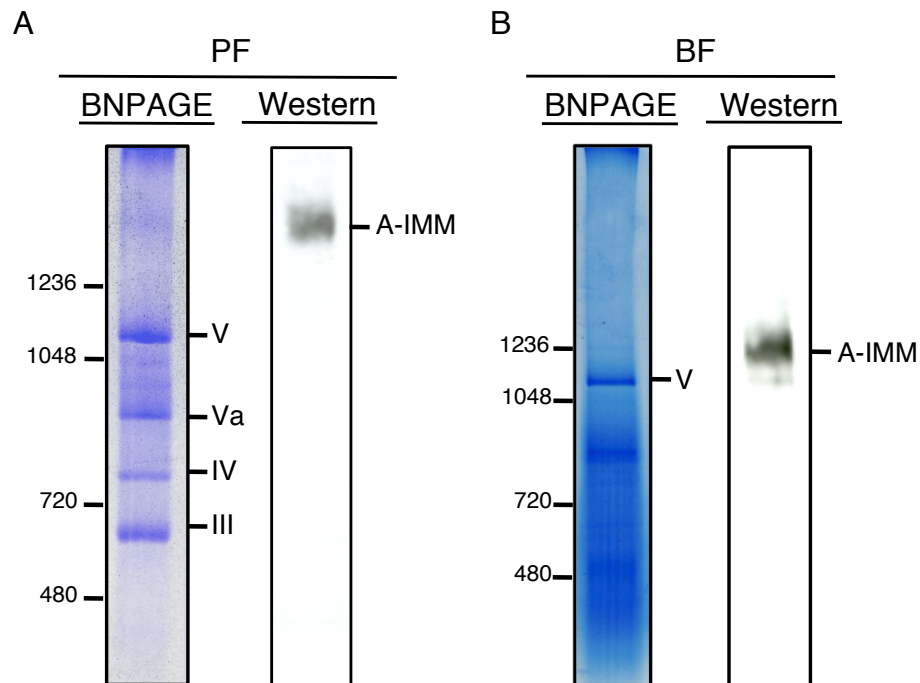


**Figure 2.4.** Differential migration of the PF and BF A-IMM. PF A) and BF B) mitochondrial membrane complexes were fractionated by BN-PAGE and analyzed by Western blot using antibodies against AEP-1 to reveal position of the A-IMM. Positions of the complexes III, IV, V and Va are also noted.

#### **Purification and composition of the A-IMM.**

The initial LC-MS/MS analysis revealed that a diverse set of proteins associated with the PF A-IMM including subunits of ATPase $F_1F_0$ , cytochrome c oxidase and  $\alpha$ -KD complexes. We used a similar crude anion exchange chromatography method as described in Priest and Hajduk (1992) to further purify the A-IMM from potential contaminating proteins (17). PF mitochondrial lysates were only used in this analysis because milligram amounts of membrane proteins could be generated and the previously

identified electron transport complexes could be used as markers during the purification. The extracted proteins were applied to a DEAE sephadex column, washed extensively and complexes were eluted with NaCl. The starting material (SM), flow through (FT), final wash (FW) and elution fractions were resolved by BNPAGE and further analyzed by Western blot. The native gel profiles differ slightly between the initial PF analysis (Figure 2.2A) and post anion exchange purification (Figure 2.6A). This is thought to be due to the differences in detergent concentrations between the membrane complex isolation and the equilibration buffers. These additional complexes were not observed in our elutions and either remained tightly bound to the DEAE resin or exited the column in the mobile phase (FT). The initial observation of the FT revealed that the ATPase- $F_1F_0$  and cytochrome c oxidase complexes were not retained by the resin (Figure 2.6A). A-IMM and complex III were both eluted between 0.1-0.3 M NaCl and relative to the cytochrome bc1, the A-IMM was recovered exclusively with 0.1 M salt (Figure 2.6A and B). This purification also reduced the heterogeneity of this structure since the 0.1 M band seems to be more compact than in the input fraction (Figure 2.6A and B). Table 1 list the proteins identified by LC-MS/MS from the 0.1 M A-IMM and 0.3 M cytochrome bc1 fraction gel bands. There was a decrease in the amount of recovered sequences for both the A-IMM and cytochrome bc1 with an 85% reduction in the A-IMM proteins as compared to the unpurified complex analysis (Table 2.1 and Table S2.1). This suggested that many of the proteins found in the initial PF analysis were either non-core components or contaminants. Remarkably, both isoforms of the E1 subunit and E2 of the soluble  $\alpha$ -KD remain associated with the A-IMM.



**Figure 2.5.** Identification of AEP-1. Alignment of bona fide COXIII (amino acids 100-150) and AEP-1 (amino acids 26-75) with diagrams of corresponding mRNA positions for each sequence. The schematic shows that the identified nine amino acid AEP-1 specific peptide (blue) is buried within the unique N-terminus (gray). Positions of the fully edited COXIII mRNA (black), pre-edited sequence (gray) and junction region (red) are indicated.

## DISCUSSION

This study utilized a proteomics approach to identify mitochondrial membrane complexes in *T. brucei*. BNPAGE, Western blot and LC-MS/MS identified a total of five membrane complexes in PF mitochondria and two in the BF. Despite the drastic compositional changes of the PF and BF mitochondrion, AEP-1 was also expressed in a mitochondrial membrane complex in PF cells. Purification of the AEP-1 associated A-IMM by anion exchange chromatography led to the identification of three subunits of the  $\alpha$ -ketoglutarate dehydrogenase complex and provided a unique localization to these historically matrix localized proteins. Additionally, a single peptide for the unique N-

terminus of AEP-1 was identified and provided the first translational evidence of an alternatively edited mRNA in the mitochondrion of *T. brucei*.

The native gel profile of mitochondrial membrane complexes in PF and BF *T. brucei* illustrated the differences in bioenergetics of this organelle during the biphasic life cycle (Figure 2.3 and Figure S2.1). Abundant proline in the insect midgut induces activation of mitochondrial pathways involved in oxidation of this amino acid and the synthesis of ATP. Complexes III and IV, which have important roles in metabolizing substrates generated from the Krebs pathway, were fractionated using our methods. Contrasting to the PF trypanosomes, BF cells proliferate in an environment that is rich in glucose and this metabolite is initially degraded in glycosomes, which subsequently leads to the production of the excretion product pyruvate. No cytochrome containing complexes were detected during the BF analysis and supported the switch from mitochondrial oxidative phosphorylation to glycosomal carbohydrate metabolism. Despite regulation of the  $\alpha$ ,  $\gamma$  and  $\epsilon$  subunits of the  $F_1$  portion of the ATPase- $F_1F_0$  in BF cells, the ATP hydrolyzing complex V had an identical mass (1.1 Mda) as the mitochondrial ATP synthase in PF trypanosomes. All of these complexes were positively identified by LC-MS/MS and suggested that tandem detergent treatment of hypotonically isolated mitochondria specifically extracted inner mitochondrial membrane complexes.

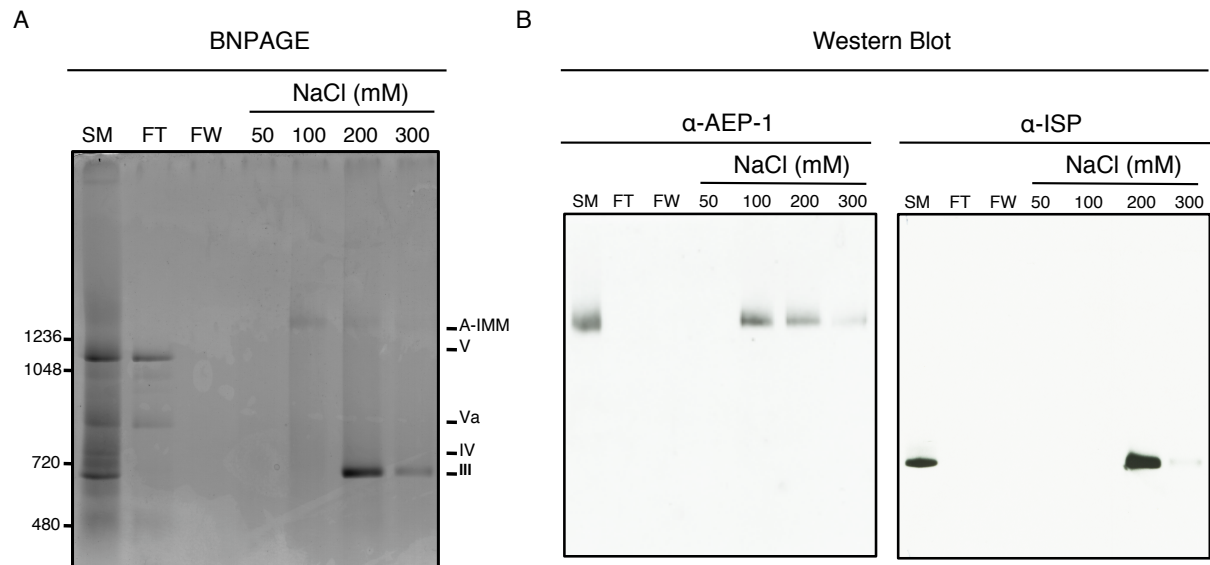


**Figure 2.6.** Purification of the A-IMM by anion exchange chromatography. Mitochondrial membrane complexes were separated on a DEAE sephadex column and proteins were eluted with a 0.05-.3M step gradient. All fractions were analyzed by BN-PAGE A) and Western Blot B) using antibodies against AEP-1 and ISP. Starting material (SM), flow through (FT), final wash (FW) and the positions of A-IMM and complexes III, IV, V and Va are indicated.

The kDNA provides insufficient genetic information for proteins that are required subunits of mitochondrial membrane complexes involved in energy production. Mitochondrial RNA editing further refines these crude sequences and creates functional transcripts that encode both conventional and unique proteins. The atypical AEP-1 was initially discovered and characterized in BF *T. brucei* because of a circulating pool of diverse COXIII mRNAs in the repressed mitochondrion (28, 29). These studies in BF cells led us to question if AEP-1 was expressed in PF cells, since preservation of the

mitochondrial genome and RNA editing is essential in this form. Our immunolocalization results revealed that AEP-1 is expressed in the mitochondrion and TAC of PF trypanosomes (Figure 2.1). The TAC localization of AEP-1 in PF cells is similar to that of the BF (22) and suggested that this protein also serves as a kDNA maintenance factor at this stage. Future studies are needed to validate this role in PF *T. brucei*.

Prior to this study, a role for the A-IMM was yet to be determined and we sought to identify subunits of this complex by LC-MS/MS to assign a function. Our BNPAGE fractionation methods successfully resolved an antibody reactive PF and BF A-IMM that both migrated above 1.2 Mda (Figure 2.4). A-IMM sequencing revealed 12 additional proteins in the larger PF complex and coincides with the considerable migration difference between the two forms (Tables S2.1 and 6). Both the PF and BF A-IMMs contained the  $\beta$  (Tb927.3.1380) and  $\gamma$  (Tb10.100.0070) subunits of complex V, E2 (Tb11.01.3550) subunit of the  $\alpha$ -KD and two hypothetical proteins (Tb10.6k15.2510 and Tb927.5.2930). Since Tb927.3.1380, Tb10.100.0070, Tb10.6k15.2510 and Tb927.5.2930 are exclusively shared by both the A-IMM and all complex V forms, we suspect that these assemblies may interact. Moreover, Schagger (2001) reviewed the effect of certain detergents and BNPAGE on respirasomes (30) and it is possible that our methods caused dissociation of subunits (streaky pattern observed on 2D in (Figure 2.3A and Figure S2.1) which can complicate LC-MS/MS analysis. Extensive purification of the PF AEP-1 complex revealed the association of  $\alpha$ -KD subunits (Table 2.1). The  $\alpha$ -

Table 2.1  
Subunits of the PF A-IMM and cytochrome c reductase (complex III) identified by LC-MS/MS post anion exchange purification

| Gene ID  | Annotation   | peptides <sup>1</sup> |
|--|--|-----------------------|
| A-IMM (0.1M NaCl <sup>3</sup> )                  |  |                       |
| Tb11.01.3550                                     | 2-oxoglutarate dehydrogenase, E2 component                   | 12                    |
| Tb11.01.1740                                     | 2-oxoglutarate dehydrogenase E1 component                    | 5                     |
| Tb11.47.0004                                     | 2-oxoglutarate dehydrogenase subunit E1 isoform              | 3                     |
| Cytochrome c reductase (0.3M NaCl <sup>3</sup> ) |  |                       |
| Tb927.5.1060                                     | mitochondrial processing peptidase, beta subunit             | 17                    |
| Tb10.389.0690                                    | mitochondrial processing peptidase subunit alpha             | 16                    |
| Tb09.211.4700                                    | reiske iron-sulfur protein , mitochondrial precursor         | 14                    |
| Tb927.8.1890                                     | cytochrome c1, heme protein                                  | 7                     |
| Tb11.01.8225 <sup>2</sup>                        | hypothetical protein   | 4                     |
| Tb10.70.3010 <sup>2</sup>                        | hypothetical protein   | 4                     |
| Tb10.70.2970                                     | ubiquinol-cytochrome c reductase complex 14 kDa subunit (VI) | 3                     |
| Tb927.5.2560 <sup>2</sup>                        | hypothetical protein   | 3                     |

<sup>1</sup> Peptides identified by BNPAGE analysis of membrane complexes

<sup>2</sup> Mitochondrial localizations based on TargetP software

<sup>3</sup> Elution fraction from anion exchange purification

KD is a Krebs pathway enzyme that has a key role in the breakdown of  $\alpha$ -ketoglutarate, thereby producing CO<sub>2</sub>, NADH and succinyl-CoA (31). This complex belongs to a group of multimeric enzymes that mainly reside in the mitochondrial matrix called  $\alpha$ -keto acid dehydrogenase complexes (includes pyruvate dehydrogenase and branched-chain alpha-keto acid dehydrogenase complexes). The  $\alpha$ -KD is composed of a succinyl transferase (E2) core that is surrounded by the  $\alpha$ -ketoglutarate dehydrogenase (E1) and dihydrolipoamide dehydrogenase (E3). Four of these subunits, including two isomers of E1, were identified in the initial sequencing of the PF A-IMM (Table S2.1). E3 was not

detected post anion exchange chromatography and suggests that the stringent conditions of the purification dissociated the protein from the A-IMM. Moreover, the E2 component was also identified in the primary LC-MS/MS analysis of the BF A-IMM (Table S2.6). The Krebs cycle is nonfunctional in BF *T. brucei* (3, 5) and the presence of E2 suggests an alternate function of this protein in the repressed mitochondrion.

Early studies of mitochondrial energy metabolism revealed complex – complex interactions between multiple Krebs cycle enzymes and also with the NADH dehydrogenase of the respiratory chain (32). These interactions also include assemblies that associate with the mitochondrial membranes and complete  $\alpha$ -KD extraction has been proven difficult, thus requiring more than simple mitochondrion disruption (32). The mediator of this membrane interaction is not known and Bogenhagen et al. (2003) proposed that the lipoyl group attached to the  $\alpha$ -KDE2 might anchor this protein to the membrane (33). Our studies have revealed that AEP-1 associates with subunits of the  $\alpha$ -KD and we suggest that this alternatively edited protein acts as the membrane anchor for this complex.

The studies reported give a description of the composition of conventional and novel mitochondrial membrane complexes in *T. brucei*. Moreover, this proteomic analysis affirmed the translation of kDNA-encoded AEP-1 and revealed the assembly of the protein with  $\alpha$ -KD subunits in the mitochondrion. A membrane bound  $\alpha$ -KD reveals a more complex level of metabolic enzyme organization and may provide the first clue of more efficient substrate channeling between the Krebs pathway and electron transport chain in *T. brucei*. Future studies are needed to identify complexes that interact with  $\alpha$ -KD at the mitochondrial membranes. Overall, additional proof is provided that

demonstrates RNA editing as not just a repair process, but also a mechanism of creating protein complex diversity in trypanosomes.

## MATERIALS AND METHODS

### **Cell culture.**

PF *T. brucei* (TRUE667) were grown in Cunningham's (SM) medium supplemented with fetal bovine serum (FBS, Gemini Bio-products, West Sacramento, CA). BF *T. brucei* (TRUE667) were maintained in HMI-9 medium containing FBS and Serum Plus media supplement (SAFC Biosciences, Lenexa, KS).

### **Fractionation of mitochondrial proteins.**

Cultured TRUE667 PF and TRUE667 BF cells isolated from Sprague-Dawley rats were hypotonically ruptured and mitochondria were purified by a method described in Harris et al. (1990) (23). The mitochondrial membrane fraction was isolated by a tandem detergent treatment as discussed in Ochsenreiter and Hajduk (2006) (15).  $1 \times 10^7$  mitochondrial equivalents of membrane proteins were denatured in a reducing SDS loading buffer and applied to gel and resolved by SDS-PAGE. Gels were either stained with coomassie or analyzed by Western blot. Mitochondrial complexes from both stages were extracted by a modified protocol demonstrated by Wittig et al. (2006) (34). 200  $\mu\text{g}$  of intact mitochondria were solubilized in buffer (2% [w/v] n-dodecyl- $\beta$ -D-maltoside [Sigma, St. Louis, MO, USA], 50 mM NaCl, 50 mM imidazole, 2 mM 6-aminohexanoic, 1mM EDTA and 1 x Complete<sup>®</sup> EDTA free protease inhibitor cocktail [Roche, Indianapolis, IN, USA], pH 7 at 4°C) for one hour on ice. Unsolubilized material was

collected by centrifugation (13,000xg for 20 min on ice) and the soluble material was saved for subsequent native analysis. 30 µg (PF) and 70 µg (BF) was loaded onto a 3.5 - 13% gradient blue native gel and fractionated at 4°C for 20 hours followed by further staining with coomassie. Unstained lanes were excised, layered on top of a 2<sup>nd</sup> dimension (2D) SDS-PAGE gel and resolved further to separate subunits. 2D gels were transferred to nitrocellulose membranes for Western analysis.

### **BNPAGE fractionation of membrane complexes.**

A 3-12% gradient acrylamide gel was prepared and run as previously described in Wittig et al. (2006) (34). 40 µg (PF) and 70 µg (BF) of mitochondrial membrane protein extract was supplemented with glycerol and Coomassie Blue G-250 (35) and applied to the blue native gel. Gels were run in a cathode buffer containing 50 mM tricine, 7.5 mM imidazole and 0.02% Coomassie Blue G-250 (pH 7.0) and an a 25 mM imidazole anode buffer at 100 V overnight at 4°C. Post electrophoresis, gels were either stained further with Coomassie or analyzed by Western blot.

### **Anion exchange purification.**

Crude anion exchange purification was performed as previously described in Priest and Hajduk (1992) with minor modifications (17). 2 mg of protein from the mitochondrial membrane fraction were isolated as described above and diluted 1:3 in a binding buffer containing 0.5% [w/v] n-dodecyl-β-D-maltoside, 50 mM NaCl, 50 mM imidazole, 2 mM 6-aminohexanoic and 1mM EDTA at pH 7.4. The diluted extract was applied to a DEAE sephadex column that was previously equilibrated with a full column volume of the same

binding buffer. The column was washed with two column volumes of binding buffer and eluted with 1 ml pulses of increasing NaCl (0.05-0.3M). A total of seven fractions were resolved by BNPAGE and evaluated by Western blot.

#### **In-gel trypsin digestion and LC-MS/MS identification.**

Proteins were digested enzymatically from excised gel band pieces using sequencing grade porcine trypsin (Promega, Madison, WI, USA) by an overnight incubation at 37°C. Gel pieces were washed with 50% and 100% acetonitrile and 100 mM ammonium bicarbonate containing 50% acetonitrile and proteins were subsequently reduced in 10 mM dithiothreitol (Sigma)/100 mM Ambic solution at 56°C for one hour. Proteins were alkylated using 55 mM iodoacetamide/100 mM ammonium bicarbonate (in the dark) and solution was adjusted to pH 8 using 100 mM ammonium bicarbonate. 100 mM ammonium bicarbonate/acetonitrile (1:1) solution was used for the initial tryptic peptide extraction followed by two more with 3% formic acid/acetonitrile (1:1). Combined extracts dried by vacuum centrifugation and resuspended in 0.1% formic acid. Samples were analyzed on an Agilent 1100 capillary LC (Santa Clara, CA) interfaced directly to a LTQ linear ion trap mass spectrometer (Thermo Fisher, San Jose, CA). The digested peptides were pressure loaded for one hour onto a PicoFrit column (New Objective, Woburn, MA) and eluted into the mass spectrometer, which was set to acquire LC-MS/MS spectra. The predicted sequences were compared to target NCBI and decoy (reverse sequence) databases and statistically significant proteins were determined at a 1% false discovery rate using ProteoIQ software (NuSep, Bogart, GA, USA).

**Western Blot Analysis.**

Protein blots were blocked in 5% (w/v) milk/TBST (150 mM NaCl, 10 mM Tris-HCl pH 8, 0.05% (v/v) Tween 20) and incubated overnight with the following primary antibodies polyclonal rabbit AEP-1 (1:4000), monoclonal mouse ISP (1:2000), polyclonal rabbit COXIV (1:100), polyclonal rabbit ATPase-F<sub>1</sub> (1:4000) and polyclonal peroxidase anti-peroxidase soluble complex (PAP, 1:5000; Sigma). Blots were washed three times and incubated with a goat anti-rabbit HRP secondary antibody (1:5000) for one hour, washed three additional times and exposed to film.

**Immunofluorescence microscopy.**

Log phase cultured PF cells were incubated with MitoTracker® (Life Technologies, Grand Island, NY, USA), washed, equilibrated with media for 30 minutes and attached to poly-l-lysine slides for 30 additional minutes. Cells were fixed with 0.5% paraformaldehyde for one minute, washed in PBS, and fixed with -20°C methanol in for 10 minutes. Slides were washed and blocked using 20% fetal bovine serum in PBS. Cells were incubated with AEP-1 polyclonal antibodies (1:500) diluted in blocking buffer and remained in primary for one hour. Slides were washed and cells were incubated with appropriate secondary antibody (1:500) for 30 minutes. Cell ghost were created by mildly fixing cells in 0.5% paraformaldehyde, washing and then incubating the cells in 0.5% Triton X-100, 10 mM NaH<sub>2</sub>PO<sub>4</sub>, 150mM NaCl, 1 mM MgCl, pH 7.2 buffer (16). After secondary, slides were rinsed in PBS and coated with 4',6'-diamidino-2-phenylindole (DAPI) containing the antifade reagent ProlongGold (Life Technologies).

Images were acquired using a Zeiss Axio Observer inverted microscope equipped with an AxioCam HSm and evaluated with AxioVision v4.6 software (Zeiss).

#### ACKNOWLEDGEMENTS

We thank Noreen Williams (ATPase-F<sub>1</sub>) and Julius Lukes (COXIV) for kindly providing antibodies. We also thank Torsten Ochsenreiter, David Seidman and members of the Hajduk lab for helpful discussions concerning the work presented in this study. Funding for this work was supported by NIH AI21401 to SLH.

#### REFERENCES

1. **Englund, P. T., S. L. Hajduk, and J. C. Marini.** 1982. The molecular biology of trypanosomes. *Annu Rev Biochem* **51**:695-726.
2. **de Souza, W., M. Attias, and J. C. Rodrigues.** 2009. Particularities of mitochondrial structure in parasitic protists (Apicomplexa and Kinetoplastida). *Int J Biochem Cell Biol* **41**:2069-2080.
3. **Vickerman, K.** 1985. Developmental cycles and biology of pathogenic trypanosomes. *Br Med Bull* **41**:105-114.
4. **Coley, A. F., H. C. Dodson, M. T. Morris, and J. C. Morris.** 2011. Glycolysis in the african trypanosome: targeting enzymes and their subcellular compartments for therapeutic development. *Mol Biol Int* **2011**:123702.
5. **van Hellemond, J. J., F. R. Opperdoes, and A. G. Tielens.** 2005. The extraordinary mitochondrion and unusual citric acid cycle in *Trypanosoma brucei*. *Biochem Soc Trans* **33**:967-971.

6. **Panigrahi, A. K., Y. Ogata, A. Zikova, A. Anupama, R. A. Dalley, N. Acestor, P. J. Myler, and K. D. Stuart.** 2009. A comprehensive analysis of *Trypanosoma brucei* mitochondrial proteome. *Proteomics* **9**:434-450.
7. **Navarro, M., X. Penate, and D. Landeira.** 2007. Nuclear architecture underlying gene expression in *Trypanosoma brucei*. *Trends Microbiol* **15**:263-270.
8. **Priest, J. W., and S. L. Hajduk.** 1996. In vitro import of the Rieske iron-sulfur protein by trypanosome mitochondria. *J Biol Chem* **271**:20060-20069.
9. **Lukes, J., H. Hashimi, and A. Zikova.** 2005. Unexplained complexity of the mitochondrial genome and transcriptome in kinetoplastid flagellates. *Curr Genet* **48**:277-299.
10. **Benne, R., J. Van den Burg, J. P. Brakenhoff, P. Sloof, J. H. Van Boom, and M. C. Tromp.** 1986. Major transcript of the frameshifted *coxII* gene from trypanosome mitochondria contains four nucleotides that are not encoded in the DNA. *Cell* **46**:819-826.
11. **Feagin, J. E., J. M. Abraham, and K. Stuart.** 1988. Extensive editing of the cytochrome c oxidase III transcript in *Trypanosoma brucei*. *Cell* **53**:413-422.
12. **Horvath, A., E. A. Berry, and D. A. Maslov.** 2000. Translation of the edited mRNA for cytochrome b in trypanosome mitochondria. *Science* **287**:1639-1640.
13. **Stuart, K. D., A. Schnauffer, N. L. Ernst, and A. K. Panigrahi.** 2005. Complex management: RNA editing in trypanosomes. *Trends Biochem Sci* **30**:97-105.
14. **Ochsenreiter, T., M. Cipriano, and S. L. Hajduk.** 2008. Alternative mRNA editing in trypanosomes is extensive and may contribute to mitochondrial protein diversity. *PLoS One* **3**:e1566.
15. **Ochsenreiter, T., and S. L. Hajduk.** 2006. Alternative editing of cytochrome c oxidase III mRNA in trypanosome mitochondria generates protein diversity. *EMBO Rep* **7**:1128-1133.
16. **Ogbadoyi, E. O., D. R. Robinson, and K. Gull.** 2003. A high-order trans-membrane structural linkage is responsible for mitochondrial genome positioning and segregation by flagellar basal bodies in trypanosomes. *Mol Biol Cell* **14**:1769-1779.

17. **Priest, J. W., and S. L. Hajduk.** 1992. Cytochrome c reductase purified from *Crithidia fasciculata* contains an atypical cytochrome c1. *J Biol Chem* **267**:20188-20195.
18. **Speijer, D., C. K. Breek, A. O. Muijsers, A. F. Hartog, J. A. Berden, S. P. Albracht, B. Samyn, J. Van Beeumen, and R. Benne.** 1997. Characterization of the respiratory chain from cultured *Crithidia fasciculata*. *Mol Biochem Parasitol* **85**:171-186.
19. **Speijer, D., A. O. Muijsers, H. Dekker, A. de Haan, C. K. Breek, S. P. Albracht, and R. Benne.** 1996. Purification and characterization of cytochrome c oxidase from the insect trypanosomatid *Crithidia fasciculata*. *Mol Biochem Parasitol* **79**:47-59.
20. **Horvath, A., T. G. Kingan, and D. A. Maslov.** 2000. Detection of the mitochondrially encoded cytochrome c oxidase subunit I in the trypanosomatid protozoan *Leishmania tarentolae*. Evidence for translation of unedited mRNA in the kinetoplast. *J Biol Chem* **275**:17160-17165.
21. **Acestor, N., A. Zikova, R. A. Dalley, A. Anupama, A. K. Panigrahi, and K. D. Stuart.** 2011. *Trypanosoma brucei* mitochondrial respiratome: composition and organization in procyclic form. *Mol Cell Proteomics* **10**:M110 006908.
22. **Ochsenreiter, T., S. Anderson, Z. A. Wood, and S. L. Hajduk.** 2008. Alternative RNA editing produces a novel protein involved in mitochondrial DNA maintenance in trypanosomes. *Mol Cell Biol* **28**:5595-5604.
23. **Harris, M. E., D. R. Moore, and S. L. Hajduk.** 1990. Addition of uridines to edited RNAs in trypanosome mitochondria occurs independently of transcription. *J Biol Chem* **265**:11368-11376.
24. **Williams, N., and P. H. Frank.** 1990. The mitochondrial ATP synthase of *Trypanosoma brucei*: isolation and characterization of the intact F1 moiety. *Mol Biochem Parasitol* **43**:125-132.
25. **Maslov, D. A., A. Zikova, I. Kyselova, and J. Lukes.** 2002. A putative novel nuclear-encoded subunit of the cytochrome c oxidase complex in trypanosomatids. *Mol Biochem Parasitol* **125**:113-125.
26. **Priest, J. W., and S. L. Hajduk.** 1994. Developmental regulation of *Trypanosoma brucei* cytochrome c reductase during bloodstream to procyclic differentiation. *Mol Biochem Parasitol* **65**:291-304.

27. **Wittig, I., and H. Schagger.** 2009. Supramolecular organization of ATP synthase and respiratory chain in mitochondrial membranes. *Biochim Biophys Acta* **1787**:672-680.
28. **Abraham, J. M., J. E. Feagin, and K. Stuart.** 1988. Characterization of cytochrome c oxidase III transcripts that are edited only in the 3' region. *Cell* **55**:267-272.
29. **Decker, C. J., and B. Sollner-Webb.** 1990. RNA editing involves indiscriminate U changes throughout precisely defined editing domains. *Cell* **61**:1001-1011.
30. **Schagger, H.** 2001. Respiratory chain supercomplexes. *IUBMB Life* **52**:119-128.
31. **Perham, R. N.** 1991. Domains, motifs, and linkers in 2-oxo acid dehydrogenase multienzyme complexes: a paradigm in the design of a multifunctional protein. *Biochemistry* **30**:8501-8512.
32. **Srere, P. A.** 1987. Complexes of sequential metabolic enzymes. *Annu Rev Biochem* **56**:89-124.
33. **Bogenhagen, D. F., Y. Wang, E. L. Shen, and R. Kobayashi.** 2003. Protein components of mitochondrial DNA nucleoids in higher eukaryotes. *Mol Cell Proteomics* **2**:1205-1216.
34. **Wittig, I., H. P. Braun, and H. Schagger.** 2006. Blue native PAGE. *Nat Protoc* **1**:418-428.
35. **Wittig, I., M. Karas, and H. Schagger.** 2007. High resolution clear native electrophoresis for in-gel functional assays and fluorescence studies of membrane protein complexes. *Mol Cell Proteomics* **6**:1215-1225.

## SUPPLEMENTAL FIGURES AND TABLES

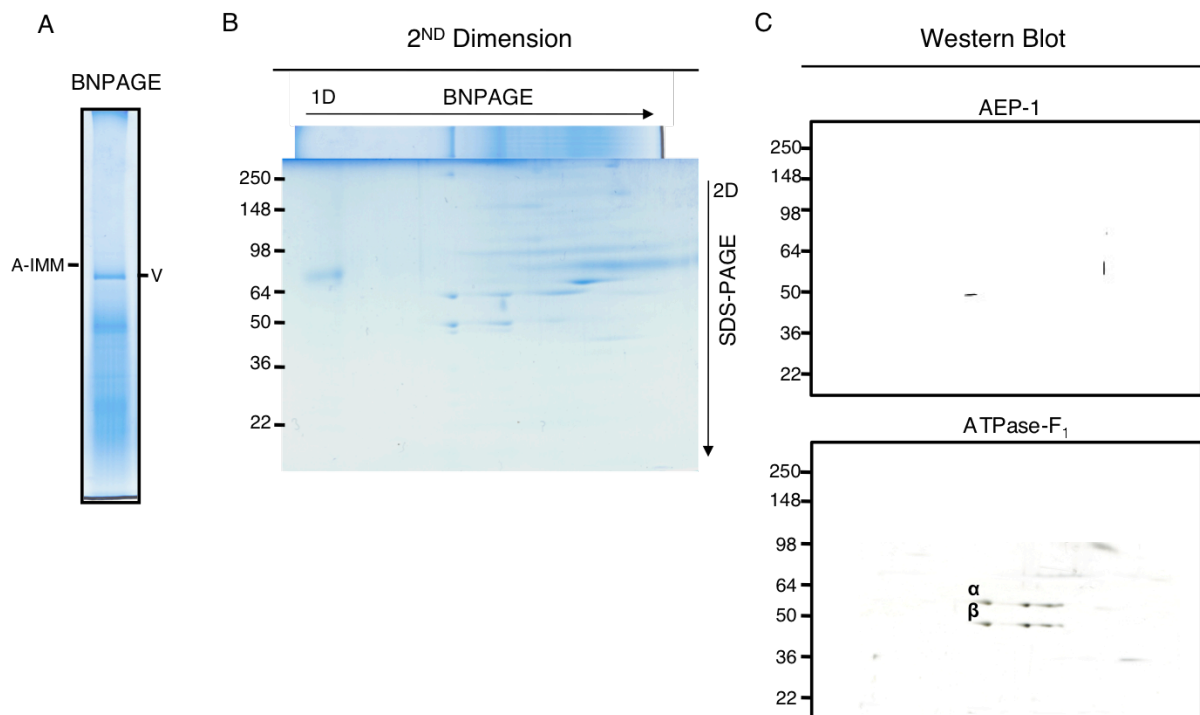


**Figure S2.1.** Native and 2D electrophoresis of mitochondrial membrane complexes from BF *T. brucei*. **(A)** Mitochondria from PF *T. brucei* were solubilized in 0.5% Triton X-100 and 2% n-dodecyl- $\beta$ -D-maltoside, loaded on a BN-PAGE gradient gel (4-13%) and coomassie-stained. **(B)** Subunits of the native complexes were separated by SDS-PAGE and stained by coomassie. **(C)** Western blot analysis of 2D gels. Western blots were analyzed using antibodies against AEP-1 and ATPase-F<sub>1</sub>. Positions of the A-IMM and complex V are shown. The  $\alpha$  and  $\beta$  subunits of the ATPase-F<sub>1</sub> are also shown.

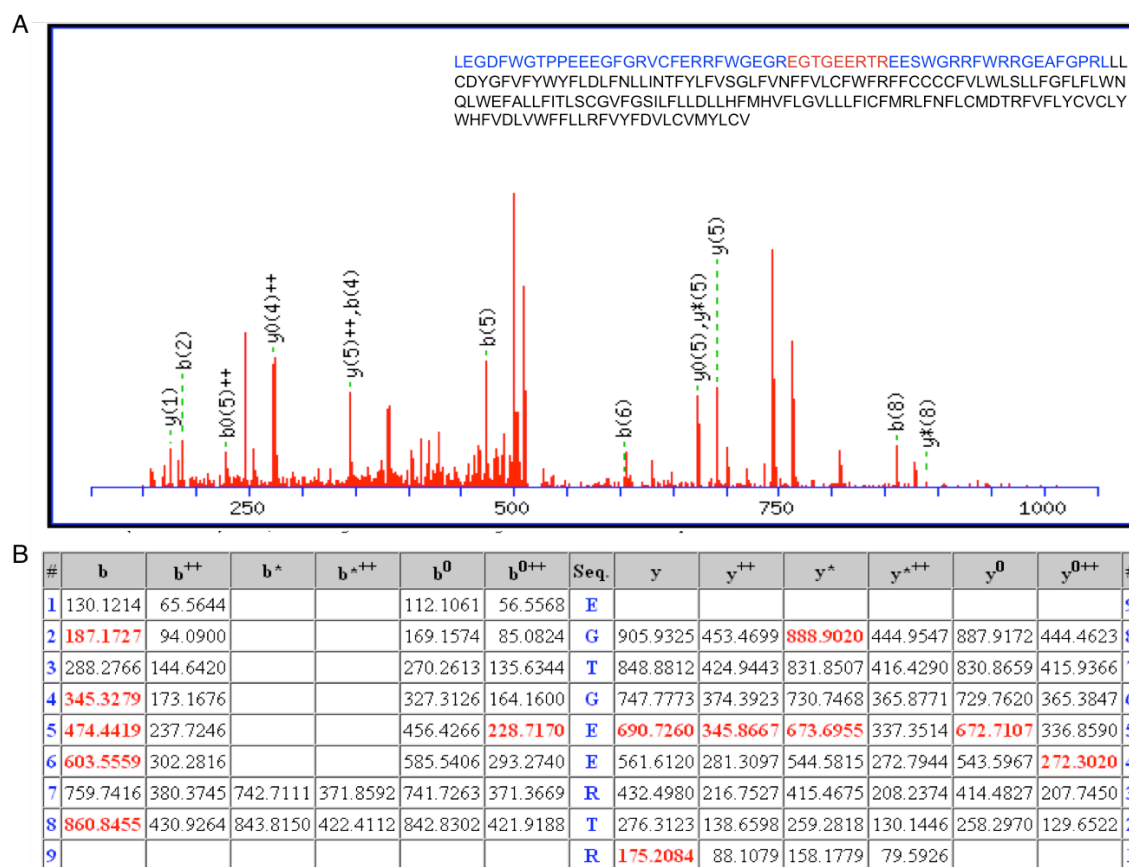


**Figure S2.2.** LC-MS/MS identification of AEP-1. **(A)** Ion spectrum from tryptic peptide EGTGEERTR (average mass of 1034.039) from the unique N-terminus of AEP-1. Sequence of AEP-1 shown with novel N-terminus (blue), identified peptide (red) and COXIII sequence (black) are shown. **(B)** Identified b and y ions for the EGTGEERTR peptide. Positively matched ions (red) are based on the 60 most intense peaks.

Table S2.1  
Subunits of the PF A-IMM identified by LC-MS/MS

| Gene ID                     | Annotation                                       | peptides <sup>1</sup> |
|-----------------------------|--|-----------------------|
| Tb11.01.1740 <sup>2</sup>   | 2-oxoglutarate dehydrogenase E1 component        | 41                    |
| Tb11.47.0004 <sup>2</sup>   | 2-oxoglutarate dehydrogenase subunit E1 isoform  | 42                    |
| Tb11.01.3550 <sup>2</sup>   | 2-oxoglutarate dehydrogenase, E2 component       | 18                    |
| Tb11.01.8470                | dihydrolipoamide dehydrogenase, E3               | 2                     |
| Tb11.0400 <sup>3</sup>      | hypothetical protein                             | 4                     |
| Tb927.8.5200 <sup>3</sup>   | hypothetical protein                             | 14                    |
| Tb10.6k15.2510 <sup>3</sup> | hypothetical protein                             | 10                    |
| Tb927.5.2930 <sup>3</sup>   | hypothetical protein                             | 20                    |
| Tb09.160.4750 <sup>3</sup>  | hypothetical protein                             | 9                     |
| Tb.11.47.0024 <sup>3</sup>  | hypothetical protein                             | 8                     |
| Tb927.3.1380                | ATP synthase beta chain, mitochondrial precursor | 18                    |
| Tb09.160.4750 <sup>3</sup>  | hypothetical protein                             | 6                     |
| Tb10.100.0070               | ATP synthase F1 subunit gamma protein            | 6                     |
| Tb11.02.0130 <sup>3</sup>   | hypothetical protein                             | 6                     |
| Tb10.70.0430                | chaperonin Hsp60, mitochondrial precursor        | 16                    |
| Tb927.6.2010 <sup>3</sup>   | hypothetical protein                             | 5                     |
| Tb11.01.2340 <sup>3</sup>   | hypothetical protein                             | 3                     |
| Tb09.211.1750               | mitochondrial carrier protein                    | 6                     |
| Tb927.7.210                 | proline oxidase                                  | 8                     |

<sup>1</sup>Peptides identified by BNPAGE analysis of membrane complexes

<sup>2</sup>Proteins also identified by SDSPAGE (2D) at calculated molecular weight

<sup>3</sup>Mitochondrial localizations based on TargetP software

Table S2.2  
Sub units of the PF ATPase-F<sub>1</sub>F<sub>o</sub> (complex V) identified by LC-MS/MS

| Gene ID                     | Annotation                                       | peptides <sup>1</sup> |
|-----------------------------|--|-----------------------|
| Tb927.5.2930 <sup>2</sup>   | hypothetical protein                             | 22                    |
| Tb11.0400 <sup>2</sup>      | hypothetical protein                             | 2                     |
| Tb10.100.0070               | ATP synthase F1 subunit gamma protein            | 9                     |
| Tb927.3.1380                | ATP synthase beta chain, mitochondrial precursor | 20                    |
| Tb10.70.7760 <sup>2</sup>   | hypothetical protein                             | 7                     |
| Tb10.6k15.2510 <sup>2</sup> | hypothetical protein                             | 5                     |
| LMJF_05_0500                | ATPase alpha subunit [Leishmania major]          | 12                    |
| Tb10.389.0690               | mitochondrial processing peptidase alpha subunit | 5                     |
| Tb09.211.1750               | mitochondrial carrier protein                    | 5                     |
| Tb927.6.4990                | ATP synthase, epsilon chain                      | 3                     |

<sup>1</sup> Peptides identified by BNPAGE analysis of membrane complexes

<sup>2</sup> Mitochondrial localizations based on TargetP software

Table S2.3  
Subunits of the PF alternative ATPase-F<sub>1</sub>F<sub>o</sub> (complex Va) identified by LC-MS/MS

| Gene ID                     | Annotation                                       | peptides <sup>1</sup> |
|-----------------------------|--|-----------------------|
| Tb10.6k15.2510 <sup>2</sup> | hypothetical protein                             | 15                    |
| Tb11.0400 <sup>2</sup>      | hypothetical protein                             | 7                     |
| Tb927.5.2930 <sup>2</sup>   | hypothetical protein                             | 24                    |
| Tb927.3.1380                | ATPase beta subunit                              | 39                    |
| Tb09.160.4310               | glutamate dehydrogenase                          | 21                    |
| Tb11.02.0250                | heat shock protein, mitochondrial precursor      | 15                    |
| Tb09.211.1750               | mitochondrial carrier protein                    | 9                     |
| Tb927.5.1710                | ribonucleoprotein p18, mitochondrial precursor   | 12                    |
| Tb10.389.0690               | mitochondrial processing peptidase alpha subunit | 7                     |
| Tb10.100.0070               | ATP synthase F1 subunit gamma protein            | 8                     |
| Tb927.7.210                 | proline oxidase                                  | 12                    |
| Tb10.70.2920                | prohibitin                                       | 11                    |
| Tb927.5.1060                | mitochondrial processing peptidase, beta subunit | 11                    |
| Tb10.6k15.0480              | hypothetical protein                             | 9                     |
| Tb10.6k15.3250              | succinyl-CoA ligase                              | 7                     |
| Tb10.70.0430                | chaperonin Hsp60, mitochondrial precursor        | 17                    |
| Tb09.211.4740 <sup>2</sup>  | hypothetical protein                             | 7                     |
| Tb927.1.4100                | cytochrome C oxidase subunit IV                  | 5                     |
| Tb09.160.1820               | cytochrome c oxidase subunit V                   | 4                     |
| Tb11.01.1900 <sup>2</sup>   | hypothetical protein                             | 4                     |
| Tb11.02.1350 <sup>2</sup>   | hypothetical protein                             | 5                     |

<sup>1</sup> Peptides identified by BNPAGE analysis of membrane complexes

<sup>2</sup> Mitochondrial localizations based on TargetP software

Table S2.4  
Subunits of the PF cytochrome c reductase (complex III) identified by LC-MS/MS

| Gene ID                   | Annotation   | peptides <sup>1</sup> |
|---------------------------|--|-----------------------|
| Tb10.389.0690             | mitochondrial processing peptidase subunit alpha     | 15                    |
| Tb927.5.1060              | mitochondrial processing peptidase, beta subunit     | 21                    |
| Tb11.02.0250              | heat shock protein, mitochondrial precursor          | 20                    |
| Tb10.70.4280              | delta-1-pyrroline-5-carboxylate dehydrogenase        | 13                    |
| Tb10.70.3010 <sup>2</sup> | hypothetical protein                                 | 9                     |
| Tb927.3.1380              | ATPase beta subunit                                  | 23                    |
| Tb10.70.2970 <sup>2</sup> | hypothetical protein                                 | 10                    |
| Tb11.01.1740              | 2-oxoglutarate dehydrogenase E1 component            | 13                    |
| Tb09.211.4700             | reiske iron-sulfur protein , mitochondrial precursor | 14                    |
| Tb09.211.1750             | mitochondrial carrier protein                        | 8                     |
| Tb10.70.0430              | chaperonin Hsp60, mitochondrial precursor            | 17                    |
| Tb10.389.0070             | elongation factor TU                                 | 7                     |
| Tb10.100.0070             | ATP synthase F1 subunit gamma                        | 7                     |
| Tb927.3.3460 <sup>2</sup> | hypothetical protein                                 | 10                    |
| Tb927.8.6580              | succinate dehydrogenase flavoprotein                 | 7                     |
| Tb927.8.1890              | cytochrome c1, heme protein                          | 11                    |

<sup>1</sup> Peptides identified by BNPAGE analysis of membrane complexes

<sup>2</sup> Mitochondrial localizations based on TargetP software

Table S2.5  
Subunits of the PF cytochrome c oxidase (complex IV) identified by LC-MS/MS

| Gene ID                   | Annotation  | peptides <sup>1</sup> |
|---------------------------|---|-----------------------|
| Tb11.0400 <sup>2</sup>    | hypothetical protein                                | 10                    |
| Tb11.02.0250              | heat shock protein, mitochondrial precursor         | 29                    |
| Tb927.1.4100              | cytochrome C oxidase subunit IV                     | 18                    |
| Tb10.389.0690             | mitochondrial processing peptidase alpha subunit    | 13                    |
| Tb927.5.1060              | mitochondrial processing peptidase, beta subunit    | 18                    |
| Tb09.160.4310             | glutamate dehydrogenase                             | 26                    |
| Tb11.01.1740              | 2-oxoglutarate dehydrogenase E1 component, putative | 19                    |
| Tb09.211.1750             | mitochondrial carrier protein                       | 10                    |
| Tb10.70.3010 <sup>2</sup> | hypothetical protein                                | 10                    |
| Tb10.70.4280              | delta-1-pyrroline-5-carboxylate dehydrogenase       | 12                    |
| Tb10.70.3010 <sup>2</sup> | hypothetical protein                                | 8                     |
| Tb10.389.0070             | elongation factor TU                                | 9                     |
| Tb927.7.210               | proline oxidase                                     | 14                    |
| Tb11.02.4810 <sup>2</sup> | hypothetical protein                                | 7                     |
| Tb10.100.0070             | ATP synthase F1 subunit gamma protein               | 10                    |
| Tb10.100.0160             | cytochrome C oxidase subunit VI                     | 10                    |
| Tb09.160.1820             | cytochrome c oxidase subunit V                      | 6                     |
| Tb11.02.2700              | fumarate hydratase class I                          | 7                     |
| Tb09.211.4700             | Reiske iron-sulfur protein precursor                | 12                    |
| Tb11.03.0230              | isocitrate dehydrogenase                            | 5                     |
| Tb927.3.1410              | cytochrome c oxidase VII                            | 7                     |
| Tb11.01.4702              | cytochrome c oxidase subunit 10                     | 4                     |

<sup>1</sup>Peptides identified by BNPAGE analysis of membrane complexes

<sup>2</sup>Mitochondrial localizations based on TargetP software

Table S2.6  
Subunits of the BF A-IMM identified by LC-MS/MS

| Gene ID                      | Annotation  | peptides <sup>1</sup> |
|------------------------------|---|-----------------------|
| Tb10.100.0070                | ATP synthase F1 subunit gamma                           | 7                     |
| Tb927.3.1380                 | ATP synthase beta chain mitochondrial precursor         | 16                    |
| Tb927.5.2930 <sup>2</sup>    | hypothetical protein                                    | 14                    |
| Tb10.70.4280                 | delta-1-pyrroline-5-carboxylate dehydrogenase, putative | 7                     |
| Tb11.01.3550                 | 2-oxoglutarate dehydrogenase, E2 component              | 5                     |
| Tb10.61.0560 <sup>2</sup>    | hypothetical protein                                    | 6                     |
| Tb 10.6k15.2510 <sup>2</sup> | hypothetical protein                                    | 5                     |

<sup>1</sup> Peptides identified by BNPAGE analysis of membrane complexes

<sup>2</sup> Mitochondrial localizations based on TargetP software

Table S2.7  
Subunits of the BF ATPase-F<sub>1</sub>F<sub>o</sub> (complex V) identified by LC-MS/MS

| Gene ID                   | Annotation                                       | peptides <sup>1</sup> |
|---------------------------|--|-----------------------|
| Tb927.3.1380              | ATP synthase beta chain, mitochondrial precursor | 18                    |
| Tb10.6k15.2510            | hypothetical protein                             | 5                     |
| Tb927.5.2930 <sup>2</sup> | hypothetical protein                             | 10                    |
| Tb10.100.0070             | ATP synthase F1 subunit gamma protein            | 4                     |
| Tb927.5.1710              | ribonucleoprotein p18, mitochondrial precursor   | 5                     |
| Tb927.6.4990              | ATP synthase, epsilon chain                      | 2                     |

<sup>1</sup> Peptides identified by BNPAGE analysis of membrane complexes

<sup>2</sup> Mitochondrial localizations based on TargetP software

## CHAPTER 3

DUAL FUNCTIONS OF  $\alpha$ -KETOGLUTARATE DEHYDROGENASE E2 IN THE KREBS  
CYCLE AND MITOCHONDRIAL DNA INHERITANCE IN *TRYPANOSOMA BRUCEI*<sup>1</sup>

---

<sup>1</sup> Sykes, S.E. and S.L. Hajduk. Accepted by *Eukaryotic Cell*.  
Reprinted here with permission of the publisher.

## ABSTRACT

The dihydrolipoyl succinyltransferase (E2) of the multi-subunit  $\alpha$ -ketoglutarate dehydrogenase complex ( $\alpha$ -KD) is an essential Krebs cycle enzyme commonly found in the matrix of mitochondria. African trypanosomes developmentally regulate mitochondrial carbohydrate metabolism and lack a functional Krebs cycle in the bloodstream of the mammal. We found that despite the absence of a functional  $\alpha$ -KD, bloodstream form (BF) trypanosomes express  $\alpha$ -KDE2 that localized to the mitochondrial matrix and inner membrane. Furthermore,  $\alpha$ -KDE2 fractionated with the mitochondrial genome, the kinetoplast DNA (kDNA), in a complex with the flagellum. A role for  $\alpha$ -KDE2 in kDNA maintenance was revealed in  $\alpha$ -KDE2 RNAi knockdowns. Following RNAi induction, bloodstream trypanosomes showed a pronounced growth reduction and often failed to equally distribute kDNA to daughter cells, resulting in accumulation of cells devoid of kDNA (dyskinetoplastic) or containing two kinetoplasts. Dyskinetoplastic trypanosomes lacked mitochondrial membrane potential and contained mitochondria of substantially reduced volume. These results indicate that  $\alpha$ -KDE2 is bifunctional both as a metabolic enzyme and as a mitochondria inheritance factor necessary for the distribution of kDNA networks to daughter cells at cytokinesis.

## INTRODUCTION

The  $\alpha$ -keto acid dehydrogenases are multienzyme assemblies that catalyze the decarboxylation of their respective  $\alpha$ -keto acid, which subsequently produces acyl-CoA and NADH (1). This family of high molecular weight (>MDa) complexes consists of pyruvate dehydrogenase (PDH), branched chain  $\alpha$ -keto acid dehydrogenase (BCKAD) and  $\alpha$ -ketoglutarate dehydrogenase ( $\alpha$ -KD). Each complex is composed of a  $\alpha$ -keto acid dehydrogenase subunit (E1), acyltransferase subunit (E2) and a dihydrolipoamide dehydrogenase subunit (E3). Multiple copies of E2 form the cores of these multimeric complexes and the remaining components (E1 and E3) surround this structure (1). In each case, the highly conserved E2 has a similar quaternary structure with a covalently attached lipoic acid prosthetic group that swings from one active site to the next (2, 3).

Although E2 has a vital role in  $\alpha$ -KD metabolism, this enzyme has also been shown to associate with prokaryotic genomes and the mitochondrial DNA of multiple eukaryotic organisms (4-9). mtDNA is organized into stable protein-DNA units called nucleoids attached to the mitochondrial inner membrane and are involved in genome replication, segregation and maintenance (10, 11). Proteins isolated from mtDNA nucleoids from higher eukaryotes revealed

the association of the E2 enzymes from the PDH and BCKAD complexes (6). Additionally,  $\alpha$ -KD E2 ( $\alpha$ -KDE2) associates with the mtDNA nucleoid of *Saccharomyces cerevisiae* and is required for mtDNA maintenance (4, 5).

The protozoan parasite *Trypanosoma brucei* possesses a distinctive mitochondrial genome termed the kinetoplast (kDNA). The kDNA is a large network structure composed of thousands of catenated DNA minicircles (~1kb) and approximately 50 maxicircles (~20kb). Maxicircles contain the coding information for components of the oxidoreductase complexes, ATP synthase and rRNAs while minicircles encode small guide RNAs (gRNAs) necessary for post-transcriptional editing of maxicircle encoded mRNAs (12).

Mitochondrial metabolism and ATP production are developmentally regulated in *T. brucei*. In mammals, the bloodstream developmental forms of trypanosomes (BF) utilize high rates of glycolysis to produce ATP and pyruvate but lack functional Krebs cycle enzymes and mitochondrial respiratory complexes needed for oxidative phosphorylation (13). Thus, all ATP is produced by glycolytic, substrate level phosphorylation. In the midgut of the insect vector, the tsetse fly, trypanosomes rapidly differentiate to the procyclic developmental form (PF) and develop a fully functional mitochondrion capable of converting proline to succinate and transferring reducing equivalents to NADH via the Krebs cycle enzymes (14).

Despite the lack of conventional oxidative phosphorylation in the BF, the kDNA must be faithfully replicated and segregated since it encodes enzymes needed in the PF and other developmental stages in the tsetse fly (15-18). A number of structural proteins and replication enzymes necessary for kDNA replication and segregation have been identified (19, 20) and the mechanism of kDNA replication has been described in detail (21). During mitochondrial S-phase minicircles are released from the kDNA network by a type II topoisomerase and relocate to the kinetoflagellar zone (KFZ), a region between one face of the kDNA disk and the basal bodies of the flagellum (22). Next, free minicircles bind the universal binding protein (UBP) at discrete foci in the KFZ where replication initiates giving rise to replicative intermediates containing theta structures (23, 24). Replicating minicircles migrate to antipodal sites on the elongated kDNA network where single strand gaps, from lagging strand replication, are filled and the newly replicated minicircles, containing a single gap at the origin of replication, are reattached to the network (11, 25-27). RNAi knockdown or conditional knockouts of several of the key replicative enzymes results in a rapid loss of minicircles (27-29). Complete kDNA replication results in a network with twice the number of minicircles and maxicircles that undergoes lateral elongation and finally segregation to daughter cells ensuring equal inheritance of minicircles and maxicircles.

While the mechanism of network segregation is poorly understood, the association of the kDNA with a specialized portion of the mitochondrial membrane, immediately adjacent to the basal bodies of the flagellum, is required for kDNA segregation (11, 30). The association of the kDNA to the basal bodies has been defined morphologically as a filamentous network of proteins known as the tripartite attachment complex (TAC) (11). The TAC maintains a physical connection between the kDNA and flagellum and fractionates with a larger flagellum-kDNA complex (FKC) upon cell solubilization with nonionic detergents (11, 31). The TAC extends from the basal bodies of the flagellum to the outer mitochondrial membrane (exclusion zone filaments) and continues across the inner mitochondrial membrane to the KFZ face of the kDNA (unilateral filaments). To date, only two components of the TAC have been identified—1) p166 was the first protein component identified in the TAC (30). This large nuclear encoded protein was initially discovered during an RNAi library screen for kDNA replication/segregation defects (30). p166 contains an N-terminal mitochondrial import signal, as well as a short transmembrane domain, and associates with the unilateral filaments of the TAC. The RNAi knockdowns of p166 resulted in altered kDNA structure due to asymmetric segregation of the kDNA, but no effect of kDNA replication was observed (30). 2) Alternatively edited protein-1 (AEP-1), encoded by an alternatively edited cytochrome oxidase III (COIII) mRNA, is a chimeric protein with a unique N-terminal 60 amino acid DNA binding domain and five C-terminal

transmembrane domains of COIII (32). AEP-1 associates with the unilateral filaments of the TAC where it serves as a maintenance factor for the kDNA (33).

The structural organization of the kDNA network has given rise to unique mechanisms of replication, segregation and inheritance of this mitochondrial genome. Central to these processes is the FKC, which ensures segregation of the newly replicated kDNA networks and distribution to daughter cells at cytokinesis. Considering the complexity of the FKC, it is likely that both structural and motor proteins, necessary for segregation and inheritance, remain to be defined (11, 21). In this study, we report the expression of  $\alpha$ -KDE2 in the oxidative phosphorylation deficient BF *T. brucei*. We show that  $\alpha$ -KDE2 is expressed and localizes to the BF mitochondria, despite the lack of  $\alpha$ -KD activity. Surprisingly, we found that  $\alpha$ -KDE2 localized to antipodal sites on the kDNA network and is a stable component of the FKC. RNAi knockdown of  $\alpha$ -KDE2 results in increased numbers of dyskinetoplasmic cells with a corresponding increase of cells with two kinetoplasts, consistent with a role for  $\alpha$ -KDE2 in distribution of kDNA at cytokinesis and not in either segregation or replication. Finally, depletion of  $\alpha$ -KDE2 results in collapse of the mitochondrial membrane potential in dyskinetoplasmic cells and a reduction in total mitochondrial volume. These data demonstrate the importance of  $\alpha$ -KDE2 as a bifunctional protein necessary for the maintenance of the kDNA and mitochondrion in *T. brucei*.

## RESULTS

### **Expression of $\alpha$ -KDE2 in BF *T. brucei*.**

Replication, segregation and the inheritance of the kDNA network requires the assembly of a novel apparatus, the FKC, to facilitate equal distribution of the kDNA to daughter cells. We reasoned that dual functioning proteins might be part of the FKC and participate in kDNA maintenance. To address this possibility we looked at the level of expression of known, nuclear-encoded mitochondrial enzymes in BF trypanosomes lacking mitochondrial oxidative phosphorylation. A similar analysis of mitochondrial encoded proteins led to the identification of an alternatively edited COIII mRNA that encoded a component of the FKC (32, 34). The developmental regulation of nuclear encoded mitochondrial proteins in *T. brucei* occurs principally at the level of RNA stability and, to a lesser extent, by differential protein stability (35, 36). High throughput RNA sequencing (RNA-Seq) provides an accurate evaluation of the life cycle dependent expression of mitochondrial proteins (37-40). Genome wide analysis of mRNA levels indicated that the expression of  $\alpha$ -KDE1,  $\alpha$ -KDE2 and E3 was not

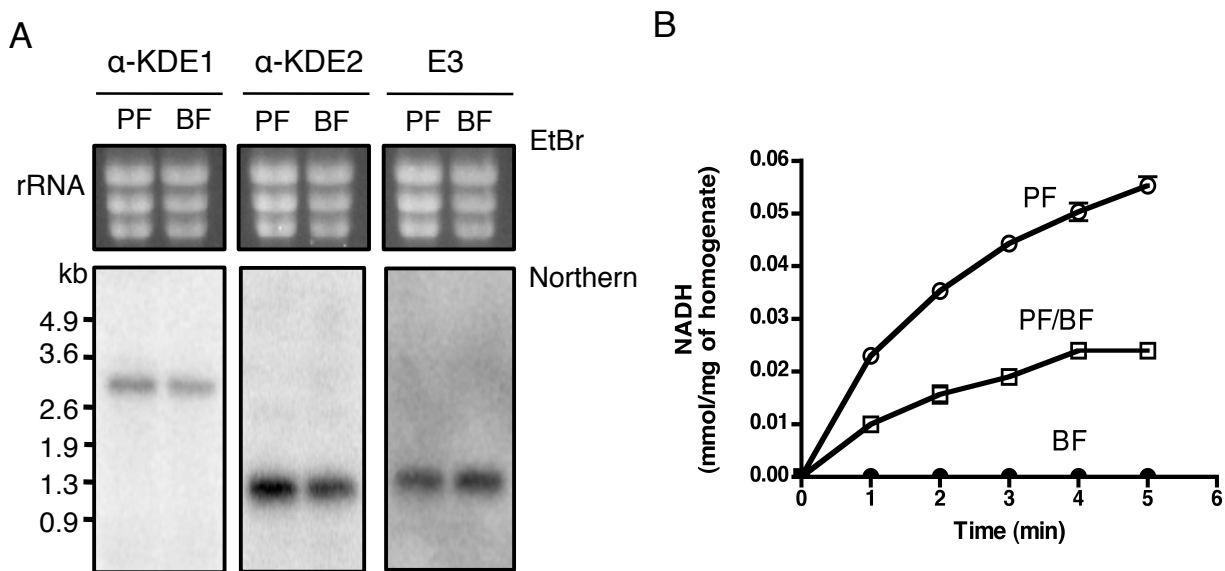


**Figure 3.1.** Stage specific mRNA expression of  $\alpha$ -KD subunits and complex activity in developmental stages. A) Northern analysis of the  $\alpha$ -KDE1,  $\alpha$ -KDE2 and E3 in PF and BF *T. brucei*. RNA from  $1 \times 10^7$  cells was probed for  $\alpha$ -KDE1,  $\alpha$ -KDE2, and E3 transcripts. Ethidium stain for rRNAs is shown for each lane. B) Activity of  $\alpha$ -KD in BF and PF *T. brucei*. Purified mitochondria were solubilized in nonionic detergents and 40  $\mu$ g of PF or BF mitochondrial protein was added to assay medium for the conversion of NAD<sup>+</sup> to NADH. For mixing experiment, 20  $\mu$ g of PF and 20  $\mu$ g of BF homogenate were combined and added to the same reaction. Each assay was measured at 340nm at 27°C.

developmentally regulated in BF and PF trypanosomes (39, 40). Unlike  $\alpha$ -KDE1 and  $\alpha$ -KDE2, the E3 subunit is a component of four distinct multienzyme mitochondrial complexes, encoded by a single trypanosome gene (41). Therefore, sequence analysis alone cannot be used to determine whether E3 mRNAs encode subunits of the  $\alpha$ -KD or other enzyme complexes (40). To verify the RNA-Seq results, total RNA from procyclic and bloodstream trypanosomes ( $1 \times 10^7$  cell equivalents) was analyzed by northern blot hybridization with probes specific for the  $\alpha$ -KDE1 (~3.0 kb),  $\alpha$ -KDE2 (~1.1 kb) and E3 (~1.4 kb) (Figure 3.1A). Hybridization was normalized relative to the rRNA ethidium stain for each lane (Figure 3.1A). Consistent with published RNA-Seq results, the mRNAs of  $\alpha$ -KDE1,  $\alpha$ -KDE2 and E3 were expressed in both BF and PF trypanosomes (39) (Figure 3.1A).

**$\alpha$ -KD activity is absent in BF *T. brucei*.**

Since previous studies have shown that BF *T. brucei* lacks metabolically active Krebs cycle enzymes, the presence of  $\alpha$ -KDE1 and  $\alpha$ -KDE2 mRNA expression in both BF and PF trypanosomes was unexpected. However, E3 has previously been shown to be essential in BF trypanosomes (41). We therefore next examined these cells for  $\alpha$ -KD activity. This mitochondrial enzyme complex specifically converts  $\alpha$ -ketoglutarate to succinyl CoA and

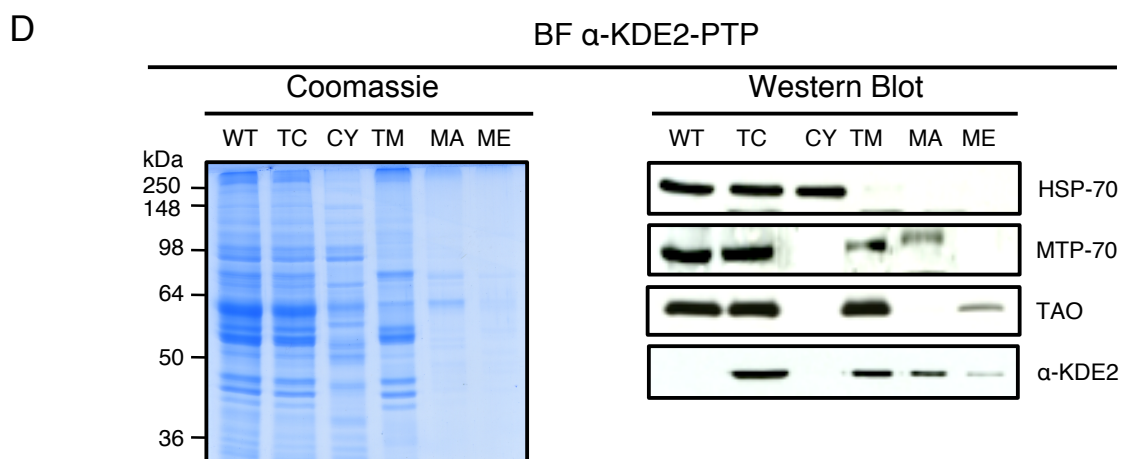
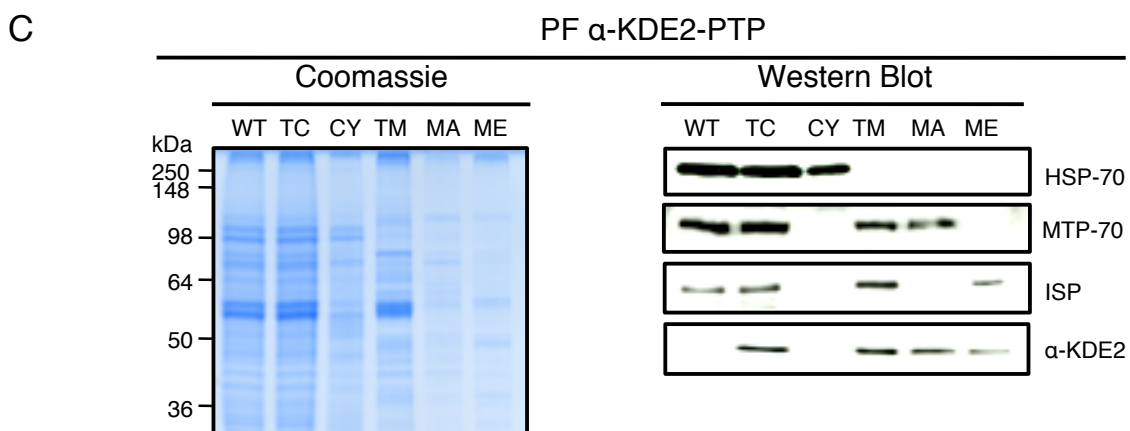
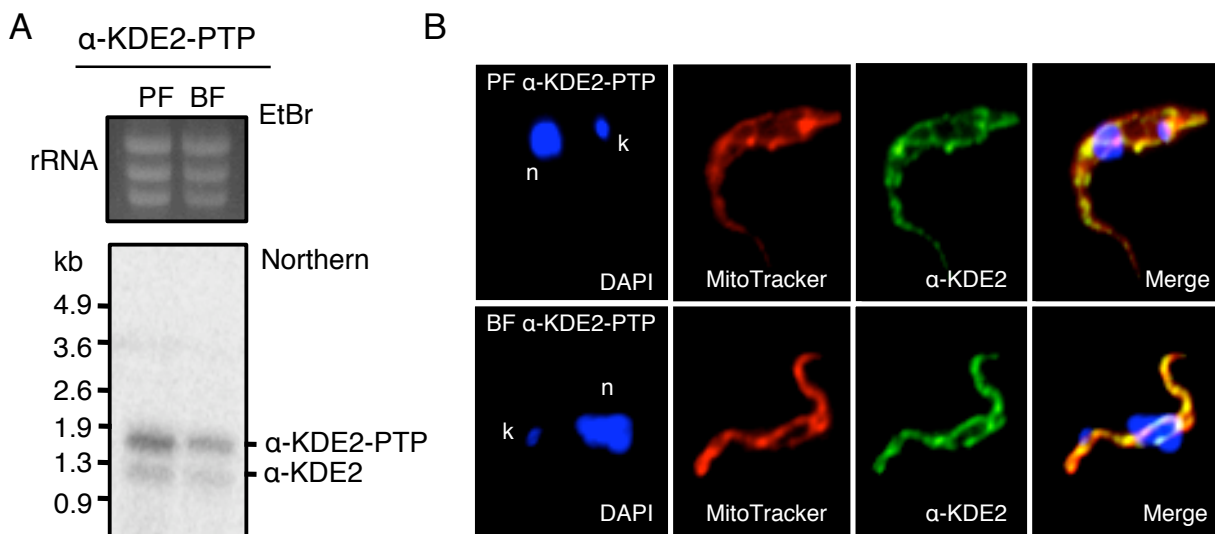


**Figure 3.2.** Localization and subcellular fractionation of  $\alpha$ -KDE2-PTP. A partial  $\alpha$ -KDE2 sequence was ligated into the C-terminal PTP expression vector (pC-PTP-NEO) and transfected into BF and PF form *T. brucei*. A) Northern analysis of  $\alpha$ -KDE2-PTP transcript expression in PF and BF developmental stages. RNA from  $5 \times 10^6$  cells was evaluated with radiolabeled probes against the  $\alpha$ -KDE2 sequence. Ethidium stain for rRNAs is shown for each lane. B) Cellular localization of  $\alpha$ -KDE2-PTP by immunofluorescence microscopy.  $\alpha$ -KDE2-PTP PF and BF cells were stained for DNA with DAPI, mitochondria with MitoTracker and  $\alpha$ -KDE2-PTP with antibodies against the Protein C epitope. C) Subcellular fractionation of procyclic form  $\alpha$ -KDE2-PTP cells. Lysates from total PF-667 (WT) cells and fractionated PF  $\alpha$ -KDE2-PTP cells (total cell, TC) were resolved by SDS-PAGE and analyzed Western Blot using antibodies against HSP-70 (cytosolic marker), MTP-70 (mitochondrial matrix marker), ISP (mitochondrial membrane marker) and Protein A epitope ( $\alpha$ -KDE2-PTP). D) Subcellular fractionation of BF  $\alpha$ -KDE2-PTP cells. Lysates from total BF-667 (WT) cells and BF  $\alpha$ -KDE2-PTP cells (TC) were fractionated and analyzed as in (C) with TAO as the mitochondrial membrane marker. The positions of the nucleus (n), kDNA (k), heat shock protein-70 (HSP-70), mitochondrial heat shock protein-70 (MTP-70), iron sulfur protein (ISP) and trypanosome alternative oxidase (TAO) are indicated. Abbreviation used for cells and organelle fractions in panels C and D. Total cell protein for non-transfected *T. brucei* 667 (WT) and  $\alpha$ -KDE2-PTP transfected (TC).

Cytosolic protein (CY), total mitochondrial protein (TM), mitochondrial matrix protein (MA) and mitochondrial membrane protein (ME).

subsequently reduces  $\text{NAD}^+$  to NADH. This dinucleotide conversion can be measured spectrophotometrically for  $\alpha$ -KD activity when  $\alpha$ -ketoglutarate is added as a substrate. At 340nm the procyclic mitochondrial lysates, but not BF mitochondrial lysates, showed increasing production of NADH (Figure 3.1B). To determine whether the lack of  $\alpha$ -KD activity in BF trypanosomes was due to an endogenous inhibitor of  $\alpha$ -KD in the BF mitochondrial fraction, an equal amount of BF and PF mitochondrial lysate were mixed and added to the same  $\alpha$ -KD assay. Since the total protein concentration during this analysis was kept constant, a two-fold reduction in the NADH produced ( $\mu\text{mol}/\text{min}$ ) was expected if no enzyme antagonists were present (Figure 3.1B). Lack of inhibition by the BF lysates indicates that the  $\alpha$ -KDE1,  $\alpha$ -KDE2, and E3, while expressed in BF mitochondria, do not assemble into a functional enzyme complex suggesting alternative functions for these proteins in BF trypanosomes. Evidence for the bifunctionality of  $\alpha$ -KDE2 in other organisms led us to examine the function of this protein in BF trypanosomes (10).

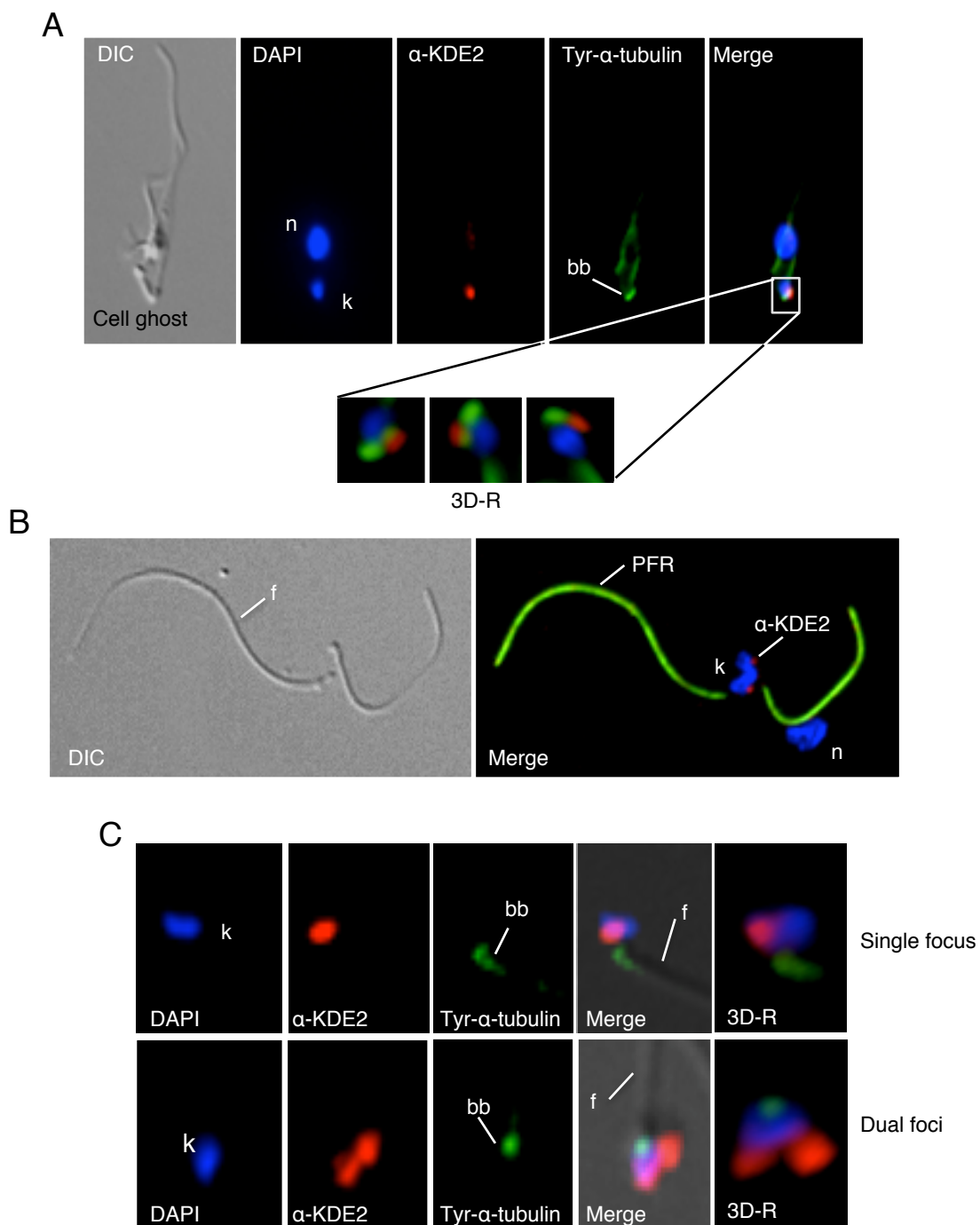


**Figure 3.3.**  $\alpha$ -KDE2-PTP associates with the FKFC. A) Mildly fixed BF  $\alpha$ -KDE2-PTP cells were incubated with 0.25% Triton X-100 to create cell ghost and stained with DAPI and

antibodies against tyr- $\alpha$ -tubulin and Protein C epitope of  $\alpha$ -KDE2-PTP. Bottom panel shows magnified three-dimensional reconstruction (3D-R) images near the kDNA. B) Cytoskeletons were created by incubating bloodstream  $\alpha$ -KDE2-PTP cells in 0.25% Triton X-100. These structures were stained with DAPI and antibodies against the PFR and  $\alpha$ -KDE2-PTP. C) BF  $\alpha$ -KDE2-PTP cells were solubilized in 0.5% Triton X-100 and microtubules were depolymerized with 1mM Ca<sup>+2</sup> to create FKCs. FKCs were stained with DAPI, and antibodies against the tyr- $\alpha$ -tubulin and  $\alpha$ -KDE2-PTP. Magnified 3D-reconstructions images (3D-R) are shown for each panel. The position of the nucleus (n), kDNA (k), flagellum (f), basal bodies (bb) and paraflagellar rod (PFR) are indicated.

#### **$\alpha$ -KDE2 distribution in the mitochondrion of trypanosomes.**

Krebs cycle associated  $\alpha$ -KDE2 is present in a soluble complex within the mitochondrial matrix. However, a fraction of E2 transferases ( $\alpha$ -KDE2, PDHE2, BCKADE2) has also been shown to be associated with DNA nucleoids, attached to the mitochondrial membrane of other cells (5-7). To evaluate the localization of  $\alpha$ -KDE2 in *T. brucei*, a C-terminal epitope tagged version of the protein ( $\alpha$ -KDE2-PTP) was constructed (42, 43). Expression of the BF and PF ( $\alpha$ -KDE2-PTP) tagged transcripts from a single allele was confirmed by northern analysis, which identified a 1.5 kb ( $\alpha$ -KDE2-PTP mRNA) and 1.1 kb bands (endogenous  $\alpha$ -KDE2 mRNA) in both cell types (Figure 3.2A). Though inserted into the endogenous  $\alpha$ -KDE2 locus,  $\alpha$ -KDE2-

PTP expression was approximately 2-fold higher than wildtype  $\alpha$ -KDE2 and is possibly a result of increased mRNA stability due to the 3' UTR sequences flanking the PTP coding sequences (Figure 3.2A) (42).

We next examined the intracellular localization of  $\alpha$ -KDE2-PTP by immunofluorescence microscopy (Figure 3.2B). Using an antibody against the Protein C epitope,  $\alpha$ -KDE2-PTP distribution was compared with MitoTracker Red staining (Figure 3.2B). Within the large and highly branched mitochondrion of the PF trypanosomes, the  $\alpha$ -KDE2-PTP and MitoTracker staining superimposed (upper panel). Similarly, while BF mitochondrion was reduced to a single, largely unbranched tubular structure, MitoTracker and  $\alpha$ -KDE2-PTP co-localized throughout the organelle (lower panel) despite the lack of  $\alpha$ -KD activity (Figure 3.1B and 3.2B). Subcellular fractionation studies confirmed the mitochondrial localization of  $\alpha$ -KDE2 in both BF and PF *T. brucei*. In western blot studies, total cell lysates from non-transfected BF and PF cells (Wild type, WT) did not contain proteins that cross-react with the antibody ( $\alpha$ -Protein A) used to detect  $\alpha$ -KDE2-PTP. Total BF and PF protein from  $\alpha$ -KDE2-PTP expressing cells (TC) and cellular fractions enriched in cytosol (CY), total mitochondria (TM), mitochondrial matrix (MA) and mitochondrial membrane (ME) were resolved by SDS-PAGE and analyzed by western blot with antibodies for marker proteins (Figure 3.2C and D).  $\alpha$ -KDE2-PTP was exclusively detected

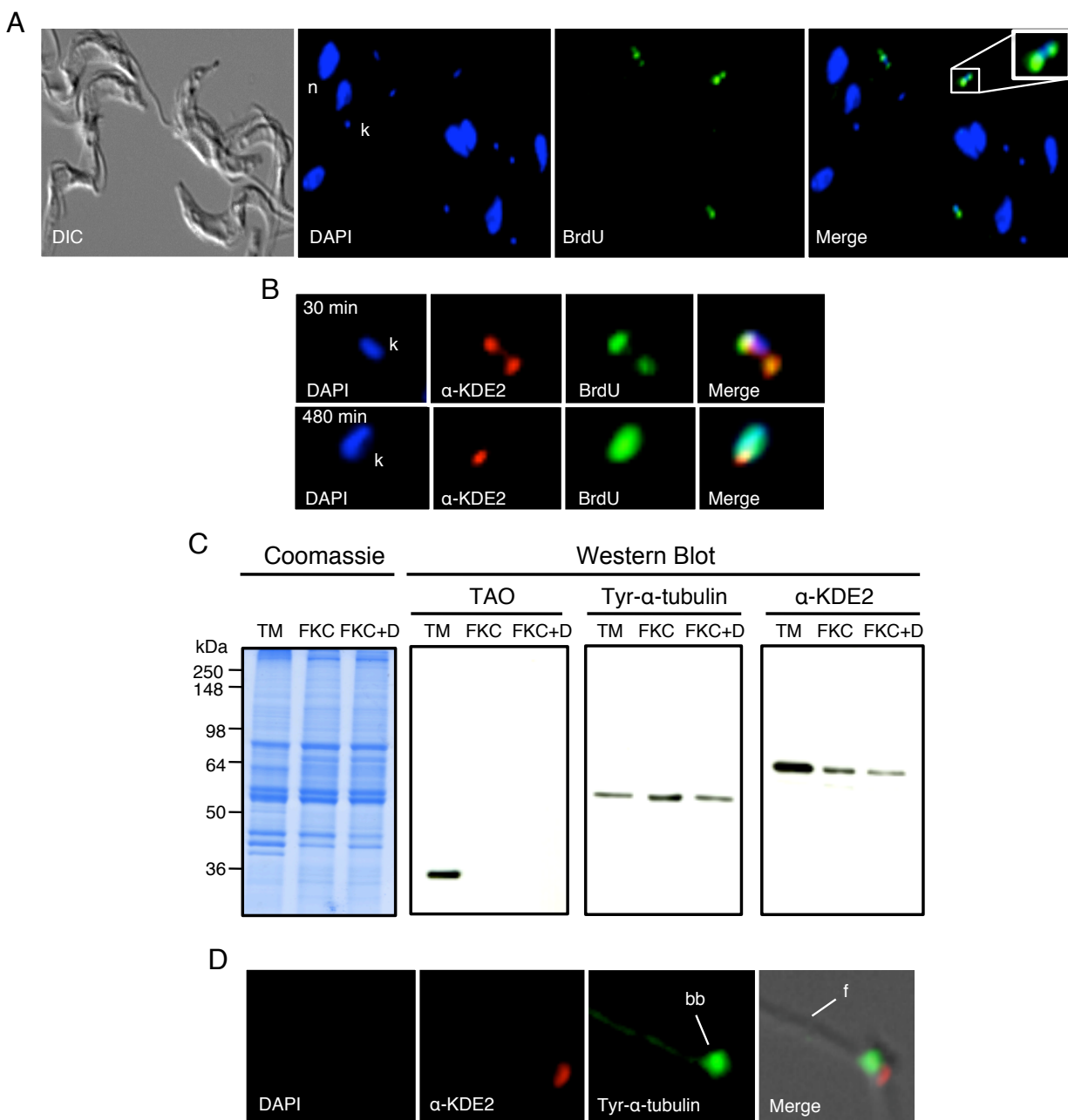


**Figure 3.4.** Antipodal localization and stable association of  $\alpha$ -KDE2-PTP with the FKCs. A) BF  $\alpha$ -KDE2-PTP *T. brucei* were incubated with BrdU for 30 min, fixed and acid treated. Cells were stained with DAPI and probed with a monoclonal antibody against BrdU to show the distribution

of recently replicated minicircle kDNA. A magnified image of newly replicated BrdU labeled minicircles reattached to the kDNA network is shown in the merged image. B) FKCs were isolated from 30 min and 480 min BrdU treated cells, heat treated and stained with antibodies against BrdU and  $\alpha$ -KDE2-PTP. C) Proteins from total mitochondria (TM), FKCs and DNase treated FKCs (FKC+D) from bloodstream form  $\alpha$ -KDE2-PTP cells were resolved by SDS-PAGE and analyzed by Western Blot. Proteins were probed with antibodies against TAO, tyr- $\alpha$ -tubulin and the Protein A domain of  $\alpha$ -KDE2-PTP. D) Immunofluorescence microscopy of DNase treated FKCs stained with DAPI and antibodies against tyr- $\alpha$ -tubulin and the Protein C domain of  $\alpha$ -KDE2-PTP. The position of the nucleus (n), kDNA (k), flagellum (f) and basal bodies (bb) are indicated.

in mitochondrial fractions relative to the cytosolic HSP-70 and the mitochondrial matrix MTP-70. Examination of the sub-mitochondrial distribution of  $\alpha$ -KDE2-PTP revealed that approximately 25% localized with the mitochondrial membrane markers, iron sulfur protein (ISP) for PF and the alternative oxidase (TAO) for BF (Figure 3.2C and D). These results confirmed the localization of  $\alpha$ -KDE2-PTP to the mitochondrion of PF and BF *T. brucei* and suggested a similar sub-mitochondrial localization in the two developmental stages. To further

evaluate the alternative function(s) of  $\alpha$ -KDE2 in trypanosome mitochondria we focused our studies on BF trypanosomes where the  $\alpha$ -KD enzymatic activity is absent.

### **$\alpha$ -KDE2 associates with the FKc.**

The kDNA network of trypanosomes is anchored to the base of the flagellum by the TAC. This association with the mitochondrial membrane is reminiscent of the attachment of the mitochondrial nucleoid in diverse organisms. Since  $\alpha$ -KDE2 is distributed in both the mitochondrial matrix and membranes it was not possible to determine whether there was a specific association with the kDNA using intact cells. To release the mitochondrial matrix and membrane associated  $\alpha$ -KDE2-PTP, cells mildly fixed with paraformaldehyde were treated with low concentrations of Triton X-100 (0.25%) to create cell ghosts. This treatment permeabilizes many subcellular organelles including the mitochondrion, while leaving the DNA-associated cytoskeleton intact (31) (Figure 3.3A). The cell ghosts were subsequently examined by immunofluorescence microscopy using anti-Protein C and anti-tyrosinated  $\alpha$ -tubulin (tyr- $\alpha$ -tubulin) antibodies to visualize  $\alpha$ -KDE2-PTP and the basal bodies of the flagellum respectively. The nucleus and kinetoplast were stained with DAPI (Figure 3.3A). The majority of the  $\alpha$ -KDE2-PTP signal was depleted in these preparations, leaving a prominent structure in close proximity to the kDNA and basal bodies. Three-dimensional reconstruction

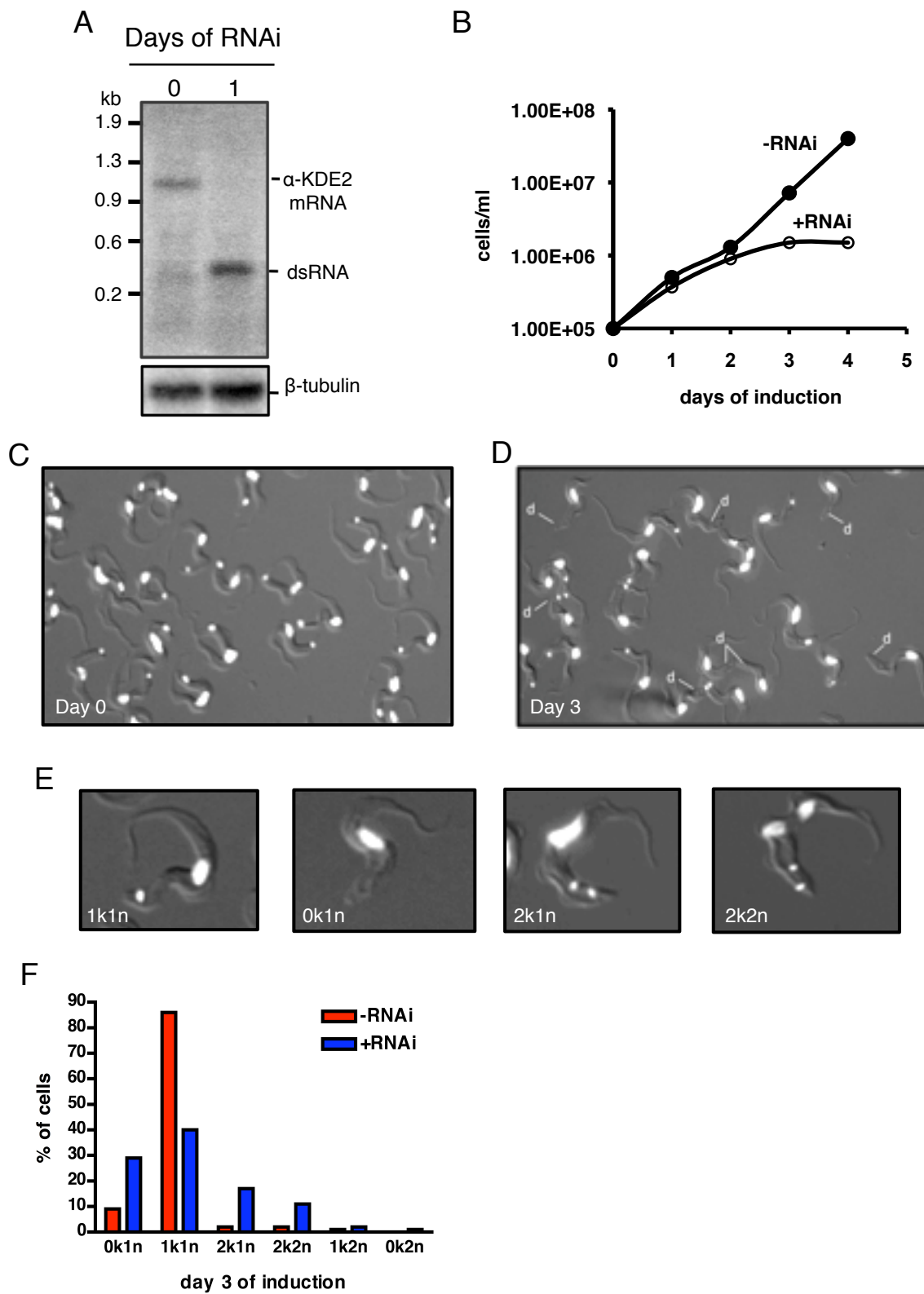


**Figure 3.5.** Effect of  $\alpha$ -KDE2 RNAi knockdown in BF *T. brucei*. BF *T. brucei* were transfected with the inducible RNAi vector containing 425 bps of  $\alpha$ -KDE2 sequence. A) Northern analysis showing the reduction of  $\alpha$ -KDE2 mRNA levels by 24 hours. Blot was evaluated with radiolabeled probes against  $\alpha$ -KDE2 and  $\beta$ -tubulin sequences. B) The effects of  $\alpha$ -KDE2 knockdown on cell growth. Cells were grown in the presence or absence of 1 $\mu$ g/ml doxycycline and monitored for changes in proliferation. C) and D) The number of kinetoplast and nuclei were examined on day zero and three days post induction by DAPI staining. E) Examples of DAPI stained (1k1n), dyskinetoplastic (0k1n), 2k1n and 2k2n cells. F) Quantitation of induced and uninduced cells types on day three of RNAi. A total of 400 DAPI stained cells were analyzed. The position of dyskinetoplastic cells (d) and double-stranded RNA (dsRNA) are indicated.

(3D-R) images further supports the close proximity of  $\alpha$ -KDE2-PTP to the kDNA and basal body (Figure 3.3A).

Since kDNA replication involves the detachment, duplication and reattachment of minicircles, the kDNA network grows laterally until it is twice the size of the kDNA network in non-replicating cells. The newly replicated kDNA network segregates and along with a newly formed flagellum are distributed to daughter cells at cytokinesis. Late in the kDNA replication cycle,  $\alpha$ -KDE2-PTP distributes with each lobe of the kDNA network in close proximity to the

old and newly formed flagellum (Figure 3.3B). In this image, a single unfixed cell treated with detergent has two flagella, one nucleus and a single V-shaped kDNA network that has completed kDNA replication and just beginning network scission (11). Interestingly,  $\alpha$ -KDE2-PTP foci are associated with this bilobed kDNA genome with a single point located on each lobe.

When cells were treated with detergent and  $\text{CaCl}_2$  there was a general depolymerization of the subpellicular microtubules leaving the kDNA associated with flagellum via the TAC (Figure 3.3C) (11).  $\alpha$ -KDE2-PTP was localized to either a single point on the kDNA (top panel) or at two points (bottom panel) in asynchronous populations. The orientation of the 3D-R images further supports the close association of  $\alpha$ -KDE2-PTP to the kDNA and also better resolves the two discrete  $\alpha$ -KDE2-PTP points in the bottom panel. The heterogeneity in  $\alpha$ -KDE2-PTP foci was likely due to cell cycle differences with a singular localization associated with kDNA networks that have recently completed replication and segregation (Figure 3.3B & C). These results show that  $\alpha$ -KDE2-PTP is closely associated with the FKC and co-fractionates with the TAC.

#### **$\alpha$ -KDE2-PTP maintains an antipodal distribution throughout kDNA replication.**

Many proteins that maintain the kDNA in *T. brucei* are organized around the network in specialized regions (21). Antipodal sites, which are structural projections that flank this

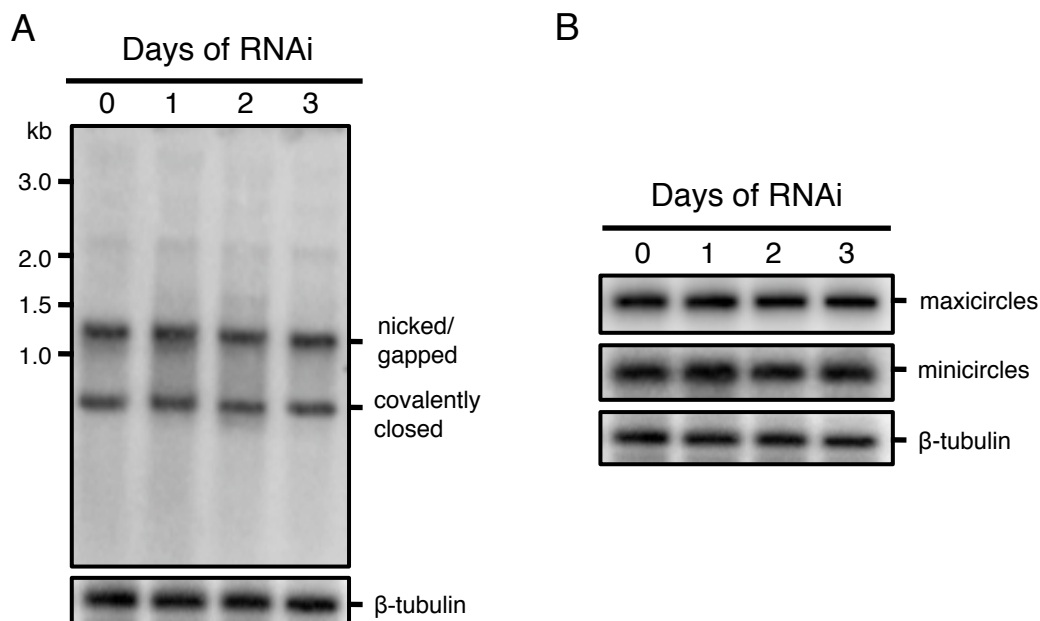


**Figure 3.6.** Effect of  $\alpha$ -KDE2 RNAi on minicircle and maxicircle abundance. A) Total genomic DNA was fractionated by agarose gel electrophoresis and analyzed by Southern blot over a three-day period post induction of  $\alpha$ -KDE2 RNAi for changes in free replicating minicircle levels. B) Southern blot analysis of XbaI and HindIII digested total genomic DNA for variations in the amounts of kDNA associated minicircles and maxicircles. Both blots were hybridized with radiolabeled probes for minicircle and maxicircle sequences. Hybridization with a  $\beta$ -tubulin probe was used as a loading control.

genome, house many of the replication proteins and are the regions where newly replicated minicircles reattach to the network. The thymidine analogue bromodeoxyuridine (BrdU) is a

synthetic base that is incorporated into the free replicating kDNA minicircles during S-phase. Initial reattachment of these minicircles to the network leads to labeling of the antipodal sites (44). To determine whether  $\alpha$ -KDE2-PTP localized to the antipodal sites, cells were incubated with BrdU for 30 minutes, fixed, treated with HCl and stained with DAPI and antibodies for BrdU. Trypanosomes in early S phase showed two sites of BrdU staining flanking the kDNA disk and revealed an antipodal distribution of minicircles (Figure 3.4A). Additionally, FKCs prepared from cells treated with BrdU for 30 minutes revealed a colocalization of these minicircles with  $\alpha$ -KDE2-PTP at the antipodal sites (Figure 3.4B). When BrdU labeling was extended to 480 minutes, replicated BrdU labeled DNA was distributed throughout the kDNA network, but the position of  $\alpha$ -KDE2-PTP remained constant. In cells that have completed kDNA replication and segregation we observed a single  $\alpha$ -KDE2-PTP staining foci as has been described for other proteins localized to the antipodal sites (45).

**$\alpha$ -KDE2-PTP is stably linked to mitochondrial structural elements.**

The antipodal localization  $\alpha$ -KDE2-PTP led us to ask whether the protein stably interacts within the FKc by direct binding to the kDNA or to TAC elements surrounding the genome. To determine if  $\alpha$ -KDE2-PTP directly associates with the kDNA, purified FKc preparations were treated with DNase and total mitochondria (TM), FKc, and DNase treated FKc (FKc+D) fractions were resolved by SDS-PAGE and analyzed by western blot (Figure 3.4C). Blots were

probed with antibodies against TAO, tyr- $\alpha$ -tubulin and  $\alpha$ -KDE2-PTP. The membrane protein TAO was present in TM but was lost during FKC purification. Both  $\alpha$ -KDE2-PTP and the basal body marker, tyr- $\alpha$ -tubulin, remained associated with the FCK following DNase treatment (Figure 3.4C). Treatment with DNase caused a mild dilution of the FKC samples since a similar reduction in signal intensity was observed in the tyr- $\alpha$ -tubulin and  $\alpha$ -KDE2-PTP FKC+D fractions. The association of  $\alpha$ -KDE2-PTP with the FKC was further confirmed by immunofluorescence microscopy of the FKC+D preparations. No kDNA was detectable by DAPI staining yet both tyr- $\alpha$ -tubulin and  $\alpha$ -KDE2-PTP were retained in the DNase treated FKC (Figure 3.4D). Together these results show that  $\alpha$ -KDE2-PTP, though localized to the antipodal sites, is directly associated with the FKC and indicates that the antipodal replication/reattachment sites interact with this complex.

#### **RNAi knockdown of $\alpha$ -KDE2 decreases growth rate and influences kDNA distribution.**

The localization of  $\alpha$ -KDE2-PTP to the FKC in BF *T. brucei* suggested the protein had an alternative function in kDNA maintenance. To examine this secondary function for  $\alpha$ -KDE2, we developed an RNAi cell line by cloning in a partial  $\alpha$ -KDE2 nucleotide sequence into the

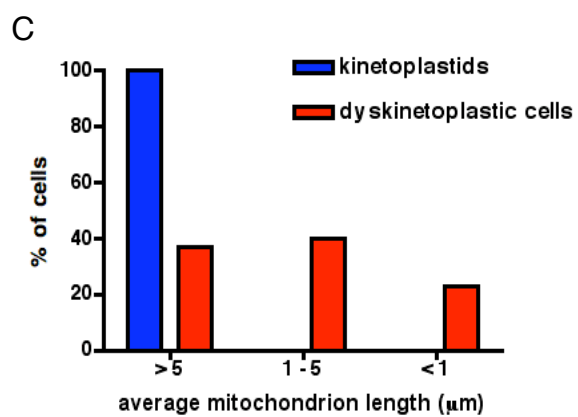
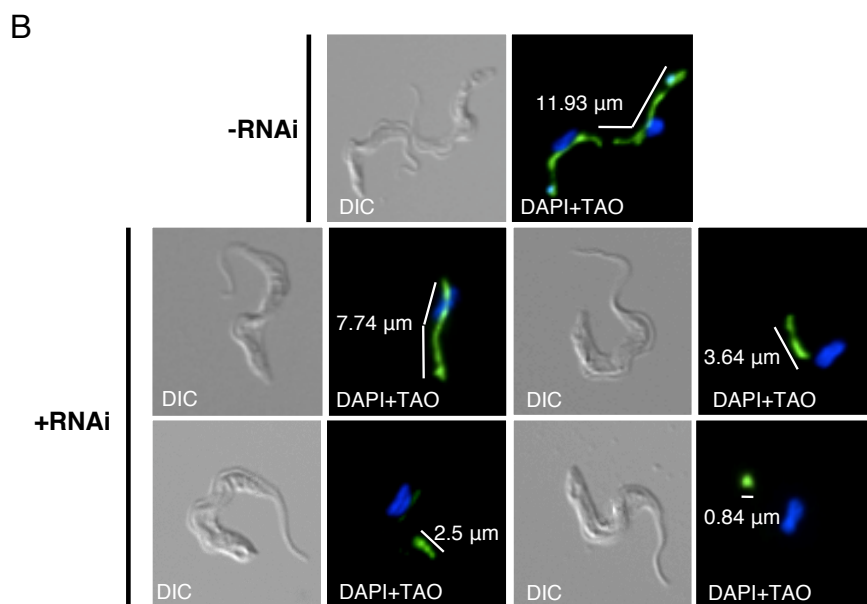
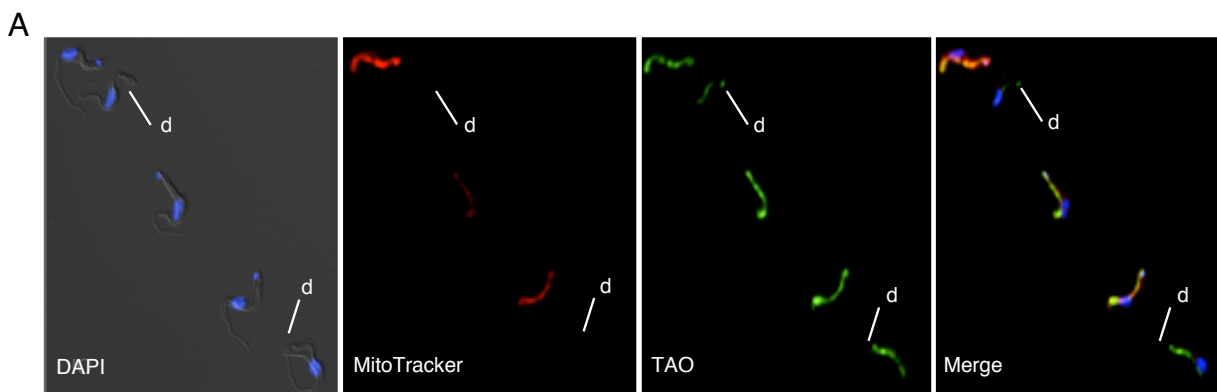


**Figure 3.7.** Mitochondrial function and morphology are altered in dyskinetoplastic cells. A) Fluorescence microscopy analysis of  $\alpha$ -KDE2 RNAi cells. Day 3 induced cells were stained for DNA with DAPI, mitochondria with MitoTracker Red and probed with antibodies against TAO. Dyskinetoplastic cells are indicated (d). B) Mitochondrial morphology of  $\alpha$ -KDE2 RNAi cells. Observed changes in mitochondria lengths of dyskinetoplastic cells in  $\mu\text{m}(\text{s})$  by TAO staining. C) Quantification of observed mitochondrion lengths for trypanosomes with and without kinetoplasts on day three. A total of 400 stained cells were analyzed.

inducible pZJM vector (46). Northern analysis of this induced cell line revealed complete loss of detectable  $\alpha$ -KDE2 mRNA 24 hours after induction (Figure 3.5A). Loss of  $\alpha$ -KDE2 mRNA levels was accompanied by a 26-fold reduction in cell number by day four (Figure 3.5B). The effect of RNAi knockdown of  $\alpha$ -KDE2 on the morphology of the kDNA network was evaluated by DAPI staining (Figure 3.5C and D). At the time of induction, over 85% of the cells contained one kinetoplast and one nucleus (1k1n) with a small fraction of cells containing 0k1n, 2k1n and 2k2n (Figure 3.5C). By day three the percentage of dyskinetoplastic cells (0k1n) lacking detectable kDNA staining had increased to 27% of the total cells (Figure 3.5D, E and F). A similar increase in the number of cells with two kinetoplasts (2k1n, 2k2n) was observed. The increased fraction of dyskinetoplastic trypanosomes and cells containing two kinetoplasts

suggested that  $\alpha$ -KDE2 maybe required for kDNA inheritance to daughter cells following segregation of the kDNA.

**kDNA abundance is not affected by  $\alpha$ -KDE2 mRNA depletion.**

Many of the enzymes localized to the kDNA antipodal sites are involved in kDNA replication. RNAi knockdown of these replication proteins leads to kDNA loss (27, 47). In order to evaluate the effect of  $\alpha$ -KDE2 RNAi knockdown on kDNA replication, the abundance of free replicating minicircles was determined in total genomic DNA isolated from induced RNAi cells over a three-day period. Free minicircles, separated by agarose gel electrophoresis, to resolve the covalently closed and nicked/gapped circles, were analyzed by Southern blot (Figure 3.6A). Hybridization with a probe specific to a conserved sequence found on all minicircles revealed no change in the abundance of both closed and nicked/gapped conformations. Additionally, the abundance of kDNA network-associated minicircles and maxicircles were also assayed and no differences were observed (Figure 3.6B). These results suggest that the overall abundance of kDNA is unaltered by RNAi knockdown of  $\alpha$ -KDE2 consistent with the coordinate increase of both dyskinetoplastic trypanosomes and cells containing two kinetoplasts. Together these studies showed that  $\alpha$ -KDE2 was necessary for inheritance of the kDNA by daughter cells at cytokinesis and not for replication or segregation of the kDNA.

**Dyskinetoplastic *T. brucei* have truncated mitochondria with decreased membrane potential.**

In the BF of *T. brucei*, the mitochondrial ATP synthase functions as an ATPase driving the movement of protons across the mitochondrial membrane establishing a membrane potential (17, 48). A single maxicircle gene encoding the mRNA for subunit A6, numerous minicircle encoded gRNAs for the editing of A6 pre-mRNA and nuclear encoded editing enzymes are all necessary for the successful production of the functional ATPase (49). An expected consequence of the generation of dyskinetoplastic trypanosomes by  $\alpha$ -KDE2 RNAi is the loss of A6 expression and the inability of these cells to maintain a mitochondrial membrane potential (Figure 3.7).  $\alpha$ -KDE2 RNAi cells were incubated with MitoTracker Red on day three of induction, washed, fixed with methanol and prepared for immunofluorescence analysis with an antibody against the mitochondrial membrane protein TAO and DAPI. All cells containing a DAPI stainable kinetoplast had overlapping signals for both MitoTracker and TAO. Cells lacking a stainable kDNA network also lacked MitoTracker staining indicating a loss of membrane potential (Figure 3.7A). These dyskinetoplastic cells also showed a dramatic reduction in mitochondrial volume based on TAO staining. A 14-fold reduction in length was observed in extreme cases. Examples of uninduced (-RNAi) and induced (+RNAi) cells with mitochondrion length in microns ( $\mu\text{m}$ ) are shown in Figure 3.7B. Quantitation revealed that 100% of the kinetoplastids on day three

contained mitochondria that were more than 5  $\mu\text{m}$  in length (Figure 3.7C). Also on day three, dyskinetoplastic trypanosomes contained mitochondria that were between 2 - 8  $\mu\text{m}$  (77%) and only 23% were 1  $\mu\text{m}$  or less (Figure 3.7C). Together the RNAi knockdown studies showed that  $\alpha$ -KDE2 was necessary for inheritance of the kDNA by daughter cells and that the production of dyskinetoplastic trypanosomes resulted in the rapid loss of mitochondrial membrane potential and reduced mitochondrial volume.

## DISCUSSION

Whether structural or enzymatic, most proteins are encoded by a single gene and have a single function. However, there are a number of proteins that are multifunctional with seemingly unrelated activities. In mammals, alternative splicing provides an important mechanism for generation of protein diversity with literally thousands of splice variants originating from a single gene (50). Trypanosomes lack conventional cis-splicing but alternative trans-splicing at the 5' end of nuclear encoded mRNAs and alternative editing of mitochondrial mRNA have recently been recognized as mechanisms for increasing the variety of proteins (32-34, 39). Expanded functional diversity can also be accomplished without differences in protein sequence or posttranslational modification, but rather by simply having multiple activities associated with the same protein. These "moonlighting proteins" also provide additional complexity to the

limited number of proteins encoded by the eukaryotic genome. Seven of the eight Krebs cycle enzymes have alternative functions in eukaryotes. Three of these proteins have been identified as mtDNA maintenance factors in different organisms suggesting a strong evolutionary trend for metabolic enzymes to be involved in genome preservation (4, 51, 52). Here, we report the moonlighting activity of  $\alpha$ -KDE2 and define its function in the inheritance of the mitochondrial genome of African trypanosomes.

The BF of *T. brucei* lack  $\alpha$ -KD activity yet expresses all three subunits of the  $\alpha$ -KD. The enzymatic activities of  $\alpha$ -KD were expected to fractionate with the mitochondrial matrix, however,  $\alpha$ -KDE2 is also associated with mitochondrial membranes (Figure 3.2). In yeast,  $\alpha$ -KDE2 also associates with the mtDNA nucleoid at the mitochondrial membrane and is necessary for maintenance of the genome (4, 5). Similarly, we found that  $\alpha$ -KDE2 in *T. brucei* associates with FKC apparatus. The association of  $\alpha$ -KDE2 with the FKC is not mediated by direct binding to kDNA but rather the protein is physically linked to the FKC in a DNase resistant manner. Despite apparent similarities in the distribution of  $\alpha$ -KDE2 in yeast and trypanosomes, the structure of the kDNA network and its mechanism of replication impose unique requirements. Immunofluorescence microscopy localized  $\alpha$ -KDE2 to discrete positions on the kDNA within the FKC. The mechanism of kDNA replication requires a spatial order of the genome, replication enzymes and segregation apparatus. The KFZ and the antipodal sites represent

defined functional zones surrounding the kDNA and are involved in replication, segregation and maintenance of the trypanosome mitochondrial genome. Pulse labeling cells with BrdU allowed the identification of the antipodal sites and shows that  $\alpha$ -KDE2 localizes here. Initially, localization of  $\alpha$ -KDE2 to the site of minicircle reattachment following replication led us to believe that  $\alpha$ -KDE2 might be directly involved in kDNA replication. Moreover, RNAi knockdown of  $\alpha$ -KDE2 mRNA resulted in a dramatic increase in cells lacking kDNA staining with DAPI. However, we also observed a corresponding increase in cells with two kDNA networks and Southern blot hybridization confirmed that the abundance of kDNA was unaltered during RNAi knockdown of  $\alpha$ -KDE2 expression despite increased number of dyskinetoplastic cells. Together these results indicate that  $\alpha$ -KDE2 is not directly involved in kDNA replication or segregation, but rather is necessary for the distribution of the replicated kDNA networks to daughter cells at cytokinesis. We propose that unequal distribution of the replicated kDNA networks gave rise to a dyskinetoplastic daughter cell and a daughter cell with two kinetoplasts.

The antipodal distribution of  $\alpha$ -KDE2 is static throughout the cell cycle suggesting a structural versus a catalytic function for  $\alpha$ -KDE2 at the FKC of *T. brucei*. In asynchronous populations  $\alpha$ -KDE2 is associated with one or both antipodal sites on the kDNA. We have found  $\alpha$ -KDE2 on a bilobed kDNA (pre-partitioned) suggesting that the  $\alpha$ -KDE2 stably associated as a single site on each lobe of the replicating kDNA network. Complete segregation of this “V

shaped” bilobed network produces daughter kDNA networks with a single podal site containing  $\alpha$ -KDE2. This is similar to the results seen in the analysis of the distribution of mitochondrial topoisomerase II in the related organism *Crithidia fasciculata* (45). Furthermore, while BrdU analysis of kDNA replication revealed an initial colocalization of newly replicated minicircles and  $\alpha$ -KDE2 at the antipodal sites, continuous uptake of BrdU led to a uniform distribution of the nucleotide analogue throughout the kDNA network whereas  $\alpha$ -KDE2 remained static at the antipodal sites (Figure 3.4B).

A possible role for  $\alpha$ -KDE2 within the FKC might involve kDNA binding and suggests that  $\alpha$ -KDE2 could serve as a bridge to the proteinaceous filaments linking the kDNA network to the mitochondrial membrane. We found that  $\alpha$ -KDE2 association with FKC resisted treatment with DNase, but additional studies are needed to determine whether  $\alpha$ -KDE2 has DNA binding properties. Within the FKC, the unilateral filaments of the TAC attach to the mitochondrial membranes and extend through the KFZ to a single face of the kDNA disk (11). Only two unilateral filament proteins (p166 and AEP-1) have been reported (30, 33) and possible interactions with  $\alpha$ -KDE2 have not been determined. The resistance of  $\alpha$ -KDE2 to detergent solubilization and DNase treatment suggests an association with unidentified proteins that makeup the structural skeleton in the mitochondria.

Two TAC proteins previously studied, p166 and AEP-1, localize to the kDNA/basal body region of *T. brucei* and purify with the FKC (30, 33). RNAi knockdown of p166 and expression of a dominant negative mutant of AEP-1 showed that both are essential for kDNA maintenance and segregation.  $\alpha$ -KDE2 RNAi had no effect on kDNA morphology or division, but resulted in an increase of dyskinetoplastic cells and a corresponding increase in cells with two kinetoplasts. This suggests that in the absence of  $\alpha$ -KDE2, newly replicated kDNA networks fail to partition into the newly formed mitochondrion leading to unequal kDNA distribution to the daughter cells.

If  $\alpha$ -KDE2 is necessary for kDNA inheritance, it is somewhat surprising that the maximum percentage of dyskinetoplastic cells never exceeds approximately 35%. It is well established that BF trypanosomes lack a functional Krebs cycle and oxidative phosphorylation and ATP is exclusively produced during glycolysis. However, mitochondrial translation is required in BF *T. brucei* suggesting an essential function is provided by a mitochondrial gene product (15). It seems likely that the depletion of  $\alpha$ -KDE2 by RNAi is lethal to BF trypanosomes due to the moonlighting function of this protein in kDNA inheritance. In BF *T. brucei* the formation of a proton gradient across the mitochondrial membrane, necessary for import of nuclear encoded mitochondrial proteins, is dependent on the expression of a functional  $F_1F_0$  ATPase. One essential component of the  $F_1F_0$  ATPase is the maxicircle encoded A6 subunit. Since dyskinetoplastic trypanosomes lack the A6 gene they cannot maintain a proton gradient and lose

the ability to import proteins from the cytoplasm. This occurs rapidly resulting in loss of membrane potential and reduced mitochondrial volume within three days of RNAi induction.

The moonlighting function of  $\alpha$ -KDE2 in kDNA distribution to daughter cells further underscores the importance of multifunctional proteins in the maintenance of the mitochondrial genome in eukaryotes. Unexpectedly we have also demonstrated the essential role of mitochondrial-encoded proteins in the duplication and inheritance of the intact mitochondrion in BF trypanosomes. The complexity of the FKC and kDNA replication cycle has driven the diversification of mitochondrial proteins in trypanosomes and as additional FKC associated proteins are identified, it is likely that new moonlighting and alternatively processed proteins will be discovered.

## MATERIALS AND METHODS

### **Cell Culture.**

Procyclic form *T. brucei* were grown in Cunningham's (SM) medium supplemented with fetal bovine serum (FBS, Gemini Bio-products, West Sacramento, CA). Bloodstream form *T. brucei* were maintained in HMI-9 medium containing FBS and Serum Plus media supplement (SAFC

Biosciences, Lenexa, KS). The  $\alpha$ -KDE2 RNAi cell line was cultured in HMI-9 medium that was supplemented with tetracycline free FBS.

### **Construction of $\alpha$ -KDE2-PTP and $\alpha$ -KDE2-RNAi cell lines.**

GGGCCCAAGATAAACTTCGAAGAGGGGCAC- 3' and 5' -  
 GCGGCCGCGGCGAGGTCGAGCACAATA- 3' against the  $\alpha$ -KDE2 (Tb11.01.3550) ORF  
 amplified a 912 bp of PF- and BF-667 genomic DNA, which were subsequently cloned into the  
 pC-PTP-NEO expression vector (42). The fragment was digested with *Apa*I and *Not*I for  
 insertion into the vector. Constructs were linearized with a unique restriction site for transfection  
 into the two *T. brucei* cell types. For  $\alpha$ -KDE2 RNAi cell line, primers 5' -  
 CCCTCGAGGCTCACGACATTCAACGAGA- 3' and 5' -  
 CCAAGCTTTCTGTGGTGGGTTGACGATA- 3' were used to amplify a partial  $\alpha$ -KDE2  
 sequence (425 bp) from BF-9013 genomic DNA and was ligated into the inducible pZJM RNAi  
 vector (46). *Not*I was used to linearize construct for transfection. All bloodstream constructs  
 were transfected using the Lonza nucleofector system (Lonza, Walkersville, MD, USA). The  
 procyclic  $\alpha$ -KDE2-PTP construct was transfected using the Bio-Rad electroporation system  
 (Bio-Rad, Hercules, CA, USA).

**Fractionation of mitochondrial proteins.**

Cultured PF *T. brucei* (TRUE667) and BF *T. brucei* (TRUE667) isolated from infected Sprague-Dawley rats, were hypotonically lysed and mitochondria were purified by a method as previously described in (53). Subcellular fractionation was performed as discussed with minor modifications (32, 54). Matrix proteins were purified by incubating mitochondria in 0.5% (v/v) Triton X-100, 20 mM Hepes-NaOH (pH 7.6) with 1xComplete<sup>®</sup> protease inhibitor cocktail (Roche Indianapolis, IN, USA) for 45 min on ice. Insoluble material was separated from matrix fraction by centrifugation at 12,000xg for 10 min at 4°C. The membrane fraction was collected post-purification of the matrix proteins by incubation of insoluble fraction in 2% (w/v) n-dodecyl- $\beta$ -D-maltoside (Sigma, St. Louis, MO, USA), 50 mM NaCl, 50 mM imidazole, 2 mM 6-aminohexanoic, 1mM EDTA and 1 x Complete<sup>®</sup> EDTA free protease inhibitor cocktail pH 7 at 4°C for one hour on ice. An insoluble fraction was collected by centrifugation at 13,000xg for 20 min at 4°C and the soluble fraction was saved for subsequent analysis. The total cell, cytosolic, total mitochondrial, matrix and membrane fractions of PF and BF *T. brucei* were denatured in a reducing SDS loading buffer and applied equivalently ( $2 \times 10^6$  cells) to gel and resolved by SDS-PAGE. Gels were either stained with coomassie or analyzed by western blot.

**Extraction of FKCs.**

We used the published method for purifying FKCs from *T. brucei* (11). For SDS-PAGE analysis, these complexes were extracted from  $6 \times 10^7$  BF cells and a fraction of these structures were treated with DNase (Roche) for one hour on ice to remove the kDNA. FKCs isolated from  $1 \times 10^7$  cells were loaded on gels, resolved, stained with coomassie and analyzed by Western.

**Western Blot Analysis.**

Protein blots were blocked in 5% (w/v) milk/TBST (150 mM NaCl, 10 mM Tris-HCl pH 8, 0.05% (v/v) Tween 20) and incubated overnight with the following primary antibodies: polyclonal rabbit HSP-70 (1:3000; Abcam, Cambridge, MA, USA), monoclonal mouse MTP-70 (1:500), monoclonal mouse ISP (1:2000), monoclonal mouse TAO (1:100), monoclonal rat YL1/2 (1:5000; Abcam) and polyclonal peroxidase anti-peroxidase soluble complex (PAP, 1:5000; Sigma). Blots were washed three times and incubated with a goat anti-rabbit HRP secondary antibody (1:5000) for one hour.

**BrdU analysis.**

The BrdU assay was performed as previously described in (44, 55) with few modifications.  $2 \times 10^6$  BF cells were incubated with 50  $\mu$ M 5-bromo-2-deoxyuridine (Sigma) and 50  $\mu$ M 2-deoxycytidine (Sigma) at 37°C for 30 and 480 minutes. Cells were washed in media, dried on a

slide and fixed in methanol ( $-20^{\circ}\text{C}$ ) for 30 minutes. After fixation, cells were rehydrated in PBS and pretreated with 2.0 M HCl for an additional 30 minutes. Slides were neutralized in PBS (three five minute washes) and prepared for immunofluorescence. For FKC localization, slides were fixed with methanol for 10 min and treated with ice cold 2% paraformaldehyde on the slide for 5 min. Next the slides were heated at  $90^{\circ}\text{C}$  in 10 mM sodium citrate (pH 6.0) for 10 minutes. Slides were removed from bath, allowed to cool to room temperature ( $27^{\circ}\text{C}$ ) and washed with PBS for immunofluorescence assay.

### **Immunofluorescence microscopy.**

Log phase cultured  $\alpha$ -KDE2-PTP BF and PF cells were incubated with MitoTracker® (Life Technologies, Grand Island, NY, USA), washed, equilibrated with media for 30 minutes and attached to poly-l-lysine slides for 30 additional minutes. Cells were fixed with 0.5% paraformaldehyde for one minute, washed in PBS, and permeabilized with ice cold 0.05% Triton X-100 in PBS for five minutes at  $4^{\circ}\text{C}$ . Slides were washed and blocked using 20% fetal bovine serum in PBS. Cells were incubated with Protein C polyclonal antibodies (1:200) diluted in blocking buffer and remained in primary for one hour. Slides were washed and cells were incubated with appropriate secondary antibody (1:500) for 30 minutes. For FKCs, intact and DNAase treated structures were dried on a slide and fixed with methanol ( $-20^{\circ}\text{C}$ ) for 10 minutes.

Slides were blocked with 0.5% BSA in PBS for 30 minutes and the following primary antibodies were diluted in the blocking buffer and added: monoclonal rat YL1/2 (1:1000) and polyclonal rabbit Protein C (1:200). Slides were washed in blocking buffer and appropriate secondary antibody (1:500) was used. BF  $\alpha$ -KDE2 RNAi cells were washed in media, dried on slide and fixed in methanol for 10 minutes. BrdU treated FKCs were blocked in 0.5% BSA in PBS for 30 minutes and incubated with polyclonal rabbit Protein C (1:200) and monoclonal mouse BrdU (1:100) primary antibodies diluted in blocking buffer for 90 minutes. Slides were washed in blocking buffer and incubated in appropriate secondary antibody (polyclonal, 1:500; monoclonal, 1:100) for one hour. After secondary, all slides were rinsed in PBS and coated with 4',6'-diamidino-2-phenylindole (DAPI) containing the antifade reagent ProlongGold (Life Technologies). Images were acquired using a Zeiss Axio Observer inverted microscope equipped with an AxioCam HSm and evaluated with AxioVision v4.6 software (Zeiss).

### **Activity of the $\alpha$ -KD.**

Purified intact PF and BF mitochondria were solubilized in buffer containing 2% (w/v) n-dodecyl- $\beta$ -D-maltoside 50 mM NaCl, 50 mM imidazole, 2 mM 6-aminohexanoic, 1mM EDTA and 1 x Complete<sup>®</sup> EDTA free protease inhibitor cocktail on ice for one hour and centrifuged at 13,000xg for 20 minutes. 40  $\mu$ g of soluble mitochondrial homogenate was incubated in one ml

of  $\alpha$ -KD assay buffer (50mM Tris-HCl, pH 7.6, 0.1 mM CaCl<sub>2</sub>, 0.05 mM EDTA, 0.3 mM thiamine pyrophosphate, 1 mM MgCl<sub>2</sub>, 3 mM  $\alpha$ -ketoglutarate, 3 mM NAD<sup>+</sup> and 0.75 mg/ml of coenzyme A at 25°C). The activity of  $\alpha$ -KD was monitored spectrophotometrically by the production of NADH per minute at 340 nm.

### **Northern and Southern analysis.**

All radiolabeled probes were prepared using Prime-It random primer labeling kit (Stratagene, Santa Clara, CA, USA). For northern analysis, total RNA was extracted from both developmental stages using TriPure Isolation Reagent (Roche). Transcripts were separated on a 7% formaldehyde 1% agarose gel, blotted to a membrane and evaluated with radiolabeled probes generated from ORF specific sequences ( $\alpha$ -KDE1,  $\alpha$ -KDE2, E3 and  $\beta$ -tubulin). Probes were hybridized in a mix containing 50% (vol/vol) formamide, 5x SSC, 5x Denhardt's solution (Sigma), 1% (w/v) SDS and 100  $\mu$ g/ml salmon sperm DNA (Life Technologies) at 55°C overnight. Blots were washed twice at 30 minute intervals in 0.2x SSC containing 0.1% SDS at 68°C. Total genomic DNA was extracted from induced ( $\alpha$ -KDE2 RNAi cells every 24 hours for Southern analysis. Undigested and digested (XbaI and HindIII) DNA was resolved by agarose and transferred to blot and analyzed for kDNA content. To evaluate minicircle sequences, probes were derived from a cloned fragment composed of predicted origin of replication (ori) and bent

helical region conserved in all minicircles. Maxicircle probes were generated from a PCR product using primers against the pre-edited 9S genomic sequence. All Southern probes were hybridized in a solution containing 50% formamide (Sigma), 3x SSC, 1x Denhardt's, 20 µg/ml salmon sperm DNA, 5% dextran sulfate and 2% SDS at 42°C overnight. Blots were washed twice in a solution containing 3x SSC/0.5% SDS at 55°C for 30 minutes and exposed to a storage phosphor screen (Molecular Dynamics) and analyzed on a STORM-860 PhosphorImager (GE Healthcare).

#### ACKNOWLEDGEMENTS

We thank D.M. Engman (MTP-70 antibody), M. Chaudhuri (TAO antibody), K. Gull (PFR antibody), A. Gunzl (c-PTP-NEO plasmid) and P. Englund (pZJM plasmid) for the reagents used in this study. We also thank members of the Hajduk lab for discussions and critical reading of this manuscript. We are particularly grateful to Torsten Ochsenreiter for important insights into mechanisms of protein diversification. This work was supported by NIH AI21401 to SLH.

## REFERENCES

1. **Perham, R. N.** 1991. Domains, motifs, and linkers in 2-oxo acid dehydrogenase multienzyme complexes: a paradigm in the design of a multifunctional protein. *Biochemistry* **30**:8501-8512.
2. **Bunik, V. I.** 2003. 2-Oxo acid dehydrogenase complexes in redox regulation. *Eur J Biochem* **270**:1036-1042.
3. **Perham, R. N.** 2000. Swinging arms and swinging domains in multifunctional enzymes: catalytic machines for multistep reactions. *Annu Rev Biochem* **69**:961-1004.
4. **Sato, H., A. Tachifuji, M. Tamura, and I. Miyakawa.** 2002. Identification of the YMN-1 antigen protein and biochemical analyses of protein components in the mitochondrial nucleoid fraction of the yeast *Saccharomyces cerevisiae*. *Protoplasma* **219**:51-58.
5. **Kaufman, B. A., S. M. Newman, R. L. Hallberg, C. A. Slaughter, P. S. Perlman, and R. A. Butow.** 2000. In organello formaldehyde crosslinking of proteins to mtDNA: identification of bifunctional proteins. *Proc Natl Acad Sci U S A* **97**:7772-7777.
6. **Bogenhagen, D. F., Y. Wang, E. L. Shen, and R. Kobayashi.** 2003. Protein components of mitochondrial DNA nucleoids in higher eukaryotes. *Mol Cell Proteomics* **2**:1205-1216.
7. **Bogenhagen, D. F., D. Rousseau, and S. Burke.** 2008. The layered structure of human mitochondrial DNA nucleoids. *J Biol Chem* **283**:3665-3675.
8. **Stein, A., and W. Firshein.** 2000. Probable identification of a membrane-associated repressor of *Bacillus subtilis* DNA replication as the E2 subunit of the pyruvate dehydrogenase complex. *J Bacteriol* **182**:2119-2124.
9. **Walter, T., and A. Aronson.** 1999. Specific binding of the E2 subunit of pyruvate dehydrogenase to the upstream region of *Bacillus thuringiensis* protoxin genes. *J Biol Chem* **274**:7901-7906.

10. **Chen, X. J., and R. A. Butow.** 2005. The organization and inheritance of the mitochondrial genome. *Nat Rev Genet* **6**:815-825.
11. **Ogbadoyi, E. O., D. R. Robinson, and K. Gull.** 2003. A high-order trans-membrane structural linkage is responsible for mitochondrial genome positioning and segregation by flagellar basal bodies in trypanosomes. *Mol Biol Cell* **14**:1769-1779.
12. **Lukes, J., H. Hashimi, and A. Zikova.** 2005. Unexplained complexity of the mitochondrial genome and transcriptome in kinetoplastid flagellates. *Curr Genet* **48**:277-299.
13. **Durieux, P. O., P. Schutz, R. Brun, and P. Kohler.** 1991. Alterations in Krebs cycle enzyme activities and carbohydrate catabolism in two strains of *Trypanosoma brucei* during in vitro differentiation of their bloodstream to procyclic stages. *Mol Biochem Parasitol* **45**:19-27.
14. **van Weelden, S. W., J. J. van Hellemond, F. R. Opperdoes, and A. G. Tielens.** 2005. New functions for parts of the Krebs cycle in procyclic *Trypanosoma brucei*, a cycle not operating as a cycle. *J Biol Chem* **280**:12451-12460.
15. **Cristodero, M., T. Seebeck, and A. Schneider.** 2010. Mitochondrial translation is essential in bloodstream forms of *Trypanosoma brucei*. *Mol Microbiol* **78**:757-769.
16. **Fisk, J. C., M. L. Ammerman, V. Presnyak, and L. K. Read.** 2008. TbRGG2, an essential RNA editing accessory factor in two *Trypanosoma brucei* life cycle stages. *J Biol Chem* **283**:23016-23025.
17. **Schnauffer, A., G. D. Clark-Walker, A. G. Steinberg, and K. Stuart.** 2005. The F1-ATP synthase complex in bloodstream stage trypanosomes has an unusual and essential function. *EMBO J* **24**:4029-4040.
18. **Schnauffer, A., A. K. Panigrahi, B. Panicucci, R. P. Igo, Jr., E. Wirtz, R. Salavati, and K. Stuart.** 2001. An RNA ligase essential for RNA editing and survival of the bloodstream form of *Trypanosoma brucei*. *Science* **291**:2159-2162.
19. **Bruhn, D. F., M. P. Sammartino, and M. M. Klingbeil.** 2011. Three mitochondrial DNA polymerases are essential for kinetoplast DNA replication and survival of bloodstream form *Trypanosoma brucei*. *Eukaryot Cell* **10**:734-743.

20. **Concepcion-Acevedo, J., J. Luo, and M. M. Klingbeil.** 2012. Dynamic Localization of *Trypanosoma brucei* Mitochondrial DNA Polymerase ID. *Eukaryot Cell* **11**:844-855.
21. **Liu, B., Y. Liu, S. A. Motyka, E. E. Agbo, and P. T. Englund.** 2005. Fellowship of the rings: the replication of kinetoplast DNA. *Trends Parasitol* **21**:363-369.
22. **Drew, M. E., and P. T. Englund.** 2001. Intramitochondrial location and dynamics of *Crithidia fasciculata* kinetoplast minicircle replication intermediates. *J Cell Biol* **153**:735-744.
23. **Englund, P. T.** 1979. Free minicircles of kinetoplast DNA in *Crithidia fasciculata*. *J Biol Chem* **254**:4895-4900.
24. **Abu-Elneel, K., I. Kapeller, and J. Shlomai.** 1999. Universal minicircle sequence-binding protein, a sequence-specific DNA-binding protein that recognizes the two replication origins of the kinetoplast DNA minicircle. *J Biol Chem* **274**:13419-13426.
25. **Ferguson, M., A. F. Torri, D. C. Ward, and P. T. Englund.** 1992. In situ hybridization to the *Crithidia fasciculata* kinetoplast reveals two antipodal sites involved in kinetoplast DNA replication. *Cell* **70**:621-629.
26. **Torri, A. F., and P. T. Englund.** 1995. A DNA polymerase beta in the mitochondrion of the trypanosomatid *Crithidia fasciculata*. *J Biol Chem* **270**:3495-3497.
27. **Wang, Z., and P. T. Englund.** 2001. RNA interference of a trypanosome topoisomerase II causes progressive loss of mitochondrial DNA. *EMBO J* **20**:4674-4683.
28. **Klingbeil, M. M., S. A. Motyka, and P. T. Englund.** 2002. Multiple mitochondrial DNA polymerases in *Trypanosoma brucei*. *Mol Cell* **10**:175-186.
29. **Downey, N., J. C. Hines, K. M. Sinha, and D. S. Ray.** 2005. Mitochondrial DNA ligases of *Trypanosoma brucei*. *Eukaryot Cell* **4**:765-774.
30. **Zhao, Z., M. E. Lindsay, A. Roy Chowdhury, D. R. Robinson, and P. T. Englund.** 2008. p166, a link between the trypanosome mitochondrial DNA and flagellum, mediates genome segregation. *EMBO J* **27**:143-154.

31. **Robinson, D. R., and K. Gull.** 1991. Basal body movements as a mechanism for mitochondrial genome segregation in the trypanosome cell cycle. *Nature* **352**:731-733.
32. **Ochsenreiter, T., and S. L. Hajduk.** 2006. Alternative editing of cytochrome c oxidase III mRNA in trypanosome mitochondria generates protein diversity. *EMBO Rep* **7**:1128-1133.
33. **Ochsenreiter, T., S. Anderson, Z. A. Wood, and S. L. Hajduk.** 2008. Alternative RNA editing produces a novel protein involved in mitochondrial DNA maintenance in trypanosomes. *Mol Cell Biol* **28**:5595-5604.
34. **Ochsenreiter, T., M. Cipriano, and S. L. Hajduk.** 2008. Alternative mRNA editing in trypanosomes is extensive and may contribute to mitochondrial protein diversity. *PLoS One* **3**:e1566.
35. **Priest, J. W., and S. L. Hajduk.** 1994. Developmental regulation of *Trypanosoma brucei* cytochrome c reductase during bloodstream to procyclic differentiation. *Mol Biochem Parasitol* **65**:291-304.
36. **Torri, A. F., and S. L. Hajduk.** 1988. Posttranscriptional regulation of cytochrome c expression during the developmental cycle of *Trypanosoma brucei*. *Mol Cell Biol* **8**:4625-4633.
37. **Siegel, T. N., K. Gunasekera, G. A. Cross, and T. Ochsenreiter.** 2011. Gene expression in *Trypanosoma brucei*: lessons from high-throughput RNA sequencing. *Trends Parasitol* **27**:434-441.
38. **Siegel, T. N., D. R. Hekstra, X. Wang, S. Dewell, and G. A. Cross.** 2010. Genome-wide analysis of mRNA abundance in two life-cycle stages of *Trypanosoma brucei* and identification of splicing and polyadenylation sites. *Nucleic Acids Res* **38**:4946-4957.
39. **Nilsson, D., K. Gunasekera, J. Mani, M. Osteras, L. Farinelli, L. Baerlocher, I. Roditi, and T. Ochsenreiter.** 2010. Spliced leader trapping reveals widespread alternative splicing patterns in the highly dynamic transcriptome of *Trypanosoma brucei*. *PLoS Pathog* **6**:e1001037.

40. **Kolev, N. G., J. B. Franklin, S. Carmi, H. Shi, S. Michaeli, and C. Tschudi.** 2010. The transcriptome of the human pathogen *Trypanosoma brucei* at single-nucleotide resolution. *PLoS Pathog* **6**:e1001090.
  
41. **Roldan, A., M. A. Comini, M. Crispo, and R. L. Krauth-Siegel.** 2011. Lipoamide dehydrogenase is essential for both bloodstream and procyclic *Trypanosoma brucei*. *Mol Microbiol* **81**:623-639.
  
42. **Schimanski, B., T. N. Nguyen, and A. Gunzl.** 2005. Highly efficient tandem affinity purification of trypanosome protein complexes based on a novel epitope combination. *Eukaryot Cell* **4**:1942-1950.
  
43. **Kelly, S., J. Reed, S. Kramer, L. Ellis, H. Webb, J. Sunter, J. Salje, N. Marinsek, K. Gull, B. Wickstead, and M. Carrington.** 2007. Functional genomics in *Trypanosoma brucei*: a collection of vectors for the expression of tagged proteins from endogenous and ectopic gene loci. *Mol Biochem Parasitol* **154**:103-109.
  
44. **Woodward, R., and K. Gull.** 1990. Timing of nuclear and kinetoplast DNA replication and early morphological events in the cell cycle of *Trypanosoma brucei*. *J Cell Sci* **95 ( Pt 1)**:49-57.
  
45. **Johnson, C. E., and P. T. Englund.** 1998. Changes in organization of *Crithidia fasciculata* kinetoplast DNA replication proteins during the cell cycle. *J Cell Biol* **143**:911-919.
46. **Wang, Z., J. C. Morris, M. E. Drew, and P. T. Englund.** 2000. Inhibition of *Trypanosoma brucei* gene expression by RNA interference using an integratable vector with opposing T7 promoters. *J Biol Chem* **275**:40174-40179.
  
47. **Liu, Y., S. A. Motyka, and P. T. Englund.** 2005. Effects of RNA interference of *Trypanosoma brucei* structure-specific endonuclease-I on kinetoplast DNA replication. *J Biol Chem* **280**:35513-35520.
  
48. **Brown, S. V., P. Hosking, J. Li, and N. Williams.** 2006. ATP synthase is responsible for maintaining mitochondrial membrane potential in bloodstream form *Trypanosoma brucei*. *Eukaryot Cell* **5**:45-53.

49. **Bhat, G. J., D. J. Koslowsky, J. E. Feagin, B. L. Smiley, and K. Stuart.** 1990. An extensively edited mitochondrial transcript in kinetoplastids encodes a protein homologous to ATPase subunit 6. *Cell* **61**:885-894.
50. **Graveley, B. R.** 2001. Alternative splicing: increasing diversity in the proteomic world. *Trends Genet* **17**:100-107.
51. **Chen, X. J., X. Wang, B. A. Kaufman, and R. A. Butow.** 2005. Aconitase couples metabolic regulation to mitochondrial DNA maintenance. *Science* **307**:714-717.
52. **Elpeleg, O., C. Miller, E. Hershkovitz, M. Bitner-Glindzicz, G. Bondi-Rubinstein, S. Rahman, A. Pagnamenta, S. Eshhar, and A. Saada.** 2005. Deficiency of the ADP-forming succinyl-CoA synthase activity is associated with encephalomyopathy and mitochondrial DNA depletion. *Am J Hum Genet* **76**:1081-1086.
53. **Harris, M. E., D. R. Moore, and S. L. Hajduk.** 1990. Addition of uridines to edited RNAs in trypanosome mitochondria occurs independently of transcription. *J Biol Chem* **265**:11368-11376.
54. **Wittig, I., H. P. Braun, and H. Schagger.** 2006. Blue native PAGE. *Nat Protoc* **1**:418-428.
55. **Tang, X., D. L. Falls, X. Li, T. Lane, and M. B. Luskin.** 2007. Antigen-retrieval procedure for bromodeoxyuridine immunolabeling with concurrent labeling of nuclear DNA and antigens damaged by HCl pretreatment. *J Neurosci* **27**:5837-5844.

## CHAPTER 4

### RNAi MEDIATED KNOCKDOWN OF $\alpha$ -KETOGLUTARATE DEHYDROGENASE E1 CAUSES RAPID SWELLING OF THE TRYPANOSOME FLAGELLAR POCKET

#### INTRODUCTION

The  $\alpha$ -ketoglutarate dehydrogenase complex ( $\alpha$ -KD) is a mitochondrial Krebs cycle enzyme involved in the breakdown of  $\alpha$ -ketoglutarate to succinyl-CoA thereby producing an electron sink which is utilized further by the electron transport chain. This large multimeric structure is a member of the  $\alpha$ -keto acid dehydrogenase family (includes pyruvate dehydrogenase and branched chained  $\alpha$ -keto acid dehydrogenase) and is composed of multiple copies of three distinct enzymatic subunits arranged for efficient transfer of substrate between the active sites (1). Briefly, the  $\alpha$ -ketoglutarate decarboxylase ( $\alpha$ -KDE1) catalyzes the initial oxidative decarboxylation of  $\alpha$ -ketoglutarate and subsequently transferring an acyl group to the lipoyl domain of the dihydrolipoyl succinyltransferase ( $\alpha$ -KDE2) (1, 2).  $\alpha$ -KDE2 combines the acyl group with CoA to form succinyl-CoA and dihydrolipoamide dehydrogenase (E3) regenerates the lipoic acid group on  $\alpha$ -KDE2 thereby producing NADH (1, 2). From bacteria to higher eukaryotes, these protein components possess distinct functions that make  $\alpha$ -KD an essential complex in metabolism.

The protozoan parasite *Trypanosoma brucei* contains a single mitochondrion that undergoes extreme morphological and functional adaptations during the biphasic (between insect and mammal) life cycle of the organism (3). In the insect, the robust mitochondrion of procyclic form (PF) *T. brucei* has an active Krebs pathway and electron transport enzymes that are utilized in the generation of ATP (4). The  $\alpha$ -KD is expressed in this form and plays an essential role in the metabolism of proline, an abundant carbon source in the midgut of the tsetse fly (5). Alternatively, the mammalian blood is rich in glucose and bloodstream form (BF) trypanosomes metabolize this sugar in organelles called glycosomes for energy (6). Therefore, the mitochondrion in this cell form is reduced and many processes and proteins including an active  $\alpha$ -KD are developmentally regulated (3).

Many of the Krebs pathway enzymes in diverse organisms have additional functions that are unrelated to the known metabolic activities of these proteins (7). A previous study conducted by our lab has shown that despite the lack of a functional  $\alpha$ -KD in BF *T. brucei*, mRNA transcripts are detectable for the  $\alpha$ -KDE1,  $\alpha$ -KDE2 and E3 enzymes (8). Epitope tagging of the  $\alpha$ -KDE2 subunit identified two alternative localizations of the protein, the mitochondrial membrane and the antipodal sites of the mitochondrial DNA body, the kinetoplast (8). Furthermore, knockdown of  $\alpha$ -KDE2 caused a kinetoplast cytokinesis defect with an increase in dyskinetoplastic cells and trypanosomes containing two kinetoplasts (8). Alternatively, only the electron transference activity has been identified for the flavoprotein E3. While the metabolic activities for  $\alpha$ -KDE1 and  $\alpha$ -KDE2 are specific for  $\alpha$ -KD, E3 is also a shared component of three additional nonrelated metabolic complexes (9). Moreover, E3 has been reported

to be essential in BF *T. brucei* cultured in the absence of thymidine and strongly suggests required participation of this enzyme with the glycine cleavage complex (9). To date, an added non-metabolic function of the  $\alpha$ -KDE1 subunit has yet to be identified in trypanosomes.

In this preliminary study, we use the RNA interference (RNAi) method to understand the function of  $\alpha$ -KDE1 in BF *T. brucei*. We found that partial knockdown of  $\alpha$ -KDE1 mRNA is adequate to drastically inhibit cell growth. Additionally, reduction in these transcripts caused rapid swelling of the flagellar pocket (FP), a highly specialized membrane invagination at the base of the flagellum that is key in endo- and exocytotic trafficking in the cell (10). These findings are similar to what was observed during depletion studies of known proteins that function in FP maintenance and we propose that  $\alpha$ -KDE1 influences this organelle by direct or indirect mechanisms.

#### REDUCTION IN THE LEVELS OF $\alpha$ -KDE1 MRNA CAUSES RAPID MORPHOLOGICAL CHANGES IN BF *T. BRUCEI*

In order to assess the function of  $\alpha$ -KDE1, a partial ORF specific for this gene was ligated into the inducible pZJM RNAi vector (11) and subsequently transfected into BF cells. Protein knockdown was initiated by 1  $\mu$ g/ml doxycycline and cells were evaluated for  $\alpha$ -KDE1 mRNA loss, changes in growth and morphological alterations. Initial observation of induced trypanosomes (+RNAi) revealed a reduction in cell number after 24 hours. More specifically, an arrest in growth was observed at the 6 hour time

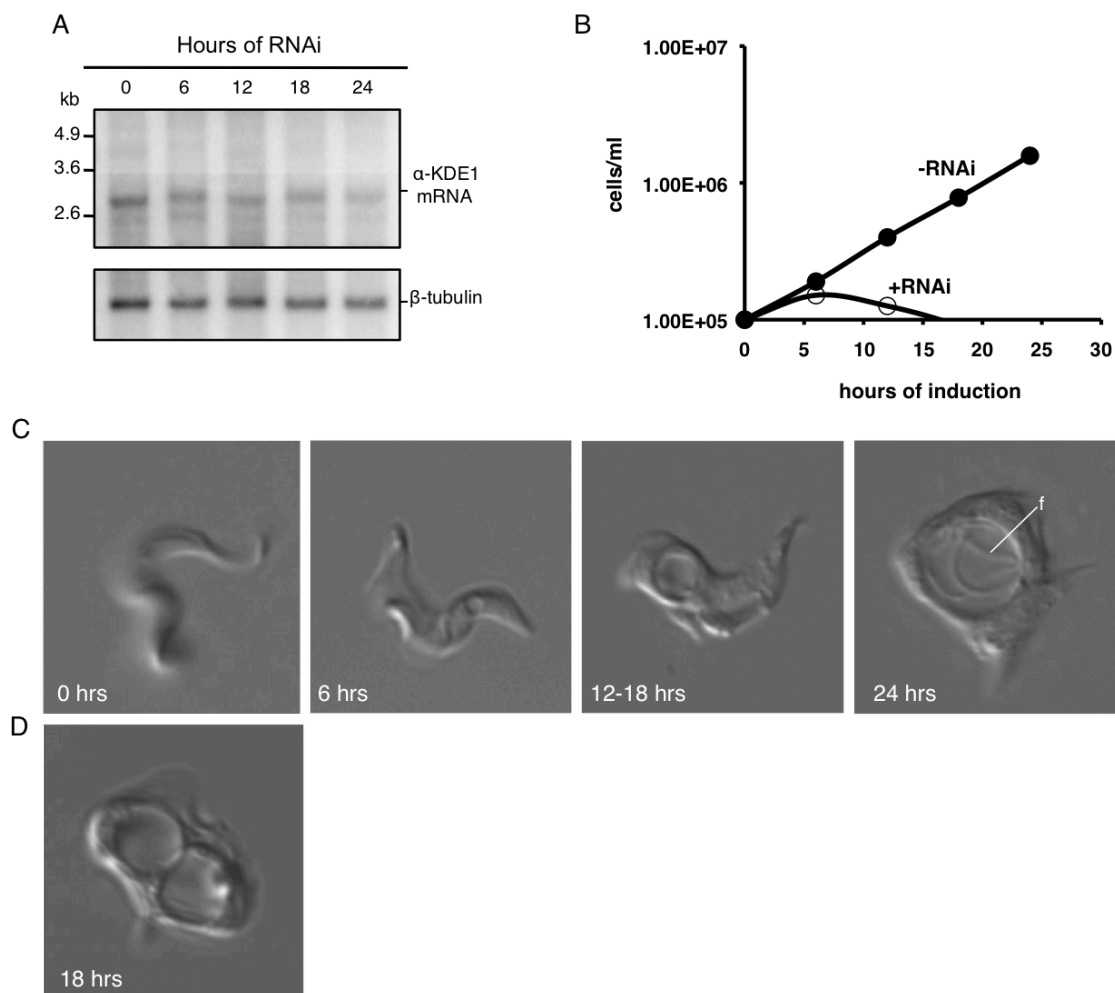


**Figure 4.1.** Effect of  $\alpha$ -KDE1 mRNA knockdown in BF *T. brucei*. BF *T. brucei* were transfected with the inducible pZJM RNAi vector containing  $\alpha$ -KDE1 ORF. A) Northern analysis showing the reduction in  $\alpha$ -KDE1 mRNA by 24 hours. Blot was analyzed with probes against  $\alpha$ -KDE1 and  $\beta$ -tubulin sequences. B) The effects of  $\alpha$ -KDE1 knockdown on cell growth. Cells were grown in the presence or absence of 1  $\mu$ g/ml doxycycline and monitored for differences in proliferation. C) and D) Still images extracted from video of induced  $\alpha$ -KDE1 RNAi cells taken at 0, 6, 12-18 and 24 hrs. Position of the flagella (f) is indicated.

point followed by a steady decrease in intact cells as compared to the –RNAi trypanosomes (Figure 4.1B). Total RNA was extracted from induced cells at 6 hour intervals over a course of 24 hours, fractionated (cell equivalents) on a denaturing formaldehyde agarose gel and transferred to a blot for  $\alpha$ -KDE1 mRNA detection. Northern blot analysis with specific probes for  $\alpha$ -KDE1 mRNA detected a band migrating around 3.0 kb (Figure 4.1A). The intensity of the bands were normalized to  $\beta$ -tubulin and knockdown of our target mRNA was confirmed by a 55 % decrease in signal at 24 hours. The inhibition of growth by mRNA depletion was accompanied by the formation of a large intracellular vesicular-like swelling that is observable by microscope at low magnification. Still DIC images of this morphology taken from video at 0, 6, 12-18 and 24 hour time points are shown in Figure 3.1C. The image at time 0 hr denoted a structurally intact cell undergoing flagella mediated tumbling that is key to vital trypanosome processes (12) and this rapid rotational motion was evident from portions of the cell body positioned in and out of the focal plane. Tumbling was restricted by 6 hours and a 1-2 $\mu$ m vesicle appeared close to the posterior tip of the cell. This enclosed compartment continued to enlarge until it encompassed the entire cell body with flagella encapsulated within this structure (24 hours). Cells with multiple swellings were also observed (Figure 4.1D).

#### $\alpha$ -KDE1 DEPLETION CAUSES FP SWELLING

*T. brucei* is a highly polarized organism that contains essential single copy organelles in the posterior portion of the cell body and includes the lysosome, Golgi,

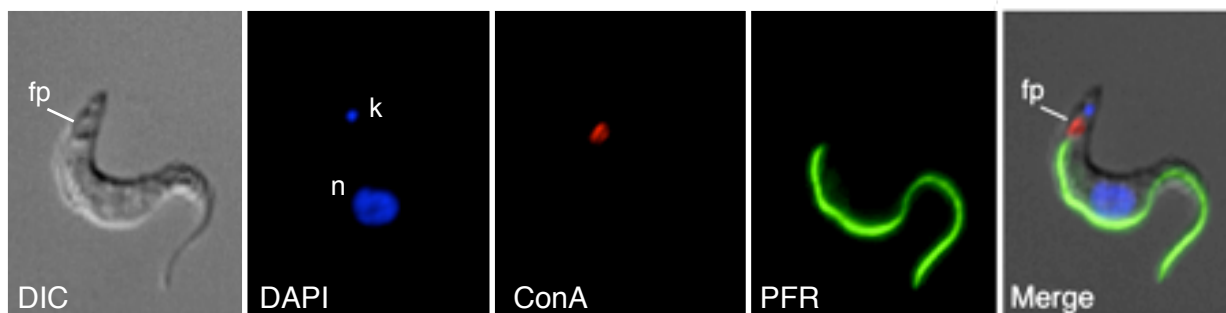


**Figure 4.2.** Cellular localization of the FP in  $\alpha$ -KDE1 RNAi cells. 6 hr induced  $\alpha$ -KDE1 RNAi BF cells were incubated with FITC-ConA at 3°C for 15 min, washed and fixed for fluorescence microscopy. Cells were also stained for DNA with DAPI and antibodies against the paraflagellar rod (PFR). Position of the FP is indicated.

endoplasmic reticulum and FP. In particular, the FP is a major hub for the rapid trafficking of glycosylphosphatidylinositol (GPI)-anchored proteins and has an important role in host immune evasion (10, 13, 14). Multiple proteins are involved in maintenance of FP function and ablation of these proteins caused extreme changes in the morphology of this organelle (15-17). The enlarged FP morphology in these studies was very similar to the phenotype observed in the  $\alpha$ -KDE1 RNAi analysis (Figure 4.1C) and we wanted to identify the position of this organelle relative to the swollen compartment in our cell line.

Concanavalin A (Con A) is a mannose-binding lectin that specifically binds GPI-anchored glycoproteins associated with the matrix of the FP and endocytotic vesicles (15). In order to localize the FP in BF trypanosomes,  $\alpha$ -KDE1 knockdown was induced for 6 hours and cells were incubated with serum-free HMI9 containing 5  $\mu$ g/ml FITC-

Con A and 1% BSA at 3°C for 15 min. Post FP labeling, cells were washed in ice cold serum-free HMI9 and fixed on ice in 1% PFA/serum-free HMI9 for 5 min. Cells were subsequently prepared for fluorescence microscopy and analyzed for the presence of FITC-Con A, paraflagellar rod (PFR) and the kinetoplast. The vesicular-like swelling was revealed in a region between the posterior tip of the PFR and kinetoplast (Figure 4.2) and previous studies have defined this area as the FP-containing domain (18). 3°C halted endocytosis and FITC-Con A bound and was restricted to the FP (15). This discrete FITC-Con A staining superimposed with 6 hour swollen compartment and confirmed that this structure is the FP (Figure 4.2 merge).

## DISCUSSION

*T. brucei* is able to developmentally regulate the pathways of energy production to meet the demands of a constantly changing extracellular environment. Though BF trypanosomes undergo major metabolic regulation of the mitochondria, altered and multifunctioning mitochondrial proteins are expressed at this stage (8, 19-21). Many metabolic enzymes have long been recognized for having two or more unrelated activities, thereby adding to the functional diversity of the genome and the mitochondrial Krebs pathway is no stranger to this phenomenon (7, 22). The roles of two  $\alpha$ -KD subunits in the repressed mitochondrion of BF *T. brucei* have been revealed (8, 9). Here we test the function of  $\alpha$ -KDE1 by RNAi analysis and show that the protein is essential in maintaining the activities of the FP.

The trypanosome FP has a very complex architecture that interacts with the endosomal and secretory systems (23-25). Diverse proteins are required to maintain FP architecture and vesicle transport, hence it is likely that this group will also include multifunctioning sequences that add to the intricacy of these structures. BILBO1 is a unique FP cytoskeletal protein exclusive to trypanosomes and its ablation prevented FP biogenesis, thus creating nonviable rounded-up BF cells after 24 hrs (26). Alternatively, clathrin is a membrane coat protein that is ubiquitous in eukaryotic organisms (27, 28) and required for plasma membrane endocytosis in BF *T. brucei* (15). Reduction in clathrin levels resulted in rapid swelling of the FP (visible within 10 hrs) and is denoted as the BigEye phenotype (15). Our data revealed that RNAi of  $\alpha$ -KDE1 caused a similar BigEye morphology with specific differences. 1) Trypanosome growth halted at 6 hrs and was immediately followed by rapid cell death. Cell lysis is mediated by pressure induced membrane disruption (data not shown) and is in agreement with what is observed for the clathrin RNAi cells. 2) An outgrowth of normal cells was not observed in our analysis and suggests that depletion of  $\alpha$ -KDE1 halts cytokinesis. 3) Flagella were embedded in the larger pockets (mainly observed between 18 to 24 hrs, Figure 4.1C) and are contrasting to the detached flagella revealed in the clathrin analysis. Perhaps the flagella remain affixed to a portion of the pocket proximal to the basal bodies and the increase luminal volume, which increases the distance between the poles of this FP, draws in these structures. Overall, knockdown of  $\alpha$ -KDE1 does not inhibit FP biogenesis (Figure 4.1D) and the swelling morphology supports a complication in vesicular trafficking.

BF *T. brucei* exhibit high rates of endo- and exocytosis (29) and explains the rapid inflation of the FP. Onset of the induced phenotype is immediate (within 6 hrs) and

may suggest that  $\alpha$ -KDE1 levels are maintained at a critical concentration or the protein is quickly turned over. The known metabolic function of  $\alpha$ -KDE1 is the initial breakdown of  $\alpha$ -ketoglutarate in the matrix of the mitochondria. Since a functional  $\alpha$ -KD is not expressed in the mitochondria of BF *T. brucei*, unique opportunities arise for  $\alpha$ -KDE1 to switch functions. The active sites for many metabolic enzymes accounts for a small portion of the exposed surface area of the protein (22) and expression of the native  $\alpha$ -KDE1 free of interacting  $\alpha$ -KD subunits ( $\alpha$ -KDE2 and E3) could liberate blocked functional domains. Also, new functions can arise through a different subcellular locale of enzymes (22), thus movement of  $\alpha$ -KDE1 from the oxidative environment of the mitochondrion to the cytosol or FP lumen may induce alternate functions. Further studies are needed to verify  $\alpha$ -KDE1 localization in this cell form.

The studies reported here add another facet to the function of diverse proteins in the complex biology of *T. brucei*. This is also the first evidence of a historically defined matrix mitochondrial enzyme affecting trafficking at the FP. The highly organized FP provides the only access between the extracellular environment and cytoplasm, thus conventional and unconventional regulators are also needed to coordinate this process. A complete understanding of the role of  $\alpha$ -KDE1 in FP maintenance will provide insight into additional proteins that are involved in the endomembrane system of trypanosomes.

## MATERIALS AND METHODS

### **Cell Culture of RNAi cell line.**

Bloodstream form *T. brucei* were maintained in HMI-9 medium containing tetracycline free FBS and Serum Plus media supplement (SAFC Biosciences, Lenexa, KS). The cell line was cultured continuously in 2.5  $\mu\text{g/ml}$  hygromycin, 2  $\mu\text{g/ml}$  G418 and 2.5  $\mu\text{g/ml}$  phleomycin. RNAi was induced with 1  $\mu\text{g/ml}$  of doxycycline.

### **Construction of $\alpha$ -KDE1 RNAi cell line.**

For  $\alpha$ -KDE1 RNAi cell line, primers 5' -CCCTCGAGTGGCGCAGAGTCACTTATTG - 3' and 5' -CCAAGCTTAATGGGACACTGAAAGGCAC - 3' were used to amplify a partial  $\alpha$ -KDE1 (Tb11.01.1740) sequence (580 bps) from BS-9013 genomic DNA and was ligated into the inducible pZJM RNAi vector (11). NotI was used to linearize construct and the sequence was transfected using the Lonza nucleofactor system (Lonza, Walkersville, MD, USA).

### **Northern analysis.**

Total RNA was extracted from the RNAi cell line using TriPure Isolation Reagent (Roche, Indianapolis, IN, USA) and transcripts were separated on a 7% formaldehyde 1% agarose gel, blotted to a membrane and evaluated with radiolabeled probes generated from ORFs specific for  $\alpha$ -KDE1 and  $\beta$ -tubulin. Radiolabeled probes were prepared using Prime-It random primer labeling kit (Stratagene, Santa Clara, CA, USA) and were hybridized in a buffer containing 50% (vol/vol) formamide, 5x SSC, 5x Denhardt's

solution (Sigma, St. Louis, MO, USA), 1% (w/v) SDS and 100 µg/ml salmon sperm DNA (Life Technologies, Grand Island, NY, USA) at 55°C overnight. Blots were washed three times at 30 minute intervals in 0.2x SSC containing 0.1% SDS at 68°C and exposed to a storage phosphor screen (Molecular Dynamics) and analyzed on a STORM-860 PhosphorImager (GE Healthcare).

### **Binding assay.**

1x10<sup>7</sup> BF  $\alpha$ -KDE1 RNAi cells were induced with 1 µg/ml doxycycline for 6 hours and washed in ice cold serum-free HMI9. Con A binding was performed as previously described in Allen et al. (2003) with minor modifications (15). Washed cells were resuspended in 3°C serum-free HMI9 containing 1% BSA and 5 µg/ml FITC-ConA and incubated for 15 min. Cells were transferred to ice for 5 minutes and subsequently washed in ice cold serum-free HMI9. The cell pellet was resuspended in 1% PFA/serum-free HMI9 for 5 min washed and prepared for fluorescence microscopy.

### **Fluorescence microscopy.**

PFA fixed  $\alpha$ -KDE1 RNAi cells were dried on a slide and fixed in -20°C methanol for 10 min. Slides were washed and blocked using 20% fetal bovine serum in PBS for 30 min. Cells were incubated with paraflagellar rod (PFR) antibodies (1:500) diluted in blocking buffer and remained in primary for one hour. Slides were washed and cells were incubated with appropriate secondary antibody (1:500) for 30 minutes in the same blocking buffer. After secondary, slides were rinsed in PBS and coated with 4',6'-diamidino-2-phenylindole (DAPI) containing the antifade reagent ProlongGold (Life

Technologies, Grand Island, NY, USA). Images were acquired using a Zeiss Axio Observer inverted microscope equipped with an AxioCam HSm and evaluated with AxioVision v4.6 software (Zeiss).

## REFERENCES

1. **Perham, R. N.** 1991. Domains, motifs, and linkers in 2-oxo acid dehydrogenase multienzyme complexes: a paradigm in the design of a multifunctional protein. *Biochemistry* **30**:8501-8512.
2. **Perham, R. N.** 2000. Swinging arms and swinging domains in multifunctional enzymes: catalytic machines for multistep reactions. *Annu Rev Biochem* **69**:961-1004.
3. **Vickerman, K.** 1985. Developmental cycles and biology of pathogenic trypanosomes. *Br Med Bull* **41**:105-114.
4. **van Hellemond, J. J., F. R. Opperdoes, and A. G. Tielens.** 2005. The extraordinary mitochondrion and unusual citric acid cycle in *Trypanosoma brucei*. *Biochem Soc Trans* **33**:967-971.
5. **van Weelden, S. W., B. Fast, A. Vogt, P. van der Meer, J. Saas, J. J. van Hellemond, A. G. Tielens, and M. Boshart.** 2003. Procylic *Trypanosoma brucei* do not use Krebs cycle activity for energy generation. *J Biol Chem* **278**:12854-12863.
6. **Parsons, M.** 2004. Glycosomes: parasites and the divergence of peroxisomal purpose. *Mol Microbiol* **53**:717-724.
7. **Sriram, G., J. A. Martinez, E. R. McCabe, J. C. Liao, and K. M. Dipple.** 2005. Single-gene disorders: what role could moonlighting enzymes play? *Am J Hum Genet* **76**:911-924.
8. **Sykes, S. E., and S. L. Hajduk.** Dual Functions of alpha-Ketoglutarate Dehydrogenase E2 in the Krebs Cycle and Mitochondrial DNA Inheritance in *Trypanosoma brucei*. *Eukaryot Cell*, in press. EC00269-12R1.

9. **Roldan, A., M. A. Comini, M. Crispo, and R. L. Krauth-Siegel.** 2011. Lipoamide dehydrogenase is essential for both bloodstream and procyclic *Trypanosoma brucei*. *Mol Microbiol* **81**:623-639.
10. **Field, M. C., S. K. Natesan, C. Gabernet-Castello, and V. L. Koumandou.** 2007. Intracellular trafficking in the trypanosomatids. *Traffic* **8**:629-639.
11. **Wang, Z., J. C. Morris, M. E. Drew, and P. T. Englund.** 2000. Inhibition of *Trypanosoma brucei* gene expression by RNA interference using an integratable vector with opposing T7 promoters. *J Biol Chem* **275**:40174-40179.
12. **Broadhead, R., H. R. Dawe, H. Farr, S. Griffiths, S. R. Hart, N. Portman, M. K. Shaw, M. L. Ginger, S. J. Gaskell, P. G. McKean, and K. Gull.** 2006. Flagellar motility is required for the viability of the bloodstream trypanosome. *Nature* **440**:224-227.
13. **Overath, P., and M. Engstler.** 2004. Endocytosis, membrane recycling and sorting of GPI-anchored proteins: *Trypanosoma brucei* as a model system. *Mol Microbiol* **53**:735-744.
14. **Shiflett, A. M., S. D. Faulkner, L. F. Cotlin, J. Widener, N. Stephens, and S. L. Hajduk.** 2007. African trypanosomes: intracellular trafficking of host defense molecules. *J Eukaryot Microbiol* **54**:18-21.
15. **Allen, C. L., D. Goulding, and M. C. Field.** 2003. Clathrin-mediated endocytosis is essential in *Trypanosoma brucei*. *EMBO J* **22**:4991-5002.
16. **Price, H. P., M. Stark, and D. F. Smith.** 2007. *Trypanosoma brucei* ARF1 plays a central role in endocytosis and golgi-lysosome trafficking. *Mol Biol Cell* **18**:864-873.
17. **Young, S. A., and T. K. Smith.** 2010. The essential neutral sphingomyelinase is involved in the trafficking of the variant surface glycoprotein in the bloodstream form of *Trypanosoma brucei*. *Mol Microbiol* **76**:1461-1482.
18. **Stephens, N. A., and S. L. Hajduk.** 2011. Endosomal localization of the serum resistance-associated protein in African trypanosomes confers human infectivity. *Eukaryot Cell* **10**:1023-1033.

19. **Ochsenreiter, T., S. Anderson, Z. A. Wood, and S. L. Hajduk.** 2008. Alternative RNA editing produces a novel protein involved in mitochondrial DNA maintenance in trypanosomes. *Mol Cell Biol* **28**:5595-5604.
20. **Saas, J., K. Ziegelbauer, A. von Haeseler, B. Fast, and M. Boshart.** 2000. A developmentally regulated aconitase related to iron-regulatory protein-1 is localized in the cytoplasm and in the mitochondrion of *Trypanosoma brucei*. *J Biol Chem* **275**:2745-2755.
21. **Ochsenreiter, T., and S. L. Hajduk.** 2006. Alternative editing of cytochrome c oxidase III mRNA in trypanosome mitochondria generates protein diversity. *EMBO Rep* **7**:1128-1133.
22. **Jeffery, C. J.** 1999. Moonlighting proteins. *Trends Biochem Sci* **24**:8-11.
23. **Lacomble, S., S. Vaughan, C. Gadelha, M. K. Morphew, M. K. Shaw, J. R. McIntosh, and K. Gull.** 2009. Three-dimensional cellular architecture of the flagellar pocket and associated cytoskeleton in trypanosomes revealed by electron microscope tomography. *J Cell Sci* **122**:1081-1090.
24. **Field, H., B. R. Ali, T. Sherwin, K. Gull, S. L. Croft, and M. C. Field.** 1999. TbRab2p, a marker for the endoplasmic reticulum of *Trypanosoma brucei*, localises to the ERGIC in mammalian cells. *J Cell Sci* **112 ( Pt 2)**:147-156.
25. **Field, M. C., and M. Carrington.** 2009. The trypanosome flagellar pocket. *Nat Rev Microbiol* **7**:775-786.
26. **Bonhivers, M., S. Nowacki, N. Landrein, and D. R. Robinson.** 2008. Biogenesis of the trypanosome endo-exocytotic organelle is cytoskeleton mediated. *PLoS Biol* **6**:e105.
27. **Seeger, M., and G. S. Payne.** 1992. A role for clathrin in the sorting of vacuolar proteins in the Golgi complex of yeast. *EMBO J* **11**:2811-2818.
28. **Wetley, F. R., S. F. Hawkins, A. Stewart, J. P. Luzio, J. C. Howard, and A. P. Jackson.** 2002. Controlled elimination of clathrin heavy-chain expression in DT40 lymphocytes. *Science* **297**:1521-1525.

29. **Engstler, M., L. Thilo, F. Weise, C. G. Grunfelder, H. Schwarz, M. Boshart, and P. Overath.** 2004. Kinetics of endocytosis and recycling of the GPI-anchored variant surface glycoprotein in *Trypanosoma brucei*. *J Cell Sci* **117**:1105-1115.

## CHAPTER 5

### CONCLUSIONS AND DISCUSSION

Protein diversification in trypanosomes is implemented by well-defined mechanisms and adds to cellular complexity by increasing the number and function of proteins expressed from a single gene (1-7). The well-defined mitochondrial RNA editing and alternative trans splicing incorporate variation at the mRNA level, however added function is inherent in moonlighting proteins and is acquired from an unmodified gene. In *T. brucei*, proteins from these diversity mechanisms help to maintain unique ultrastructural features that carry out fundamental processes that are critical for cell viability and expansion (8-10). Over the last decade major advances have been made in understanding the differentially expressed trypanosome mitochondrion, which includes notable detail in the energy metabolism, RNA editing and mitochondrial genome (kinetoplast) maintenance. Despite these advances, specific details are still obscure and we propose that understanding the contribution of unorthodox proteins will aid in elucidating cryptic steps in these mechanisms. Because of the expression of a single developmentally regulated mitochondrion, *T. brucei* becomes an excellent model system for understanding the many facets of this eukaryotic organelle.

To begin understanding the contribution of mitochondrial RNA editing to protein diversity, we previously dissected a primary role for alternatively edited protein-1 (AEP-

1), a sequence generated through alternative editing of the kinetoplast (kDNA) encoded cytochrome c oxidase III (COXIII) gene and revealed that this protein serves as a maintenance factor for the mitochondrial genome (1, 4). In bloodstream form trypanosomes (BF), over 60% of AEP-1 is sequestered to the tripartite attachment complex (TAC), a highly organized structure that physically associates with the kDNA and is important for positioning and segregation of the mitochondrial genome (4, 11). Further characterization of BF AEP-1 also identified a second fraction of the protein that is distributed throughout the mitochondrial membranes in a high molecular weight complex (A-IMM) (1). A-IMM became important to our studies since the size and structure of the TAC made it difficult to analyze for potential AEP-1 interacting proteins and the only other identified sequence, p166, was detected through an RNA interference (RNAi) library screen (12). We proposed that a proteomics approach for analyzing the A-IMM would be ideal for the identification of interacting subunit proteins, thus providing insight into the specific function of the AEP-1 and the TAC. Moreover, evidence of AEP-1 expression was limited to antisera and reverse genetics analyses (1, 4) and like many mitochondrial-encoded proteins, translational confirmation of AEP-1 by direct sequencing techniques was lacking.

The peculiarity of COXIII transcripts detected in the reduced (cytochrome deficient) mitochondrion of BF trypanosomes led to the initial identification and characterization of AEP-1 in this developmental stage (1). Since the kDNA provides important coding information for multiple subunits of membrane complexes involved in energy generation, a fundamental question was raised concerning AEP-1 expression in *T. brucei*—Is AEP-1 expressed in the mitochondrion of procyclic form (PF) trypanosomes?

Enzymes involved in kDNA replication, segregation and RNA editing are essential in this form (12-14) and thus maintenance of the mitochondrial genome is a requirement for proper organelle function. We detected AEP-1 in the mitochondrion, including the TAC, of this form and this evidence suggests nonconventional RNA editing occurs at the insect developmental stage (Chapter 2, Figure 2.1).

This work provides strong evidence that AEP-1 is expressed and assembles into at least two structurally distinct complexes, the TAC and the A-IMM (Chapter 2). The translation of alternatively edited mRNAs was confirmed when a unique nine amino acid peptide specific to the novel N-terminus of AEP-1 was identified (Figure 2.5 and S2.2). This fragment was recovered from an AEP-1 antibody reactive protein band that was resolved by second dimension SDS-PAGE post native fractionation of the A-IMM (Figure 2.3 and 2.4). Is the identification of a single peptide adequate to confirm AEP-1 expression? The composition of the AEP-1 N-terminus is extremely hydrophilic and peptides from this region are not amiable to popular mass spectrometry techniques; for example these sequences associating with the mobile phase during reverse-phase high-performance liquid chromatography (15), thus detection of these amino acids is often likely to fail. Using alternative mass spectrometry separation techniques and sequencing methods such as Edman degradation (16-18) will provide greater confidence for the identification of AEP-1 and other edited proteins.

Anion exchange chromatography and tandem mass spectrometry revealed  $\alpha$ -ketoglutarate dehydrogenase complex ( $\alpha$ -KD) subunits assembling with the A-IMM and one identified enzyme,  $\alpha$ -KDE2, was not detected at the TAC by C-terminal epitope tag ( $\alpha$ -KDE2-PTP) studies analyzing flagellum-kinetoplast complexes (FKCs) (Chapter 3,

Figure 3.3 and 4). However,  $\alpha$ -KDE2-PTP was detected at specialized domains termed antipodal sites that flank the kDNA and are involved in replication of this genome (Figure 3.4). Previous studies of these sites have revealed the association of proteins involved in replication (13, 19, 20), but any structural proteins that may be important to factors like antipodal site architecture have yet to be identified. There is a prevalence of moonlighting metabolic enzymes with a nonenzymatic secondary function (6, 21) and we propose that  $\alpha$ -KDE2 incorporates at the antipodal sites as a structural protein. This is supported from our unsuccessful attempts to localize replication proteins to purified FKCs and  $\alpha$ -KDE2 remained stably associated with the structural elements of this complex post removal of the kDNA (Figure 3.4) (22).

The role of  $\alpha$ -KDE2 in kDNA inheritance remains obscure. The unilateral filaments of the TAC maintain a physical attachment between the kDNA and mitochondrial membranes and is important for genome positioning in the mitochondrion (11). Knockdown of p166 produces kinetoplasts that are asymmetrical and further supports a genome segregation function of the TAC (12). The unique inheritance phenotype caused by  $\alpha$ -KDE2 depletion suggests that this protein associates with a structural apparatus embedded in the mitochondrion that allows for successful distribution of a single kDNA into the newly generated mitochondrion. It would be of interest to determine other factors involved in mitochondrial DNA inheritance since the kDNA provides genomic detail for key proteins in this organelle. Immunoprecipitation studies using fractionated BF  $\alpha$ -KDE2-PTP cell lysates could identify proteins that may closely associate with  $\alpha$ -KDE2 at the antipodal sites.

Additionally, AEP-1 provides a membrane localization of the Krebs cycle enzyme,  $\alpha$ -KD. Classic observations of this system (23) led to the accepted dogma that describes positioning of the electron transport chain at the mitochondrial membranes and Krebs cycle enzymes circulating free in the matrix. Several observations from studies performed over four decades ago ruled against Krebs cycle enzymes solely diffusing with the matrix including experiments that showed a tethered malate dehydrogenase and citrate synthase enzyme system led to a more efficient rate of oxidation (24-26). Past studies dealing with mitochondrial metabolic complex interactions (27, 28), substrate channeling (28, 29) and data presented in this work on the A-IMM (Chapter 2) allows us to propose a function for a membrane associated  $\alpha$ -KD. *T. brucei* is similar to most eukaryotes in that they express many of the mitochondrial membrane complexes involved in energy production as large macromolecular assemblies (17, 30). These large complexes allow for the close association of subcomplexes and would increase metabolic flow, thereby decreasing intermediate loss to unassociated competing enzymes. Sumegi and Srere (1984) revealed the ability of NADH dehydrogenase (complex I) to bind NAD-linked enzymes (27), such as  $\alpha$ -KD and this complex I- $\alpha$ -KD interaction has been identified in trypanosomes (17). A membrane bound  $\alpha$ -KD (A-IMM) may promote a more stable interaction with complex I and could allow for the assembly of additional peripheral metabolic enzymes. In *T. brucei*  $\alpha$ -KD has a major role in the metabolism of proline, a major carbon source found in the midgut environment of the tsetse fly. This generates a large electron sink that can be efficiently transferred to the cytochrome c reductase and cytochrome c oxidase complexes by a complex I- $\alpha$ -KD multienzyme that can catalyze NAD reduction and NADH oxidation in tandem.

Our methods failed to resolve any nuclear or mitochondrial encoded proteins of complex I in our sequencing analysis of A-IMM. It has been noted that certain nonionic detergents in combination with coomassie dye from Blue Native PAGE can create a mild anionic environment that can dissociate physiological multienzyme complexes (31). One such detergent, dodecyl maltoside, was shown in mammalian and yeast systems to resolve mainly monomeric complexes (31) and was similar to what we observed during our analysis (Chapter 2). To address whether a functional complex I-A-IMM exists, milder detergents such as digitonin could be used to solubilize PF mitochondria. Alternatively, techniques such as immunoprecipitation and gel filtration could also be utilized. Purified complex I-A-IMM multienzymes could be analyzed *in vitro* for the  $\alpha$ -ketoglutarate specific reduction of coenzyme Q to ubiquinol in the presence or absence of a complex I inhibitor (rotenone).

Understanding  $\alpha$ -KD expression in BF trypanosomes also led to the identification of an unexpected secondary function of  $\alpha$ -KDE1. RNAi of  $\alpha$ -KDE1 in BF cells induced a rapid swelling of the major vesicle trafficking organelle of trypanosomes, the flagellar pocket (FP). Previous studies characterizing factors involved in endocytosis revealed that knockdown of clathrin heavy chain, which is a mediator of plasma membrane vesicle formation, induced a similar phenotype that resembled an eye socket and was labeled the “BigEye” (32). BigEye formation by  $\alpha$ -KDE1 depletion is initially observed at six hours (Chapter 4, Figure 4.1) and the rapidness of this morphology suggest that this protein may physically interact with the organelle or essential factors involved in trafficking and raised the possibility of an altered localization of  $\alpha$ -KDE1. Saas et al. (2000) revealed the moonlighting Krebs cycle enzyme aconitase was shown to undergo

multicompartmentalization in the mitochondrion and cytosol of *T. brucei* and is closely related to the iron-regulatory protein-1 in mammalian cells (7). A conventional mitochondrial targeting signal is not observed for *T. brucei* aconitase (7) and suggests that an altered localization of  $\alpha$ -KDE1 would be regulated by another mechanism.

Two important questions arise from the  $\alpha$ -KDE1 RNAi studies—1) Does  $\alpha$ -KDE1 have an alternative localization in BF trypanosomes? Antisera or a C-terminal epitope tag version of  $\alpha$ -KDE1 could be generated to identify the compartments that contain this enzyme. This analysis could also address if  $\alpha$ -KDE1 specifically associates with the architecture of the FP or factors important to vesicular trafficking. 2) Is endocytosis or exocytosis affected by  $\alpha$ -KDE1 knockdown? Various techniques have been utilized to understand and differentiate between FP endocytosis and exocytosis in *T. brucei* (32-35). Concanavalin A (ConA) is a lectin binding protein that was used in our initial experiments to bind glycoproteins housed in the FP matrix at 4°C (Chapter 4, Figure 4.2). At 37°C, ConA bound glycoproteins should be endocytosed and restriction to the FP at this temperature would suggest an endocytosis defect (32). N-linked glycans containing poly-N-acetyllactosamine and the trypanosome lytic factor receptor can also be monitored for endocytosis using specific binding factors (33, 35). Defects in exocytosis can be monitored by analyzing variant surface glycoprotein (VSG) recycling. VSG is an essential glycosylphosphatidylinositol anchored glycoprotein that covers approximately 90% of the external cell surface and is essential for trypanosome immune evasion (8). Exocytosis in  $\alpha$ -KDE1 RNAi cells can be monitored by introducing a N-terminal tagged VSG to this cell line and observing the changes in acetylated versus antibody bound VSG on the plasma membrane (34). Since *T. brucei*  $\alpha$ -KDE1 has only a

42% identity to the human enzyme, the lethality of this moonlighting protein suggests that it may be a strong candidate for drug targeting.

The expression of diverse mitochondrial proteins is essential for required processes in *T. brucei*. In this study, we have provided evidence that alternative RNA editing is necessary for a membrane localization of matrix metabolic enzymes. We also identified moonlighting mitochondrial proteins that are factors for kDNA inheritance and proper function of the FP. Observations from this work will aid in identifying the specific functions of these proteins, including functions of interacting subunits. Based on these findings, we can conclude that utilizing a detailed proteomics approach is highly effective in characterizing the roles of diverse proteins in eukaryotic organisms.

#### REFERENCES

1. **Ochsenreiter, T., and S. L. Hajduk.** 2006. Alternative editing of cytochrome c oxidase III mRNA in trypanosome mitochondria generates protein diversity. *EMBO Rep* **7**:1128-1133.
2. **Nilsson, D., K. Gunasekera, J. Mani, M. Osteras, L. Farinelli, L. Baerlocher, I. Roditi, and T. Ochsenreiter.** 2010. Spliced leader trapping reveals widespread alternative splicing patterns in the highly dynamic transcriptome of *Trypanosoma brucei*. *PLoS Pathog* **6**:e1001037.
3. **Vassella, E., R. Braun, and I. Roditi.** 1994. Control of polyadenylation and alternative splicing of transcripts from adjacent genes in a procyclin expression site: a dual role for polypyrimidine tracts in trypanosomes? *Nucleic Acids Res* **22**:1359-1364.
4. **Ochsenreiter, T., S. Anderson, Z. A. Wood, and S. L. Hajduk.** 2008. Alternative RNA editing produces a novel protein involved in mitochondrial DNA maintenance in trypanosomes. *Mol Cell Biol* **28**:5595-5604.

5. **Ochsenreiter, T., M. Cipriano, and S. L. Hajduk.** 2008. Alternative mRNA editing in trypanosomes is extensive and may contribute to mitochondrial protein diversity. *PLoS One* **3**:e1566.
6. **Jeffery, C. J.** 1999. Moonlighting proteins. *Trends Biochem Sci* **24**:8-11.
7. **Saas, J., K. Ziegelbauer, A. von Haeseler, B. Fast, and M. Boshart.** 2000. A developmentally regulated aconitase related to iron-regulatory protein-1 is localized in the cytoplasm and in the mitochondrion of *Trypanosoma brucei*. *J Biol Chem* **275**:2745-2755.
8. **Field, M. C., and M. Carrington.** 2009. The trypanosome flagellar pocket. *Nat Rev Microbiol* **7**:775-786.
9. **Vickerman, K.** 1985. Developmental cycles and biology of pathogenic trypanosomes. *Br Med Bull* **41**:105-114.
10. **Englund, P. T., S. L. Hajduk, and J. C. Marini.** 1982. The molecular biology of trypanosomes. *Annu Rev Biochem* **51**:695-726.
11. **Ogbadoyi, E. O., D. R. Robinson, and K. Gull.** 2003. A high-order transmembrane structural linkage is responsible for mitochondrial genome positioning and segregation by flagellar basal bodies in trypanosomes. *Mol Biol Cell* **14**:1769-1779.
12. **Zhao, Z., M. E. Lindsay, A. Roy Chowdhury, D. R. Robinson, and P. T. Englund.** 2008. p166, a link between the trypanosome mitochondrial DNA and flagellum, mediates genome segregation. *EMBO J* **27**:143-154.
13. **Wang, Z., and P. T. Englund.** 2001. RNA interference of a trypanosome topoisomerase II causes progressive loss of mitochondrial DNA. *EMBO J* **20**:4674-4683.
14. **Guo, X., N. L. Ernst, and K. D. Stuart.** 2008. The KREPA3 zinc finger motifs and OB-fold domain are essential for RNA editing and survival of *Trypanosoma brucei*. *Mol Cell Biol* **28**:6939-6953.
15. **Chin, E. T., and D. I. Papac.** 1999. The use of a porous graphitic carbon column for desalting hydrophilic peptides prior to matrix-assisted laser desorption/ionization time-of-flight mass spectrometry. *Anal Biochem* **273**:179-185.

16. **Horvath, A., T. G. Kingan, and D. A. Maslov.** 2000. Detection of the mitochondrially encoded cytochrome c oxidase subunit I in the trypanosomatid protozoan *Leishmania tarentolae*. Evidence for translation of unedited mRNA in the kinetoplast. *J Biol Chem* **275**:17160-17165.
17. **Acestor, N., A. Zikova, R. A. Dalley, A. Anupama, A. K. Panigrahi, and K. D. Stuart.** 2011. *Trypanosoma brucei* mitochondrial respiratome: composition and organization in procyclic form. *Mol Cell Proteomics* **10**:M110 006908.
18. **Horvath, A., E. A. Berry, and D. A. Maslov.** 2000. Translation of the edited mRNA for cytochrome b in trypanosome mitochondria. *Science* **287**:1639-1640.
19. **Liu, B., H. Molina, D. Kalume, A. Pandey, J. D. Griffith, and P. T. Englund.** 2006. Role of p38 in replication of *Trypanosoma brucei* kinetoplast DNA. *Mol Cell Biol* **26**:5382-5393.
20. **Downey, N., J. C. Hines, K. M. Sinha, and D. S. Ray.** 2005. Mitochondrial DNA ligases of *Trypanosoma brucei*. *Eukaryot Cell* **4**:765-774.
21. **Sriram, G., J. A. Martinez, E. R. McCabe, J. C. Liao, and K. M. Dipple.** 2005. Single-gene disorders: what role could moonlighting enzymes play? *Am J Hum Genet* **76**:911-924.
22. **Sykes, S. E., and S. L. Hajduk.** Dual Functions of alpha-Ketoglutarate Dehydrogenase E2 in the Krebs Cycle and Mitochondrial DNA Inheritance in *Trypanosoma brucei*. *Eukaryotic Cell*, in press. EC00269-12R1.
23. **Green, D. E., W. F. Loomis, and V. H. Auerbach.** 1948. Studies on the cyclophorase system; the complete oxidation of pyruvic acid to carbon dioxide and water. *J Biol Chem* **172**:389-403.
24. **Lopes-Cardozo, M., W. Klazinga, and S. G. van den Bergh.** 1978. Evidence for a homogeneous pool of acetyl-CoA in rat-liver mitochondria. *Eur J Biochem* **83**:635-640.
25. **Matlib, M. A., W. A. Shannon, Jr., and P. A. Srere.** 1977. Measurement of matrix enzyme activity in isolated mitochondria made permeable with toluene. *Arch Biochem Biophys* **178**:396-407.

26. **Srere, P. A., B. Mattiasson, and K. Mosbach.** 1973. An immobilized three-enzyme system: a model for microenvironmental compartmentation in mitochondria. *Proc Natl Acad Sci U S A* **70**:2534-2538.
27. **Sumegi, B., and P. A. Srere.** 1984. Complex I binds several mitochondrial NAD-coupled dehydrogenases. *J Biol Chem* **259**:15040-15045.
28. **Fahien, L. A., M. J. MacDonald, J. K. Teller, B. Fibich, and C. M. Fahien.** 1989. Kinetic advantages of hetero-enzyme complexes with glutamate dehydrogenase and the alpha-ketoglutarate dehydrogenase complex. *J Biol Chem* **264**:12303-12312.
29. **Fukushima, T., R. V. Decker, W. M. Anderson, and H. O. Spivey.** 1989. Substrate channeling of NADH and binding of dehydrogenases to complex I. *J Biol Chem* **264**:16483-16488.
30. **Panigrahi, A. K., A. Zikova, R. A. Dalley, N. Acestor, Y. Ogata, A. Anupama, P. J. Myler, and K. D. Stuart.** 2008. Mitochondrial complexes in *Trypanosoma brucei*: a novel complex and a unique oxidoreductase complex. *Mol Cell Proteomics* **7**:534-545.
31. **Schagger, H.** 2001. Respiratory chain supercomplexes. *IUBMB Life* **52**:119-128.
32. **Allen, C. L., D. Goulding, and M. C. Field.** 2003. Clathrin-mediated endocytosis is essential in *Trypanosoma brucei*. *EMBO J* **22**:4991-5002.
33. **Nolan, D. P., M. Geuskens, and E. Pays.** 1999. N-linked glycans containing linear poly-N-acetyllactosamine as sorting signals in endocytosis in *Trypanosoma brucei*. *Curr Biol* **9**:1169-1172.
34. **Engstler, M., L. Thilo, F. Weise, C. G. Grunfelder, H. Schwarz, M. Boshart, and P. Overath.** 2004. Kinetics of endocytosis and recycling of the GPI-anchored variant surface glycoprotein in *Trypanosoma brucei*. *J Cell Sci* **117**:1105-1115.
35. **Stephens, N. A., and S. L. Hajduk.** 2011. Endosomal localization of the serum resistance-associated protein in African trypanosomes confers human infectivity. *Eukaryot Cell* **10**:1023-1033.